Abstracts, Division of Biological Chemistry, 188th National Meeting of the American Chemical Society, August 26–31, 1984

E. Cordes, Chairman; V. Bloomfield, Secretary
J. J. Villafranca and Rowena Matthews, Program Cochairmen

Monday Morning—Symposium on Protein–Macromolecule Interactions—K. Johnson, Symposium Chairman

1. Microtubule–Dynein Interactions and the Pathway of ATP Hydrolysis. *Kenneth A. Johnson.* Department of Biochemistry, Pennsylvania State University, University Park, PA 16802.

ATP hydrolysis is coupled to the interaction of dynein with microtubules in cilia and flagella to generate the force for a sliding movement that is coupled to wave propagation in these organelles. The kinetics of ATP binding and hydrolysis and product release have been measured by chemical quench flow methods. In parallel experiments, the kinetics of dissociation and reassociation of the microtubule–dynein complex have been measured by stopped-flow light scattering. Previously published work has established that ATP binding induces a rapid dissociation of the microtubule–dynein complex and that hydrolysis is at least 20-fold slower. The rate limiting step in the steady state is product release. Microtubules activate the steady-state ATPase approximately 10-fold and our current data suggest that the cycle is completed by the rebinding of the dynein–ADP–P_i intermediate with the microtubule and the release of products. We have also measured the rate of ATP synthesis using steady-state and transient-state methods as well as ^{18}O–P_i–H_2O exchange methods. These data indicate that there are large free changes associated with ATP binding and product release and that ATP hydrolysis at the active site is near equilibrium.

2. Interference of Nucleotide Hydrolysis in the Polymerization of Tubulin and Actin. M.-F. Carlier, T. L. Hill, D. Pantaloni, and *E. D. Korn.*

Abstract not available at time of publication.

3. Cooperativity Resulting from Association of Specific Enzyme Forms—Trapping of Active Monomer as Active Oligomer. *Paul M. Anderson.* Department of Biochemistry, University of Minnesota, Duluth, Duluth, MN 55812.

Changes in specific activity or apparent cooperativity with changes in enzyme concentration are usually considered as evidence that the observed cooperativity is a result of reversible association–dissociation in which the different oligomeric states have different properties. We have considered the possibility that similar properties can arise when the active species is specifically subject to self-association, but the different states of association are equivalent with respect to specific activity and/or ligand affinity. Calculations for schemes such as

$$E'' \rightleftharpoons E' \underset{-S}{\overset{+S}{\rightleftharpoons}} ES \rightleftharpoons (ES)_2 \rightleftharpoons (ES)_4$$

(in which ES, $(ES)_2$, and $(ES)_4$ are equivalent with respect to specific activity) show that specific activity vs. concentration of S can be sigmoidal and that the degree of cooperativity and the specific activity are affected by enzyme concentration. These effects are due simply to mass action, formation of active oligomer serving as a thermodynamic trap of active monomer. This scheme will be discussed with reference to carbamoyl phosphate synthetase and CTP synthetase.

4. Influence of Actin Binding Proteins on the Mechanism of Actin Polymerization. *C. Frieden,* Y. Doi, and T. Arakawa. Department of Biological Chemistry, Washington University School of Medicine, St. Louis, MO 63110.

The mechanism of the Mg^{2+}-induced polymerization of actin at pH 8 and 20 °C has been shown to involve a Mg^{2+}-induced conformational change followed by the binding of a second mole of Mg^{2+} prior to dimerization and subsequent elongation. We have investigated the effects of two actin binding proteins on polymerization. These are the microtubule-associated protein, which cross-links actin filaments, and brevin, which binds to actin and prevents growth at the fast growing end. In the former case, cross-linking occurs only after polymerization is complete and the protein has little or no effect on the rate of polymerization. In the latter case, brevin stimulates actin polymerization and the rate constant for monomer addition to and dissociation from the filaments can be calculated. The on rate constant is markedly dependent on Mg^{2+} concentration.

Monday Afternoon—Symposium on Nucleotide and Nucleic Acid Utilizing Enzymes—R. J. Suhadolnik, Symposium Chairman

5. Metabolism of Queuine. *W. R. Farkas.* Department of Environmental Practice, University of Tennessee College of Veterinary Medicine, Knoxville, TN 37901-1071.

Queuine is the only pyrrolopyrimidine known to occur in tRNA where it is found in the first or wobble position of $tRNA^{Asp}$, $tRNA^{Asn}$, $tRNA^{His}$, and $tRNA^{Tyr}$. The other modified nucleosides found in tRNA are synthesized at the polynucleotide level. Queuine is synthesized separately from the tRNA and is then inserted into the tRNA by an enzyme that removes a guanine residue from the wobble position of the original transcript and replaces it with queuine. The mouse and probably other higher mammals have a dietary requirement for queuine. The enzyme that transfers queuine into tRNA has been purified to homogeneity from rabbit erythrocytes. The enzyme is a dimer consisting of a 60 000 and 43 000 MW subunit. The enzyme is potently inhibited by 2,3-butanedione. Surprisingly, 1,3-cyclohexanedione but not 1,2-cyclohexanedione inhibits the enzyme.

0006-2960/84/0423-3346$01.50/0

6. Plant Oligonucleotides: Enzymatic Synthesis and Biological Activity. *Y. Devash*, I. Sela, M. Reichman, N. L. Reichenbach, and R. J. Suhadolnik. Temple University School of Medicine, Philadelphia, PA, and Hebrew University of Jerusalem, Rehovot, Israel.

We have reported on the crossover between the animal and plant kingdoms with respect to the inhibition of virus replication in plants by human leukocyte interferon and mammalian 2′,5′-adenylates (Reichman et al., *Virology 128*, 240 (1983); Devash et al., *J. Biol. Chem. 259*, 3482 (1984)). More recently, we have observed the inhibition of protein synthesis in reticulocyte lysates (RL) and in wheat germ cell-free system (WG) by plant oligoadenylates. When tobacco plants are inoculated with either tobacco mosaic virus (TMV), treated with human leukocyte interferon, or treated with plant antiviral factor (AVF), a dsRNA-dependent enzyme converting ATP to oligoadenylates is stimulated. These oligoadenylates (MW >1000) have charges of 5–, 6–, and 7– as determined by DEAE-cellullose chromatography and DEAE-cellulose TLC. The oligoadenylates with charges of 6– and 7– are potent inhibitors of protein synthesis in RL and WG systems. Unlike the mammalian 2′,5′-oligoadenylates, the plant oligoadenylates inhibit protein synthesis in RL *without* binding to and activation of the 2′,5′-adenylate dependent endonuclease. Structural elucidation is in progress.

7. Recognition of Methionine tRNAs by *E. coli* Methionyl-tRNA Synthetase. *LaDonne H. Schulman*, Heike Pelka, Dario Valenzuela, and Oscar Leon. Department of Developmental Biology and Cancer, Albert Einstein College of Medicine, Bronz, NY 10461.

Recent work from this laboratory has established that the anticodon region of $tRNA^{fMet}$ contains structural elements required for recognition of the tRNA by methionyl-tRNA synthetase (MetRS). An extensive series of variant tRNAs containing single base changes in this region have been synthesized in vitro using RNA ligase. Base substitutions in the wobble position have been found to reduce aminoacylation rates by at least five orders of magnitude. Derivatives having base substitutions in the other two positions of the anticodon are aminoacylated 50 to 18 000 times slower than normal. Analysis of the accessibility of specific nucleotides in $tRNA^{fMet}$ to modification with dimethyl sulfate and to limited nuclease digestion has provided further evidence for direct interaction of MetRS with the anticodon sequence and for induction of conformational changes in the tRNA on binding to the protein. Four different sites in the tRNA have been covalently coupled to specific lysine residues at or near the tRNA binding site of MetRS in order to construct a three-dimensional model of the protein–nucleic acid complex.

8. Further Evidence for Significance of Covalent Enzyme—tRNA Interaction. *Paul Schimmel* and *Ruth Starzyk*. Department of Biology, M.I.T., Cambridge, MA 02139.

Previous work has showed that aminoacyl tRNA synthetases (1) have a site which makes a covalent Michael adduct with the uracil ring, (2) are inactivated by a site-directed reagent which labels the uridine interaction site, and (3) evidently make a transient Michael adduct with uridine 8 in the tRNA structure (a uridine is present at position 8 in all prokaryote and cytoplasmic eukaryote tRNAs which have been sequenced to date). We now show that elimination of the electrophilic center at carbon 6, in the uracil ring of uridine 8 (in a specific tRNA) eliminates aminoacylation. The modification is achieved by sodium borohydride reduction of 4-thiouridine 8 in *E. coli* tyrosine-specific tRNA. Extensive kinetic and chromotographic data demonstrate that it is this alteration—which prevents transient covalent bond formation with the synthetase—that is responsible for the inactivation. The data add further evidence that covalent bond formation is essential for aminoacylation.

9. Nucleoside α-Thiotriphosphates: Their Use with the DNA Polymerases. *S. J. Benkovic*, A. Gupta, V. Mizrahi, J.-T. Chen, and P. Benkovic. Department of Chemistry, The Pennsylvania State University, University Park, PA 16802.

The use of nucleoside α-thiotriphosphates to examine the mechanism of action of enzyme involved in DNA synthesis or excision will be illustrated. These compounds furnish the opportunity to investigate the nature of the rate-limiting steps in Pol I catalyzed polymerization as well as in the associated 3′ → 5′-exonuclease activity since nonenzymatic reference reactions show that sulfur vs. oxygen substitution leads to isotope effects on the order of 500-fold with the thiophosphate being the slower. The polymerization reactions catalyzed by Pol I on a poly(dA)·oligo(dT) template primer system have been examined with dTTP and dTTPαS with no apparent effect on either pre- or steady-state kinetics. In contrast the 3′ → 5′-exonuclease activity of Pol I is severely inhibited by a 3′ → 5′-thiophosphate linkage with the rate being some 100-fold slower than the corresponding oxygen-substituted ester. We have exploited this large difference in sensitivity toward these two activities to employ Pol I in the selective incorporation of mismatches within the dihydrofolate reductase gene.

10. Thio and Amino Sugars and Their Phosphorylated Derivatives as Probes of Enzyme Reaction Mechanisms. *W. B. Knight* and W. W. Cleland. Department of Biochemistry, University of Wisconsin, Madison, WI 53706.

6-Thioglucose-6-P (I) was oxidized by glucose-6-P dehydrogenase at the same V as glucose-6-P, but with $K_m \times 10$. 6-Thiogluconate-6-P showed 11% the rate of 6-P-gluconate with 6-P-gluconate dehydrogenase. By contrast, I and MgADP reacted at 0.0025% the rate of glucose-6-P with hexokinase. With glycerokinase the 3-OH of racemic 1-thioglycerol was phosphorylated with $V \times 0.006$ and $K_m \times 780$ relative to glycerol. While no phosphorylation of the 1-thiol was seen, 1-thioglycerol-1-P and MgADP gave $V \times 0.00004$. The unprotonated amino group of racemic 1-aminopropanediol was phosphorylated ($V \times 0.0035$, $K_m \times 11$ relative to glycerol) >10-fold faster than the 3-OH. In contrast to the kinase reactions, alkaline phosphatase hydrolyzed I at 109% the rate for glucose-6-P, and phosphoglucomutase catalyzed conversion to the 1-phosphate at 11% of the glucose-1-P to glucose-6H rate. Since K_{eq} was 46, the free energy of hydrolysis of the phosphorylated thiol is 7.3 kcal/mol. The ability of the latter two enzymes to cleave P–S bonds as rapidly as P–O bonds, contrasted with the very slow reactions of kinases, suggests different phosphoryl transfer mechanisms for these enzymes.

Monday Afternoon—Poster Session—J. J. Villafranca, Chairman

11. Isotope Effect Studies of the Chemical Mechanism of TPN Isocitrate Dehydrogenase with 3-Fluoroisocitrate. *Charles B. Grissom* and W. W. Cleland. Department of

Biochemistry, University of Wisconsin—Madison, Madison, WI 53706.

threo-D-3-Fluoroisocitrate (3-FIc) is a substrate which is oxidatively decarboxylated by pig heart TPN isocitrate dehydrogenase. While *threo*-D-isocitrate (Ic) is very sticky (i.e., it reacts to give products much faster than it dissociates), 3-FIc is less so on the basis of the dependence of kinetic parameters on solution viscosity. The lower external commitment of 3-FIc allows the observation of significant deuterium and C-13 kinetic isotope effects at neutral pH. At pH 7.0, $^{D}(V/K) = 1.5 \pm 0.3$, $^{D}V = 1.02 \pm 0.07$, and $^{13}(V/K) = 1.013 \pm 0.001$. At pH 5.2, $^{13}(V/K)$ increases to 1.019 ± 0.001, showing that a small external commitment still remains at neutral pH. The K_m for 3-FIc is the same (1.7 ± 0.3 μM) and the V_{max} is 30-fold slower than for Ic. The recently developed method of intermediate partitioning (C. B. Grissom and W. W. Cleland, *Fed. Proc. 43*, in press (1984)) with 3-fluorooxalosuccinate will allow the determination of the intrinsic deuterium and C-13 isotope effects with 3-FIc and permit a comparison of the free energy reaction profile with Ic and 3-FIc.

12. The Regiochemistry and Stereochemistry of Proton Transfer in the Yeast Inorganic Pyrophosphatase Reaction. *D. Dunaway-Mariano*, I. Lin, and W. B. Knight. Department of Chemistry, University of Maryland, College Park, MD 20742.

Yeast inorganic pyrophosphatase catalyzes the hydrolysis of pyrophosphate to orthophosphate. The active substrate in this reaction has been shown to be the fully ionized P^1,P^2-bidentate $[Mg(H_2O)_4PP]^{2-}$ complex. The leaving group in the reaction, Mg^{2+} complexed PO_4^{3-} is quite basic and therefore we might expect an enzyme mediated proton transfer to occur to this group during the course of catalysis. A priori, protonation of the MgPP complex may occur at the P–O–P bridge oxygen atom or at one of the two available P–O isolated oxygen atoms. In order to distinguish between these two possible protonation sites we have prepared and studied the substrate activities of two different probes. First, the P^1,P^2-bidentate $Co(NH_3)_4$(imididodiphosphate) was found not to be a substrate under conditions in which the isosteric complex, P^1,P^2-bidentate $Co(NH_3)_4$(pyrophosphate) was rapidly turned over. Second, pyrophosphatase was shown to be stereospecific for the P^1,P^2-bidentate $Co(NH_3)_4$(thiopyrophosphate) enantiomer having the *R* configuration at the thiophosphoryl center. These results are interpreted to suggest that proton transfer occurs to the pro-*R* oxygen atom of the leaving group in the pyrophosphatase catalyzed $Mg(PP)^{2-}$ hydrolysis reaction.

13. Examination of the Structure of the Nucleotide Substrate for the Rat Liver Mitochondrial Proton Pump ATPase. *Mary Carpin*, D. Dunaway-Mariano, and Pete Pedersen. Department of Chemistry, University of Maryland, College Park, MD 20742 (M.C. and D.D.-M.), and Johns Hopkins School of Medicine, Baltimore, MD 21205 (P.P.).

The proton-translocating ATPase of rat liver mitochondria is a group of large membrane bound proteins. In the present study we have examined the question of whether free ATP or the MgATP complex is recognized as substrate by the ATPase. The exchange inert MgATP analogue, $Rh(H_2O)_nATP$ was tested as a substrate and as an inhibitor of the F_0F_1ATPase. The $Rh(H_2O)_nATP$ is a competitive inhibitor vs. MgATP at pH 6.0 with a $K_i = 115$ μM. The substrate activity of [γ-^{32}P]$Rh(H_2O)_nATP$ was tested using an assay for [^{32}P]P_i (liberated from the $Rh(H_2O)(ADP)(P_i)$ product complex by EDTA). No product was detected indicating that while the $Rh(H_2O)_nATP$ (which consists of a 1:1 mixture of α,β-bidentate and α,β,γ-tridentate isomers) binds to the ATP binding site, it is not turned over at an appreciable rate. The binding affinities of the two α,β-bidentate $Rh(H_2O)_4ADP$ screw sense isomers were also measured by testing them as competitive inhibitors vs. MgATP. The K_i values are 55 μM and 74 μM. While the ATPase is not stereospecific in binding the $Rh(H_2O)_4ADP$ isomers, the tightness of the binding of these isomers as well as the $Rh(H_2O)_nATP$ isomers might suggest that a metal–nucleotide complex is preferred over the free nucleotide. The stereospecificity of the ATPase toward M(II) complexes of ATPβS and ATPαS will also be reported.

14. P^1,P^2-Bidentate $Co(NH_3)_4$(thiopyrophosphate): A Stereochemical Probe. *Irene Lin* and D. Dunaway-Mariano. Department of Chemistry, University of Maryland, College Park, MD 20742.

α,β-Bidentate $Co(NH_3)_4ADP\alpha S$ was separated into a set of Δ and Λ isomers which are coordinated at the α-P via the oxygen atom and a set coordinated at the α-P via the sulfur atom. The sets of stereoisomers were converted to the corresponding O,O-coordinated and O,S-coordinated P^1,P^2-bidentate $Co(NH_3)_4$(thiopyrophosphate) complexes via treatment with $NaIO_4$. The O,O-coordinated $Co(NH_3)_4PPS$ complex shows a λ_{max} at 520 nm and a ^{31}P NMR spectrum which has doublets ($J = 24.6$ Hz) at 50.6 and 2.0 ppm. The O,S-coordinated $Co(NH_3)_4PPS$ complex shows a ^{31}P NMR spectrum having doublets ($J = 27.7$ Hz) at 37.6 and 7.2 ppm. The Δ and Λ O,O-coordinated $Co(NH_3)_4ADP\alpha S$ isomers were cleaved to the corresponding O,O-coordinated P^1,P^2-bidentate $Co(NH_3)_4PPS$ enantiomers. The CD spectra of these enantiomers are characterized by a λ_{max} at 525 nm ($\theta = (-)1068$ and $(+)1068$ deg·cm^2/dmol, respectively). Preliminary studies of the oxidative elimination of the coordinated α,β-bidentate $Cr(H_2O)_4ADP\alpha S$ isomers indicate that optically active solutions of the P^1,P^2-bidentate $Cr(H_2O)_4PPS$ enantiomers are formed. The M(III)PPS enantiomers can serve as a relay between the known configuration at the α,β-bidentate M(III)ADPαS diastereomers and the unknown configuration at the thiophosphoryl center of M(III)ATPγS or M(III)ADPβS diastereomers.

15. Investigation of the Kinetic Mechanism of *Bacteroides symbiosus* Pyruvate Phosphate Dikinase. *H.-C. Wang*, D. Dunaway-Mariano, Wolfgang von der Saal, and J. J. Villafranca. Department of Chemistry, University of Maryland, College Park, MD 20742 (H.-C.W. and D.D.-M.), and Department of Chemistry, Pennsylvania State University, University Park, PA 16802 (W.v.d.S. and J.J.V.).

The kinetic mechanism of pyruvate phosphate dikinase (PPDK) from *Bacteroides symbiosus* has been investigated using steady-state kinetic and isotope exchange techniques. PPDK catalyzes [^{14}C]Pyr $\rightleftharpoons$ PEP exchange in the absence of cosubstrates. [^{32}P]$P_i \rightleftharpoons$ PP exchange takes place only in the presence of AMP/ATP. Similarly, [^{32}P]AMP $\rightleftharpoons$ ATP exchange takes place only in the presence of P_i/PP. ^{18}O Positional isotope exchange (PIX) of the α,β-bridge ^{18}O of ATP labeled with ^{18}O at this position and the two nonbridging β-P-O positions into a nonbridging α-P-O position was used to monitor E + ATP $\rightleftharpoons$ EPP + AMP and exchange into the β,γ-bridge position to monitor EPP + P $\rightleftharpoons$ EP + PP. The requirement of the presence of P_i for appreciable PIX into the

α-P-O position supports, along with molecular isotope exchange data, a bi (ATP, P_i) bi (AMP, PP) uni (pyr) uni (PEP) mechanism. Most noticeable among the initial velocity patterns measured is the $1/V$ vs. $1/[AMP]$ at fixed [PEP] and varying [PP] pattern which, consistent with the above kinetic mechanism, is intersecting. A detailed kinetic analysis of this system will be reported.

16. Recent Developments in the Area of Exchange-Inert Metal–ATP Complexes. *A. L. Shorter*, I. Lin, and D. Dunaway-Mariano. Department of Chemistry, University of Maryland, College Park, MD 20742.

Rh(III)ATP complexes have been prepared for use as exchange inert, diamagnetic probes of enzyme active site structure and as probes of metal–ATP complex structure and stability. Reaction of the perchlorate salt of $Rh(H_2O)_6^{3+}$ with ATP yielded a mixture of α,β-bidentate and α,β,γ-tridentate $Rh(H_2O)_n$ATP isomers. Chromatography of this mixture on a Sephadex G-10 column allowed us, as determined by ^{31}P NMR, to separate the bidentate and tridentate structural isomers. Separation of the stereoisomers can be effected on cycloheptaamylose columns and on reverse-phase HPLC columns. The equilibration of the isomers has been studied by using NMR and HPLC techniques. The tridentate stereoisomers differ dramatically in their kinetic stabilities. The equilibration rates of the bidentate–tridentate structural isomers (as mixtures of stereoisomers) are approximately equal. These properties are quite different from those of the Cr(III)ATP and Co(III)ATP complexes. The mechanism of Rh(III)ATP isomerization and the spectral properties and kinase substrate activities of the pure Rh(III)ATP isomers will be reported.

17. EPR Studies of the Central Complexes of Creatine Kinase. *T. S. Leyh*, P. J. Goodhart, G. H. Reed, A. C. Nguyen, and G. L. Kenyon. Department of Biochemistry and Biophysics, University of Pennsylvania School of Medicine, Philadelphia, PA 19104 (T.S.L., P.J.G., and G.H.R.), and Department of Pharmaceutical Chemistry, University of California, San Francisco, CA 94143 (A.C.N. and G.L.K.).

The EPR spectrum for Mn(II) in the two central complexes of the creatine kinase reaction mixture has been identified. The signals that correspond to each central complex have been assigned with the aid of the spectrum for the enzyme–Mn(II)ATP complex with a nonreactive analogue of creatine, 1-(carboxymethyl)-2-iminoimidazolidin-4-one. The EPR spectra show that the enzyme–Mn(II)ATP–creatine and enzyme–Mn(II)ADP–phosphocreatine complexes are present in a ratio of approximately 1.4 to 1, and chromatographic assays for ADP and ATP following an acid quench of samples give virtually the same result. Coordination of the oxygens from the substrate and product phosphate groups to Mn(II) in these complexes has been investigated using regiospecific ^{17}O ($I = {}^5/_2$) enrichment at the various phosphate positions. EPR measurements with these labeled samples show equivalent inhomogeneous broadening from ^{17}O in all of the EPR signals irrespective of the position of the label. These results show that Mn(II) is coordinated to all three available phosphate groups in both the substrate and product complexes in the equilibrium mixture.

18. Electron Paramagnetic Resonance Studies of Vanadyl Complexes with Pyruvate Kinase. *Kenneth A. Lord* and George H. Reed. Department of Biochemistry and Biophysics, University of Pennsylvania, Philadelphia, PA 19104.

Vanadyl ion (VO^{2+}) binds to pyruvate kinase (PK) competitively with respect to Mg^{2+} with a stoichiometry of one per subunit. EPR spectra for the enzyme–VO^{2+} complexes in solution exhibit powder pattern line shapes with axially symmetric g and ^{51}V hyperfine tensors. The ^{51}V hyperfine tensor and the g values vary slightly with formation of ternary complexes with substrates and analogues that have carboxyl and hydroxyl functional groups. EPR spectra for ternary complexes with the substrates, thioglycolate and thiolactate, have g values and ^{51}V hyperfine tensors that are indicative of direct coordination between VO^{2+} and the sulfur ligand. Superhyperfine coupling with ^{17}O of labeled glycolate and oxalate show that VO^{2+} is coordinated to the carboxylate groups of oxalate and glycolate and to the hydroxyl group of glycolate. VO^{2+} gives a rate 4% that of an equivalent concentration of Mg^{2+} in the overall reaction of PK. Because of the dual divalent cation requirement of PK, in these assays VO^{2+} must also interact with the nucleotide substrate; either role could limit activity.

19. ENDOR Studies of the Iron–Molybdenum Cofactor of Nitrogenase and Its Interactions with Substrates. *M. J. Nelson*, M. A. Levy, W. H. Orme-Johnson, R. A. Venters, J. E. Roberts, and B. M. Hoffman. Massachusetts Institute of Technology, Cambridge, MA 02139, and Northwestern University, Evanston, IL 60201.

Electron nuclear double resonance spectroscopy has been applied to the study of ^{57}Fe, ^{95}Mo, ^{97}Mo, and ^{33}S-enriched molybdenum–iron proteins of nitrogenase. From the iron ENDOR spectra we have made approximations to the hyperfine coupling tensors for six distinct iron sites in the iron–molybdenum cofactor. Based on these data, we suggest three of these irons are high-spin ferrous, and three high-spin ferric. Observation of a molybdenum resonance demonstrates the integration of that metal into the spin system of the cofactor. Further, the small magnitude of the molybdenum hyperfine coupling implies zero or integer spin, consistent with an even oxidation state for that metal. ENDOR spectra of these proteins in the presence of substrates of nitrogenase reveal specific interactions between these substrates and certain metals in the iron–molybdenum cofactor cluster.

20. Attempts To Trap an Oxyanion Intermediate in the Ring Opening of Epoxides Catalyzed by Glutathione *S*-Transferase. *R. N. Armstrong* and Wen-Jian Chen. Department of Chemistry, University of Maryland, College Park, MD 20742.

Isozyme C_2 of rat liver glutathione *S*-transferase catalyzes the trans addition of glutathione (GSH) stereospecifically to the oxirane carbon of *R* absolute configuration in several arene oxide substrates such as phenanthrene 9,10-oxide, **1**. Whether this xenobiotic metabolizing enzyme has evolved to the extent that it is capable of protonating the incipient alkoxide in the transition state for the reaction is being questioned by attempts to trap oxyanion intermediates along the reaction coordinate. A potential intramolecular oxyanion trap has been incorporated into **1** by the synthesis of racemic 1-acetoxyphenanthrene 9,10-oxide, **2**. Isozyme C_2 catalyzes the addition of GSH to racemic **2** to give at least two products which have the anticipated 9*S*,10*S* absolute configuration. Demonstration of transfer of the acetyl group from the 1-position to the 10-position in the stereospecific addition GSH to (9*R*,10*S*)-**2** but not in (9*S*,10*R*)-**2** would constitute strong evidence for an oxyanion intermediate in the enzyme-catalyzed reaction. With this in mind, the chemical and stereochemical identification of reaction products is being pursued.

21. Conformationally Locked Vicinal Diols as Probes of the Conformer Selectivity of UDP-glucuronosyltransferase. Richard N. Armstrong and *Deborah A. Lewis*. Department of Chemistry, University of Maryland, College Park, MD 20742.

UDP-glucuronosyltransferase (EC 2.4.1.17) catalyzes the stereoselective transfer of the glucuronosyl group of uridine 5′-diphosphoglucuronate to vicinal dihydrodiols of polycyclic aromatic hydrocarbons (Lewis & Armstrong (1983) *Biochemistry 22*, 6297). Inasmuch as dihydrodiols exist in solution as a rapidly interconverting mixture of two conformers the conformer selectivity of the enzyme is difficult to determine. For this reason the kinetically stable conformers of 3,4,5,6-tetramethyl-9,10-dihydroxy-9,10-dihydrophenanthrene, **1**, have been prepared. Racemic *cis*-**1** obtained by OsO_4 oxidation of the aromatic hydrocarbon is converted to *trans*-**1** by oxidation to the orthoquinone followed by stereoselective reduction with KBH_4 to give racemic *trans*-**1E** with diequatorial hydroxyl groups. Racemic *trans*-**1A** (diaxial hydroxyl groups) is obtained by heating *trans*-**1E** in H_2O/CH_3OH. Antipodes of *cis*-**1** and *trans*-**1A** can be resolved by chiral HPLC. Preliminary evidence with racemic substrates suggests *trans*-**1E** is the preferred substrate for the enzyme with *cis*-**1** and *trans*-**1A** being less effective substrates.

22. Substrate Specificity of Ribonucleotide Triphosphate Reductase from *L. leichmannii*. *G. Harris*, J. Stubbe, and M. J. Robins. Department of Biochemistry, University of Wisconsin, Madison, WI 53706 (G.H. and J.S.), and Department of Chemistry, University of Alberta, Edmonton, Alberta, Canada (M.J.R.).

The substrate specificity of ribonucleotide reductase (RTPR) has been examined with a variety of 2′-substituted 2′-deoxynucleotides:

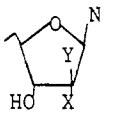

(N, X, Y) Urd, F, H; Urd, Cl, H; A, N_3, H; A, Cl, H; A, Br, H; A, I, H; C, F, H; A, H, N_3; A, H, Cl; A, H, Br. All of these compounds result in rapid time dependent inactivation of RTPR with $t_{1/2}$ min of 24, 0.7, 9, 0.25, 1.3, 8, 24, <0.25, 0.9, 4.5, respectively. Both ClUTP and FUTP can partition between a normal reduction reaction to produce 2′dUTP and inactivation. Incubation of both ribo and ara BrATP in the absence of reductant results in three to five turnovers per inactivation. This inactivation is accompanied by release of both adenine and Br^-, as well as change in the protein absorption spectrum at 320 nm. The mechanism by which these halogenated derivatives inactivate RTPR appears to be quite similar to that established for ClUTP. Both the ara and ribo N_3ATP's are also potent irreversible inhibitors of RTPR, whose mechanism appears to be different than that for the halogenated derivatives. A reductant appears to be necessary for rapid inactivation, and no change in the protein absorption spectrum accompanies inactivation.

23. Ribonucleotide Reductase: Catalysis of a Rearrangement Reaction. *M. Ator*, G. Harris, and J. Stubbe. Department of Biochemistry, University of Wisconsin, Madison, WI 53706.

Interaction of 2′-chloro-2′-deoxynucleotides ClUDP (ClUTP) with *E. coli* ribonucleotide reductase (RDPR) or *L. leichmannii* reductase (RTPR) results in cleavage of the 3′ C–H bond, production of PP_i (PPP_i), release of uracil, and formation of 2-methylene-3(2*H*)-furanone (I). Compound I is responsible for rapid inactivation of these enzymes. Evidence is presented that I is generated in solution by the decomposition of 3′-keto-2′-deoxynucleotide produced at the enzymes' active sites. Incubation of [3′-^{3}H]ClUDP (ClUTP) with reductase results in the production of ^3H_2O and [ara-2′-^{3}H]-3′-keto-deoxynucleotide. The 3′-keto-2′-deoxynucleotide was identified by trapping with $NaBH_4$. 2′-DeoxyUDP (UTP) and the 3′ epimer were isolated in a 1:4 mixture. After removal of the phosphates from these reduced products, the stereochemistry of this ^{3}H transfer was established using deoxyuridine hydroxylase. Ribonucleotide reductase can catalyze a rearrangement of hydrogen from the 3′ position of ClUDP (ClUTP) to the 2′ position (top face) of 3′-ketonucleotide. Given the unique role of AdoCbl in the *L. leichmannii* enzyme these results may provide insight into the mechanism of AdoCbl dependent rearrangement reactions.

24. Interaction of 2′-Azido-2′-deoxyuridine 5′-Diphosphate with *E. coli* Ribonucleotide Reductase: Evidence for Generation of a New Radical. M. Ator, *S. Salowe*, and J. Stubbe. Department of Biochemistry, University of Wisconsin, Madison, WI 53706.

Interaction of 2′-azido-2′-deoxyUDP (N_3UDP) with *E. coli* ribonucleotide reductase results in rapid time dependent inactivation of the enzyme accompanied by cleavage of the 3′ C–H bond, production of PP_i and release of uracil. Only one equivalent of N_3UDP per equivalent of B_2 subunit is required for complete inactivation. This process is accompanied by loss of the tyrosine radical on the B_2 subunit of RDPR and formation of a new radical identical to that reported by Sjöberg et al. with N_3CDP [*J. Biol. Chem.* (1983) *258*, 8060]. The EPR spectrum of this new radical consists of a large (25G) triplet of smaller (6G) doublets which was assigned by these workers to a nitrogen radical with a hyperfine coupling to a hydrogen. We have found that [2′-^{15}N]N_3UDP collapses the triplet signal of the new radical to a doublet, demonstrating unequivocally that spin density is located on a nitrogen derived from the azide moiety. Substitution of ^{2}H on the 1′, 2′, or 3′ carbons of N_3UDP does not alter the EPR signal, indicating that the 6G coupling is not due to a hydrogen at any of these positions. A V/K isotope effect of approximately 2 exists for [3′-^{2}H]N_3UDP inactivation of the enzyme. The isotope effect can also be observed upon tyrosine radical loss as monitored by A_{410} or EPR. Together these results suggest that formation of the new radical parallels the normal reaction pathway which is hypothesized to involve a radical cation mechanism.

25. Synthesis of Chirally Deuterated *S*-Adenosylmethylthiopropylamines and Their Use in the Elucidation of the Mechanism of Spermidine Synthase. *G. R. Orr*, D. Kullberg, and J. K. Coward. Department of Chemistry, Rensselaer Polytechnic Institute, Troy, NY 12181.

Chiral [4-^{2}H]-γ-aminobutyric acids were converted through several steps to their respective *N*-(3-(*N*′-nitroso-*p*-toluenesulfonamido)-1-propyl)phthalimides, **1a** and **1b**. Thermal rearrangement of these intermediates afforded the corresponding tosylates, **2a** and **2b**. Coupling of **2a** and **2b** with 2′,3′-isopropylideneadenosyl-5′-thiolate followed by deprotection and S-methylation gave the title compounds **3a** and **3b**. Spermidines obtained by enzyme-catalyzed aminopropyl transfer to perdeuterioputrescine were converted to their N_1,N_7-diBoc-spermidine-N_4-camphanamides. Analysis of these derivatives by ^{1}H NMR allowed elucidation of the stereo-

chemical course of the enzymatic reaction.

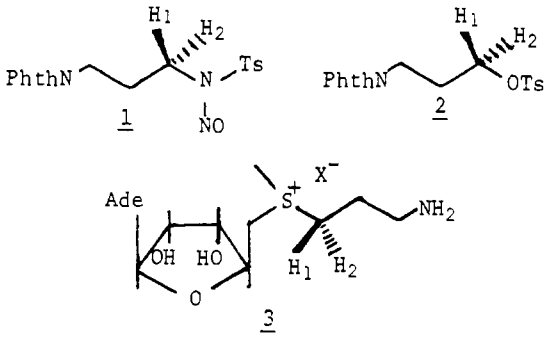

a) H_1 = D, H_2 = H b) H_1 =, H_2 = D

26. Probes of Acyl Enzyme Mechanisms for Lipolytic Enzyme Catalysis. *Daniel Quinn* and Jay Stout. Department of Chemistry, University of Iowa, Iowa City, IA 52242.

The mechanisms of lipoprotein lipase (LpL) and cholesteryl esterase (CEase) have been probed using water-soluble substrates and inhibitors. LpL-catalyzed hydrolysis of *p*-nitrophenyl butyrate (PNPB) is rapidly inhibited by diethyl *p*-nitrophenyl phosphate. The inhibition involves rapid formation of a phosphoryl-LpL intermediate and consequent slow dephosphorylation and is exploited to quantitate [LpL] by active site titration. V_{max} and K_m of CEase-catalyzed hydrolysis of PNPB are increased by addition of alcohols, which is consistent with nucleophilic trapping of a butyryl-CEase intermediate:

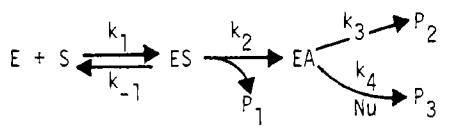

For $k_2 >> k_3$: $V_{max} = (k_3 + k_4[Nu])[E]_T$; $K_s = (k_2 + k_{-1})/k_1$; $K_m = K_s(k_3 + k_4[Nu])/k_2$. V_{max} activation follows the order 1-butanol >> ethanol > methanol. V_{max} and K_m for CEase-catalyzed hydrolysis of PNPB are increased ~2-fold by addition of sonicated phospholipid vesicles, which suggests that interfacial activation of the enzyme is a specific effect on rate-determining deacylation.

27. Effects of Interactions with Substrate, O_2, and Cofactor on the Iron Center of Phenylalanine Hydroxylase. *L. M. Bloom*, S. J. Benkovic, and B. J. Gaffney. Department of Chemistry, The Pennsylvania State University, University Park, PA 16802 (L.M.B. and S.J.B.), and Department of Chemistry, Johns Hopkins University, Baltimore, MD 21218 (B.J.G.).

The iron center of phenylalanine hydroxylase (PAH) was probed by EPR and iron chelation with *o*-phenanthroline during the reductive, activating, and catalytic steps of hydroxylation. These studies are based on the EPR spectrum of the holoenzyme in which signals arising from two iron environments are observed, a half-apo form which gives only one set of EPR signals, and apoenzyme. Changes in the EPR spectra and the accessibility of iron to *o*-phenanthroline have been correlated with the steps of the reaction.

28. Inhibition of Trypsin by Organophosphinates. *C. A. Broomfield*, S. Wingertsahn, J. R. Grothusen, J. H. Clark, M. D. Green, T. M. Brown, and C. N. Lieske. U.S. Army Medical Research Institute of Chemical Defense, Aberdeen Proving Ground, MD (C.A.B., S.W., J.H.C., M.D.G., and C.N.L.), and Department of Entomology, Fisheries and Wildlife, Clemson University, Clemson, SC (J.R.G. and T.M.B.).

It is well-known that many organophosphorus compounds are strong inhibitors of the "serine" proteases and esterases, such as trypsin, chymotrypsin, elastase, and the cholinesterases. While inhibition of these enzymes by organophosphates and organophosphonates has been the subject of numerous investigations, the organophosphinates have received little attention. Presently we have studied the initial rate constants of nine 4-nitrophenyl organophosphinates with trypsin, measuring spectrophotometrically the 4-nitrophenol released. The enzymatic rate constants lie between 493 and 13170 M^{-1} min^{-1}, with no apparent relationship between base-catalyzed hydrolysis rates of the esters and their rates of reaction with trypsin. That is, a plot of log k_i vs. log k_{obsd} has a correlation coefficient of 0.77. The optical isomers of one of the inhibitors [4-nitrophenyl ethyl(phenyl)phosphinate] were separated by HPLC on a commercial (*R*)-*N*-(3,5-dinitrobenzoyl)phenylglycine chiral-phase column and then tested separately as trypsin inhibitors. The P(+) isomer had a k_i of 661 M^{-1} min^{-1} (standard deviation = 66) compared to 627 M^{-1} min^{-1} (standard deviation = 9) for the racemic mixture. The P(−) isomer was inactive. This pronounced stereospecificity differs from the phosphonylation of trypsin according to observations reported to Ooms in *Biochem. Pharmacol. 16*, 1653 (1967).

29. Facile Synthesis of $^{17}O,^{18}O$-Phosphoryl-Labeled Oligonucleotides and Two-Dimensional NMR Method for the Assignment of Deoxyribose Proton NMR Signals in d(ApGpCpT). D. O. Shah, K. Lai, M. Miyazaki, K. Taira, and *D. G. Gorenstein*. Department of Chemistry, University of Illinois at Chicago, Chicago, IL 60680.

Simple modification of the solid-phase phosphoramidite procedure for the synthesis of oligonucleotides has allowed the introduction of oxygen isotopes into the phosphoryl oxygen of the tetramer d(ApGpCpT). At each nucleotide addition cycle, oxidation of the phosphite with iodine in either H_2O enriched in ^{17}O or ^{18}O (or unenriched with normal ^{16}O) has provided the specifically labeled d(Ap(^{17}O)Gp(^{18}O)Cp(^{16}O)T. The introduction of these oxygen labels has allowed the unambiguous assignment of the three ^{31}P NMR signals, and combined with a 2-D $^{31}P/^{1}H$ chemical shift correlated NMR spectral method has provided a novel means for the ready assignment of the H5′ and H3′ protons coupled to the phosphates. ^{31}P NMR spectra of the duplex complex of this labeled tetramer with the drug actinomycin D reveals that the two resonances of the Gp(^{18}O)C units are shifted dramatically downfield. This confirms that the drug intercalates between the base-paired GpC group.

30. ^{13}C and ^{2}H NMR Spectroscopy of Transition-State Analogue Complexes of *N*-Acyl-*p*-phenylalaninals and α-Chymotrypsin. *D. O. Shah*, K. Lai, and D. G. Gorenstein. University of Illinois at Chicago, Chicago, IL 60680.

Enzymes are predicted to bind transition-state structures more tightly than the ground-state structures and hence a "transition-state analogue", a molecule that resembles the transition state should have a higher affinity for the enzyme than the substrate or product analogue structures. Evidence in support of the transition-state analogue hemiacetal structure formed between the enzyme active site and the aldehyde carbonyl has largely been indirect. However, in a proton and fluorine NMR investigation of *N*-acetyl- and *N*-benzoyl-DL-*p*-fluorophenylalaninal and *N*-acetyl-L-*p*-fluorophenylalaninal binding to α-chymotrypsin, Gorenstein & Shah (1982) provided the first direct observation of signals (fluorine) representing the hemiacetal structure and the noncovalent Michaelis

complex. We now present C-13 and H-2 spectra of these transition-state analogue complexes as additional evidence supporting the earlier ^{19}F NMR assignments.

31. New Transition State Analogue Inhibitors of Aspartate Transcarbamylase. F. C. Wedler and *G. K. Farrington.* Department of Biochemistry, The Pennsylvania State University, University Park, PA 16802.

Aspartate transcarbamylase (ATCase) catalyzes the first committed step in de novo pyrimidine biosynthesis: L-Asp + C-P → *N*-carbamyl-L-Asp + P_i. Four new potential inhibitors have been designed, synthesized, and tested with ATCase. The compounds contain a tetrahedral sulfur center in place of the carbonyl group of carbamyl phosphate so as to mimic the tetrahedral transition state of ATCase.

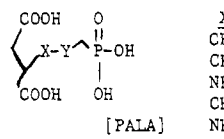

	X	Y	Ki(μM)L-isomer	r(Å)
α	CH_2	S	86	
	CH_2	S(O)	62	∼ 6.3
	NH	$S(O)_2$	55	
	CH_2	$S(O)_2$	45	
[PALA]	NH	C(O)	[.027]	∼ 5.3

Affinities of these inhibitors for ATCase (relative to PALA) correlate inversely with the overall αC to P distance (*r*). Thus, steric factors appear to override geometric (tetrahedral vs. trigonal) considerations, in agreement with the "compression" mechanism proposed by Stark [*The Enzymes*, IX (1973), part B, p 225].

32. Enzyme Generated Transition State Analogues. *Thomas I. Kalman.* Department of Medicinal Chemistry, State University of New York, Buffalo, NY 14260.

The rational design of transition state analogue inhibitors of enzymes requires detailed knowledge of the structure of transient reaction intermediates and transition states. Even when such knowledge exists, the construction of analogues with closely resembling, but chemically stable structures presents practical difficulties. In addition, analogues of intermediates on the catalytic pathway of substrate to product conversion may have limited access to the enzyme active site (small k_{on}). To circumvent these problems, the principle of suicide enzyme inactivation can be applied. Instead of unmasking a latent function group, the enzyme converts the suicide substrate into a high-affinity form resembling a transient intermediate on the reaction pathway. Due to the intrinsic reversibility of the process, temporary paralysis rather than death of the enzyme will occur. Structural features of the analogue should promote the stabilization of its enzyme-bound form. In the case of the covalent catalysis, the enzyme would generate covalently bound transition state analogues. It is recognized that many known enzyme inhibitors fall into this latter category, but have rarely been considered transition state analogues. The rationales for the design of enzyme inhibitors of this type will be discussed and examples reviewed.

33. Distribution of Reaction Intermediates on Chicken Liver Fatty Acid Synthase. *V. E. Anderson* and G. G. Hammes. Department of Chemistry, Cornell University, Ithaca, NY 14853.

The relative concentrations of different chain length intermediates on fatty acid synthase have been determined by the use of radioactive substrates. With limiting malonyl-CoA, only saturated thio esters are found with a relative abundance of 1.0, 0.51, 0.16, 0.17, 0.15, 0.01, and <0.01 for C_6, C_8, C_{10}, C_{12}, C_{14}, C_{16}, and C_{18}, respectively. The observed decrease in abundance with increasing chain length can be attributed to an increase in the rate of the elongation reaction or of the thioesterase activity with increasing chain length. The equilibrium constant for transesterification between 4′-phosphopantetheine and the essential sulfhydryl residue has been determined for enzyme without thioesterase activity. The equilibrium constant decreases monotonically from 2 for C_4 to 1 for C_{14} and dropped to 0.16 and <0.1 for C_{16} and C_{18}. Thus steric constraints on the intramolecular transesterification reaction also influence the distribution of reaction intermediates. The relative abundance of 3-keto and 3-hydroxy intermediates of varying chain lengths and of oxy and thio esters also is being determined.

34. In Vitro Effects of Nitrous Oxide on Purified Methionine Synthase. Verna Frasca, Barbara S. Stephenson, and *Rowena G. Matthews.* Department of Biological Chemistry, University of Michigan, Ann Arbor, MI 48109.

In model studies, cob(I) alamin is oxidized by nitrous oxide (N_2O) with the formation of N_2 [Blackburn, R., Kway, M., and Swallow, A. J., *J. Chem. Soc., Faraday Trans. 73*, 250–255 (1976)]. Prolonged exposure of mammals to N_2O results in loss of activity of methionine synthase (N^5-methyltetrahydrofolate:homocysteine methyltransferase), a cobalamin-dependent enzyme. We have now demonstrated that highly purified cobalamin-dependent enzymes from both *E. coli* and pig liver are irreversibly inactivated during turnover in solutions equilibrated with N_2O which contain the normal assay components, viz., methyltetrahydrofolate, homocysteine, adenosylmethionine, and a reducing system. Because the standard reducing system for in vitro assays utilizes cobalamin as a mediator, we have determined that inactivation also occurs in the absence of added cobalamin, utilizing a reducing system consisting only of dithiothreitol for the pig liver enzyme and the physiological reducing system consisting of NADPH, an NADPH-flavodoxin oxidoreductase and flavodoxin for the *E. coli* enzyme. We hypothesize that N_2O oxidizes the enzyme-bound cob(I)alamin to an inactive cob(III)alamin which is stabilized by coordination with a protein amino group.

35. Solid-State PTN NMR Studies of Penicillin Effects on *Aerococcus viridans*. *G. Edwin Wilson, Jr.*, Gary S. Jacob, and Jacob F. Schaefer. Clarkson University, Potsdam, NY 13676 (G.E.W.), and Monsanto Company, St. Louis, MO 63166 (G.S.J. and J.F.S.).

Solid-state ^{15}N NMR has emerged as an excellent tool for following the metabolism of nitrogen-containing compounds in intact cells. Solid-state techniques are particularly useful for investigating highly cross-linked matrices such as the bacterial cell wall. The effects of sublethal doses of benzylpenicillin on both the quantity and cross-link index of peptidoglycan biosynthesized by *A. viridans* have been quantitatively determined by generally applicable NMR methods. The methods will be presented, and the implications of the results on the mechanism of penicillin action on *A. viridans* will be discussed.

36. Kinetic Studies of the Hydrolytic Reactions Catalyzed by *E. coli S*-Adenosylmethionine Synthetase. *G. D. Markham.* Institute for Cancer Research, Philadelphia, PA 19111.

S-Adenosylmethionine (AdoMet) synthetase (ATP:L-methionine *S*-adenosyltransferase) catalyzes a reaction in which tripolyphosphate is formed as an intermediate but is hydrolyzed to yield P_i and PP_i before PPP_i can be released. ^{31}P NMR has been used to monitor the incorporation of ox-

ygen into P_i formed in reactions conducted in ^{18}O-enriched H_2O. P_i formed in the AdoMet synthetase reaction contains more than one oxygen from solvent; the amount of oxygen incorporation indicates that the [enzyme·AdoMet·PP_i·P_i] complex partitions equally between product dissociation and resynthesis of PPP_i. The same result is obtained for the hydrolysis of added PPP_i when AdoMet is present as activator, a reaction which has twice the V_{max} of the AdoMet synthetase reaction. Without AdoMet, PPP_i hydrolysis is ~10-fold slower, and the P_i formed contains only one oxygen from solvent; thus product release is fast compared to the rate of resynthesis of PPP_i from the [enzyme·PP_i·P_i] complex. In the enzyme-catalyzed hydrolysis of ATP to ADP and P_i, which only occurs in the absence of methionine, only one oxygen is incorporated into P_i. Single turnover experiments monitoring $^{32}P_i$ formation from [γ-^{32}P]ATP are consistent with bond cleavage being rate determining in ATP hydrolysis.

37. Studies on the Active Site of Succinyl-CoA:Tetrahydrodipicolinate *N*-Succinyltransferase. David A. Berges, *Walter E. DeWolf*, George L. Dunn, David J. Newman, Stanley J. Schmidt, and Charles Gilvarg. Departments of Natural Products, Pharmacology and Medicinal Chemistry, Smith Kline & French Laboratories, Philadelphia, PA 19101 (D.A.B., W.E.D., G.L.D., D.J.N., and S.J.S.), and Department of Biological Sciences, Princeton University, Princeton, NJ 08544 (C.G.).

Succinyl-CoA:tetrahydrodipicolinate *N*-succinyltransferase, one of the enzymes in the biosynthetic pathway for diaminopimelate in bacteria, catalyzes the conversion of tetrahydrodipicolinate to *N*-succinyl-2-amino-6-oxo-L-pimelic acid. In the course of testing compounds for inhibitory activity against this enzyme, it was discovered that both acyclic and cyclic dicarboxylic acids were inhibitory. In the acyclic series, strikingly, several of the aminodicarboxylic acids were substrates for the enzyme. In the cyclic series, which included examples from the cyclohexane, tetrahydropyran, tetrahydrothiapyran, and piperidine series, the trans isomers were more active than the cis isomers. Conclusions concerning the geometry of the active site will be discussed.

38. Role of Oligomer Formation in the Catalytic and Regulatory Functions of Carbamoyl Phosphate Synthetase. *Paul M. Anderson.* Department of Biochemistry, University of Minnesota, Duluth, Duluth, MN 55812.

Carbamoyl phosphate synthetase is subject to self-association to tetramer when ornithine (a positive effector) and phosphate are present and to dimer when phosphate and/or UMP (a negative effector) are present [Anderson, P. M., and Marvin, S. V. (1970) *Biochemistry 9*, 171–178; Powers, S. G., Meister, A., and Haschemeyer, R. H. (1980) *J. Biol. Chem. 255*, 1554–1558]. Current studies employing gel filtration chromatography have shown that the enzyme exists as monomer in the presence of UMP and/or phosphate, and also as fully active monomer in the presence of all substrates (±-ornithine, and Mg^{2+} at concentrations which are either equimolar or in excess of ATP) at concentrations which support maximal activity, when the concentration of enzyme is as low as that normally employed in kinetic assays. These results support previously reported evidence indicating that the catalytic activity and the regulatory properties of this enzyme are not directly linked to oligomer formation [Anderson, P. M. (1977) *Biochemistry 16*, 583–586].

39. Interactions of Cr(III)GDP and Cr(III)GTP Complexes with Phosphoenolpyruvate Carboxykinase. P. Kramer and T. Nowak. Department of Chemistry, University of Notre Dame, Notre Dame, IN 46556.

The tetraaquo and tetraamino bidentate Cr(III)GDP coordination complexes and the β,γ complexes of CrGTP have been synthesized and interact with P-enolpyruvate carboxykinase (PEPCK). $Cr(H_2O)_4GDP$ is a potent linear competitive inhibitor of PEPCK vs. Mn-GDP at pH 6.0 with a K_i of 30 μM. At pH above 6.0 with 3 mM Mn^{2+} hydrolysis yields free GDP and Cr. The rates of formation of free GDP were measured enzymatically with PEPCK and with pyruvate kinase and free GDP was also detected by reverse phase HPLC. The rate constant for hydrolysis at pH 6.0 in 3 mM $MnCl_2$, is estimated at 0.048 min^{-1}. Hydrolysis of $Cr(NH_3)_4GDP$ is negligible at pH 6.0. At this pH, the K_i of $Cr(NH_3)_4GDP$ is approximately 0.25 mM. $Cr(H_2O)_4GTP$ inhibits PEPCK competitively vs. MgITP with K_i = 0.59 mM at pH 6.9 in the presence of 50 μM Mn. The diastereomeric forms of Cr(III)GDP and Cr(III)GTP complexes are separable by the reverse-phase HPLC method developed by Gruys & Schuster (*Biochemistry 22*, 5055 (1983)) for CrADP complexes. It should be possible to determine the specificity of the PEPCK interaction with metal nucleotides.

40. Misonidazole and Glutathione Peroxidase Activity. *K. S. Kumar* and Joseph F. Weiss. Biochemistry Department, Armed Forces Radiobiology Research Institute, Bethesda, MD 20814.

Endogenous protective enzyme systems may have a role in the detoxification of reactive oxygen species and metabolites resulting from the generation of radiation-induced free radicals. Xenobiotics and their metabolism may affect these enzyme systems, thus modifying radiation damage. The present study concentrates on the in vitro and in vivo effects of the 2-nitroimidazole radiosensitizer misonidazole (MISO) on glutathione peroxidase (GSHPx) activity. MISO strongly inhibited GSHPx activity in mouse liver cytosol using cumene hydroperoxide as substrate. Our hour after IP injection of MISO (800 mg/kg) in mice, GSHPx activity in liver was depressed to one-half that of control values, and the depression was maintained at 2 and 3 h. GSHPx activity in spleen was depressed to 40% at 1 h only. In lung, there was a persistent decrease (20%) at all time periods studied, whereas no effect was observed in kidney. These differences may reflect the differential ability of tissues to metabolize MISO. Products formed during MISO metabolism (free radical oxygen species, reduced MISO) could inhibit GSHPx or suppress its synthesis, which may contribute to the radiosensitizing and/or toxic effects of MISO.

41. Biochemical Properties of NADH:Nitrate Reductase from *Cucurbita maxima*. Margaret G. Redinbaugh and *Wilbur H. Campbell*. Chemistry Department, State University of New York, College of Environmental Science and Forestry, Syracuse, NY 13210.

NADH:nitrate reductase (EC 1.6.6.1) was extracted from five-day-old squash cotyledons and applied to blue Sepharose. Nitrate reductase was specifically eluted by NADH in buffer containing leupeptin, PMSF, *p*-aminobenzamidine and TLCK to limit proteolytic degradation. The eluted enzyme was directly applied to a Zn–chelate column and after washing, was eluted by lowering the pH. After concentration by ammonium sulfate, enzyme was gel filtered using Bio-Gel A1.5m in a

buffer with leupeptin. Yield was 0.3 mg/kg of cotyledon, which was a 7.5% recovery. The nitrate reductase was homogeneous in one-dimensional native and SDS gels and yielded a single spot in two-dimensional gels. The native M_r was 240 kDa with a subunit of 115 kDa, which indicates a homodimeric structure. Analysis for FAD and hemin content indicated two each per native nitrate reductase. Spectra of nitrate reductase had maxima 274 and 413 nm for oxidized and 424, 527, and 556 nm for reduced with mM extinction coefficients of 245, 135, 180, 13, and 25.5, respectively. Amino acid composition and contents of Fe and Mo are being analyzed. The enzyme has also been shown to contain a Mo-pterin identical to the one from chicken liver sulfite oxidase.

42. Role of Peroxidase–IAA Oxidase Isoenzymes in the Immune System of Maple Trees. *W. C. Shortle.* USDA Forest Service, Durham, NH 03824.

The most productive plant meristem on earth is the vascular cambium of trees. Injury and infection of trees initiate an immune response which protects the cambium without which a tree cannot survive. Key features of the response are increased mitotic activity followed by anomalous differentiation of cambial derivatives into an infection resisting layer, IRL. Samples of differentiating cambial cells were taken from wounded trees during IRL formation. Nonwounded stems of clonal material served as controls. Homogenates were assayed for peroxidase and IAA oxidase activity. Isoenzymes were separated by high-resolution isoelectric focusing in pH gradients on polyacrylamide gel slabs. Results indicated a flux in cathodic isoenzymes during the growing season. These isoenzymes appeared to be initially suppressed in wounded trees, followed by a brief period of strong activity. Changes in the cathodic isoenzymes may alter IAA levels causing anomalous cambial growth and differentiation as part of the immune response.

43. Hydrogen Exchange of Human Erythrocyte Spectrin and Band 3. *E. S. Benson*, B. E. Hallaway, S. A. Booth, J. A. Norman, and A. Rosenberg. University of Minnesota, Minneapolis, MN 55455.

The shape of the red blood cell is largely controlled by the membrane cytosketal proteins, site of interaction with hemoglobin. We have studied the dynamic conformational properties of these two proteins using hydrogen exchange kinetics and varying temperature, pH, and ionic strength. Comparing spectrin to proteins of similar high helical content, it is not as tightly folded as myoglobin, but it has regions that are more rigid than tropomyosin, a rodlike protein. Temperature dependence of exchange shows activation energies considerably higher than those of lysozyme and several other globular proteins. Similar studies of the cytoplasmic fragment of band 3 protein indicate that this protein has a very rigid, nonfluctuating core similar to that of carbonic anhydrase. The exchange properties of this segment are not affected by hemoglobin binding. These results will be discussed in relationship to the proposed models of structural behavior of these two proteins.

44. Studies on Mammalian Glycinamide Ribonucleotide Transformylase. *Carol A. Caperelli.* Department of Chemistry, New York University, New York, NY 10003.

Glycinamide ribonucleotide transformylase (EC 2.1.2.2), the first folate dependent enzyme in the pathway of de novo purine biosynthesis, has been purified 1500-fold from the murine lymphoma cell line L5178Y. The purification was achieved through the application of two folate-analogue affinity chromatographic procedures, one of which featured biospecific elution of the desired enzymatic activity. The mammalian enzyme is a monomer of M_r 110000 and the initial velocity studies indicate that the kinetic mechanism for this enzyme is sequential. Although the natural cofactor for the transformylation reaction is L-(−)-10-formyltetrahydrofolate, the enzyme efficiently uses the folate analogue, 10-formyl-5,8-dideazafolate, as an alternate cofactor, while the 10-acetyl-5,8-dideazafolate is a potent competitive inhibitor against 10-formyl-5,8-dideazafolate. The isolation and characterization of this important enzyme, which may be a target for some of the antifolates, should contribute to our understanding of de novo purine biosynthesis and its relationship to folare cofactor metabolism.

45. Covalent Cross-Linking of the Active Site Subunit of Bovine Heart Mitochondrial NADH → Ubiquinone Reductase. J. A. Gondal, B. Chambers, and *W. M. Anderson.* Northwest Center for Medical Education, Indiana University School of Medicine, Gary, IN 46408.

Bovine heart mitochondrial NADH → ubiquinone reductase (complex I) was cross-linked with the following reagents: dithiobis(succinimidyl propionate) (DSP), 3,3′-dithiobis(sulfosuccinimidyl propionate) (DTSSP, a water soluble derivative of DSP), and dimethyl 3,3′-dithiobis(propionimidate) dihydrochloride (DTBP). All three reagents cross-linked complex I in a time and concentration dependent manner with the following order of effectiveness: DSP > DTBP > DTSSP. Direct evidence of cross-linking of the 53 kDa FMN containing active site subunit by DSP and DTBP was shown by disappearance of this polypeptide band from SDS–polyacrylamide gels. Indirect evidence of cross-linking of this subunit includes (a) inhibition of enzymatic activity, (b) quenching of FMN fluorescence in the cross-linked complex, and (c) decrease of FMN absorbance at 410 nm in the cross-linked complex. NADH (150 μM) partially protects the 53 kDa subunit from cross-linking by DSP and DTBP. Kinetics of enzyme inhibition upon cross-linking with DSP or DTBP revealed distinct patterns depending upon the artificial electron acceptor used, suggesting that dissimilar mechanisms for electron transfer are utilized by different acceptors.

46. Inhibition of Soybean Lipoxygenase 1 by Phenylhydrazine and Related Molecules. Morton J. Gibian and *Kuldip Singh.* Department of Chemistry, Seton Hall University, South Orange, NJ 07079.

It had earlier been reported that a series of hydrazones showed varying degrees of inhibition toward soybean and other lipoxygenases and that neither the ketone nor hydrazine themselves were inhibitory. Desiring to examine the nature of these inhibitions, several preliminary experiments along with appropriate controls were carried out in this laboratory. Contrary to the prior report, it was found that phenylhydrazine at less than micromolar level is an extremely potent time-dependent irreversible inhibitor of soybean lipoxygenase 1. Among a rather wide variety of related molecules which were tested, phenylhydrazine, *p*-nitrophenylhydrazine, and acetophenone phenylhydrazone are the most potent inhibitors (second-order deactivation rate constants are approximately 8, 44, and 0.5×10^6 M^{-1} min^{-1}). Neither hydrazine itself nor 2,4-dinitrophenylhydrazine exhibit significant inhibition. Several hydroxylamines, benzenediazonium salts, and hydroxamic acids are much weaker irreversible inhibitors. The

inactivation by phenylhydrazine is strongly (probably absolutely) O_2 dependent.

47. A Microradiometric Assay for the Determination of Salivary Cholinesterase. *N. F. Dalessandro*, R. A. Miller, and A. C. Ibay. U.S. Army Institute of Dental Research, Walter Reed Army Medical Center, Washington, DC 20307.

The amount of saliva required by available techniques for the determination of salivary cholinesterase ranges from 0.5 to 2.0 mL. This often requires analyzing pooled samples. The micro radiometric assay permits the analysis of 20 μL of whole, parotid or extra-parotid saliva and measures the amount of tritiated acetic acid hydrolyzed from the tritiated acetylcholine substrate by salivary cholinesterase. The saliva and tritiated acetylcholine were allowed to react in an appropriate buffer for a few minutes. The reaction was then quenched with a stop solution and mixed with a volume of scintillation cocktail. By radiometrically measuring the amount of tritiated acetate, the amount of acetylcholinesterase can be calculated based on the turnover rate. The method was validated by comparing the results from human saliva, which ranged from 0.29 to 1.37 units/L, to the results from methods cited in the literature.

48. A Modification of the Technicon Autoanalyzer System for Monitoring Peptide Uptake. *Peter J. McCarthy*, David J. Newman, and Louis J. Nisbet. Department of Natural Products Pharmacology, Smith Kline & French Laboratories, Philadelphia, PA 19101.

Studies involving alterations in the extracellular concentration of amine-containing substrates are enhanced by the use of a continuous monitoring system. A readily available system for continuous analysis is the Technicon Autoanalyzer. This paper will describe modifications of this system in conjunction with the fluorescamine method of amine assay for use in microbial transport studies. Particular emphasis will be placed upon peptide uptake by *Candida albicans* and the advantages of this novel system in studying the energization and kinetics of transport. Other potential uses of the monitoring system will be indicated.

49. Predicted Secondary Structure of Cholera Toxin A-Subunit: Functional Areas Defined by Helical Regions. *L. K. Duffy*, A. Kurosky, and C.-Y. Lai. Harvard Medical School, Boston, MA, University of Texas Medical Branch, Galveston, TX, and Roche Institute of Molecular Biology, Nutley, NJ.

The NAD-glycohydrolase and ADP-ribosyltransferase activities of cholera toxin reside on its A-subunit. The A-subunit is also noncovalently bound to a β_5-subunit to make up the intact toxin. Using the method of Chou and Fasman ((1978) *Annu. Rev. Biochem. 47*, 251) we found that the predicted secondary structure consists of approximately 35% β-structure and 15% α-helix. The major β-sheet region consists of six strands in the amino-terminal half of the molecule (residues 33–106). The β-sheet domain leads into the active site domain which is characterized by alternating β-sheets and α-helix. This $\beta\ \alpha\ \beta\ \alpha$ type structure has been found in other NAD binding proteins. In addition, two regions (residues 14–18 and 200–214) are α-helical and are located in areas of the A-subunit which have been implicated by both chemical modification studies and monoclonal antibody binding to be sites of interaction with the β_5-subunit (Kurosky et al. (1982) *Fed. Proc. 41*, 6548).

50. Temperature Dependence of the Circular Dichroism Spectra of β_2-Microglobulins. *Eleanor M. Brown* and Merton L. Groves. Eastern Regional Research Center, ARS, U.S. Department of Agriculture, Philadelphia, PA 19118.

β_2-Microglobulin (β_2-m) is a small highly conserved protein, related to both the immune and histocompatibility antigen systems. Spectral properties of β_2-m from different species are generally similar, but there are significant differences in the circular dichroism (CD) spectrum with changes in temperature. At pH 6, and 25 °C, the near-ultraviolet CD spectra of cow, goat, and human β_2-m consist of maxima at 293 and 286 nm and a minimum near the base line, centered at 275 nm. At 5 °C the spectrum of human β_2-m remains unchanged, while the spectra of the cow and goat β_2-m contain the 293-nm maximum and a stronger negative band at 275 nm with the 286-nm band becoming an inflection point between these peaks. Examination of the sequences of these proteins suggests the presence of conformational changes in the environment of tyrosine, tryptophan, and cystine residues caused by proline isomerization. The observed conformational changes in cow and goat β_2-m could be due to cis–trans isomerization of Pro-Pro sequences at residues 4–5, 14–15, and 32–33 where only single proline residues are found in human β_2-m.

51. The Role of Phosphate Compounds on the Transfer of In-111 and Ga-67 from Transferrin (TF) to Horse Ferritin (FE). *R. E. Weiner*. Department of Diagnostic Radiology, University of Kansas Medical Center, Kansas City, KS 66103.

A variety of compounds found intracellularly stimulate in vitro the transfer of the radiopharmaceutical, Ga-67, from TF to FE. To further investigate this transfer phenomena the movement of In-111 from TF to FE and the influence of ATP and pyrophosphate (PP_i) on the TF nuclide complexes have been examined. A two chamber dialysis system, ion exchange or gel chromatography, distinguished between TF, FE, and nonprotein bound radionuclide. There was little transfer of In-111 from TF to FE without mediators. Upon the addition of ATP or ascorbate (1 mM each) significant transfer to FE occurred. At equilibrium the distribution percent with ATP was TF = 15, FE = 84, and free = 1, which was similar to that observed with Ga-67 transfer. However the equilibrium time was significantly longer for In-111. This difference in equilibrium time was partially related to the rate of binding to FE. Also, when ATP or PP_i was added to a TF*Ga-67 solution the percent of bound Ga-67 rapidly decreased. In contrast, the addition of ATP to TF*In-111 caused no decrease in TF bound In-111. These results suggest that the comparatively rapid translocation of Ga-67 from TF to FE in the presence of ATP is dependent on the ability of this compound to cause the dissolution of the TF*Ga-67 complex.

52. Fluorescence Investigation of Polymer-Bound Alcohol Dehydrogenase. *S. L. Haynie*. AT&T Bell Laboratories, Murray Hill, NJ 07974.

Chemical modification of an enzyme by covalent attachment to a synthetic polymer usually results in some loss in catalytic activity. The observed change in activity may be directly linked to a change in one or more catalytic parameters, e.g., substrate specificity, binding constants, or pH profile. In most detailed investigations of immobilized systems, the catalytic parameters are well characterized, however, structural questions are rarely directly addressed. In this investigation, we have examined the conformation of immobilized yeast and horse-liver alcohol dehydrogenases using fluorescence tech-

niques. The enzymes are covalently bound to a soluble acrylamide copolymer (poly(acrylamide-*co*-N-acryloxysuccinimide), PAN) and to the cross-linked gel of PAN. The intrinsic fluorescence from the tryptophan residues of the alcohol dehydrogenases in monitored using steady-state and lifetime fluorescence measurements. The spectral characteristics of the polymer-bound enzymes will be compared with those of the native proteins. We will discuss the consequences of the enzyme modification reaction in relation to the conformational integrity and the overall activity of the enzyme.

53. Equilibrium and Kinetic Studies of the Nature of Metal-Ion Binding in Parvalbumin. *Erich K. Hild*, Patrick J. Breen, Kenneth A. Johnson, and William DeW. Horrocks, Jr. The Pennsylvania State University, 152 Davey Laboratory, University Park, PA 16802.

Parvalbumin is a small (MW ~12000) calcium-binding protein containing two primary metal-binding sites. In this study tripositive lanthanide ions have been used as probes of the structure, thermodynamics, and kinetics of metal-ion binding to a tryptophan-containing parvalbumin isotype from codfish. The change in the UV absorption spectrum of tryptophan in parvalbumin (centered at 290 nm), in going from the apo form to fully bound, was monitored as a function of the amount of metal ion added. In addition, the change in the tryptophan emission spectrum, centered near 320 nm, was studied. Rate constants for the dissociation of these metal ions from parvalbumin were measured using the change in tryptophan emission at 340 nm (λ_{ex} = 280 nm) as the metal ion chelator DCTA was mixed with the metal-loaded protein in a stopped-flow spectrophotometer. Tryptophan sensitized Tb(III) luminescence at 545 nm was also utilized to monitor metal ion exchange or removal from parvalbumin. Energy transfer between neodymium and terbium ions bound at the two sites in parvalbumin was quantitated by measuring the luminescence lifetime of terbium in varying ratios with neodymium. From this, estimates of relative occupation of the two sites were obtained.

54. NMR Studies of the Phosphoribosyl Pyrophosphate–Yeast Orotate Phosphoribosyltransferase Complexation. *D. B. Syed*, R. S. Strauss, L. Mayer, and D. L. Sloan. Department of Chemistry, City College of CUNY, New York, NY 10031.

Kinetic analysis suggests that divalent metal ion complexes of phosphoribosyl pyrophosphate (PRibPP) and yeast orotate phosphoribosyltransferase (OPRTase) interact to form a phosphoribosyl-enzyme intermediate, which then catalyzes the conversion of orotate to orotidylate (Victor, J., Leo-Mensah, A., and Sloan, D. L. (1979) *Biochemistry 18*, 3597–3604). The structures of metal ion–PRibPP complexes bound to OPRTase and free in solution have been examined from NMR measurements of the longitudinal relaxation rates ($1/T$) of the six PRibPP protons at 220 and 400 MHz. Metal ions, Mg(II), Mn(II), Co(II), Cr(III), and Rh(III) were employed in studies of the solution PRibPP conformation. The calculated paramagnetic ion–proton distances suggest direct binding of metal to the pyrophosphate group. In the presence of OPRTase, these absolute and relative PRibPP $1/T$ values do not change until metal ions are also added to the solution. Calculated Mn(II)–proton distances for enzyme-bound PRibPP suggest a more open conformation for this substrate on the OPRTase active site. The CUNY-NMR facility (400 MHz) and the Rockefeller University NMR facility (220 MHz) were utilized in these studies.

55. ^{207}Pb NMR Characterization of Pb Complexes Containing Oxygen, Nitrogen, and Sulfur Ligands. *E. K. Jaffe*. Biochemistry Department, Thomas Jefferson University, Philadelphia, PA 19107.

Although Pb(II) is widely accepted as a biological toxin, and some Pb(II) complexes have been characterized by ^{207}Pb NMR [Nakashima, T. T., and Rabenstein, D. L. (1983) *J. Magn. Res. 51*, 223–232], this NMR probe has not yet been applied to biological samples. Therefore, in order to determine the practicability of using ^{207}Pb ($I = {}^1/_2$, 22% n.a.) as a biochemical probe, the chemical shifts, line widths, and relaxation times of Pb(II) complexes with oxygen, nitrogen, and sulfur ligands have been determined. The chemical shift range from $Pb(NO_3)_2$ to $Pb(DTT)_2$ is 5500 ppm. Like ^{113}Cd, there is a general trend that chemical shifts caused by oxygen ligands < nitrogen ligands < sulfur ligands. The Pb(II) complexes of ATP, imidazole, EDTA, ENTMP, DTT, and mercaptoethanol all have T_1 values from 0.04 to 0.1 s and T_2 values less than 0.015 s, thus making data aquisition on dilute (biological) samples practicable. All observed ^{207}Pb resonances shift downfield upon heating, with magnitudes as large as 1 ppm/°C.

56. Nitrogen-15 NMR Evidence for a Hydrogen Bond between Histidine and Serine in the Catalytic Triad of Serine Proteases and for Protein Conformational Changes in the Catalytic Mechanism. *W. W. Bachovchin*. Department of Biochemistry and Pharmacology, Tufts University School of Medicine, Boston, MA 02111.

Nitrogen-15 NMR results have been obtained which indicate that a rather strong hydrogen bond links the histidine and serine residues of the catalytic triad of α-lytic protease in the resting enzyme in solution. This result is at odds with current interpretations of the X-ray diffraction data of α-lytic protease [Brayer, G. D., Delbaere, L. T. D., & James, M. N. G. (1979) *J. Mol. Biol. 131*, 743] and other serine proteases [Kraut, J. (1977) *Annu. Rev. Biochem. 46*, 331; Steitz, T. A., & Shulman, R. G. (1982) *Annu. Rev. Biophys. Bioeng. 11*, 419] which now indicate that the serine and histidine residues are too far apart (3.2 to 3.7°) and not properly aligned for the formation of a hydrogen bond. Nitrogen-15 NMR results have been obtained which demonstrate that protonation of the histidine imidazole ring triggers the disruption of the aspartic acid, histidine hydrogen bond when the enzyme is complexed to inhibitors which are tetrahedral intermediated analogues. These results suggest that the enzyme may function in a more dynamic manner than previously thought by undergoing specific conformational changes in response to specific events at the active site.

57. Temperature Dependence of the Longitudinal Relaxation and Exchange Rates of Amide Protons in Peptide Substrates of Protein Kinase. *P. R. Rosevear*, D. C. Fry, and A. S. Mildvan. Johns Hopkins Medical School, Baltimore, MD 21205.

The longitudinal relaxation rates ($1/T_{1,app}$) of the amide protons of two peptide substrates for protein kinase, Arg-Arg-Ala-Ser-Leu and Leu-Arg-Ala-Ser-Leu-Gly, were measured as a function of temperature. Exchange rates of these protons with water ($1/\tau_{ex,H_2O}$) were also measured, using the saturation-transfer technique. At all temperatures, $1/T_{1,app}$ was found to be the sum of two components: $1/\tau_{ex,H_2O}$ and $1/T_1$, the intrinsic relaxation rate. The NH protons of carboxy-terminal residues exchanged >10-fold slower than

those of internal residues, and this behavior was duplicated by the NH protons of *N*-acetylserine and *N*-acetylserine amide respectively. A 50-fold variation of the exchange rates at 25 °C was detected among the internal residues. While the $\Delta H^{\ddagger}$ values ranged from 16 to 19 kcal/mol, differences in rates of exchange were due primarily to unequal entropy barriers. The NH_2 protons of *N*-acetylserine amide exchanged both with water and with each other. For these protons, $1/T_{1,app}$ could be adequately described as the sum of three components: $1/T_1$; $1/\tau_{ex,H_2O}$; and $1/\tau_{ex,NH_2}$, the rate of cross-exchange. Despite the various exchange rates of the amide protons, all exhibited similar changes in chemical shift with temperature.

58. Measurement of Absolute Interproton Distances by Frequency-Dependent Nuclear Overhauser Effects: Conformation of Bound MgATP on Adenylate Kinase and on a Peptide Fragment of the Enzyme. *D. C. Fry*, S. A. Kuby, and A. S. Mildvan. Johns Hopkins Medical School, Baltimore MD 21205, and University of Utah Research Park, Salt Lake City, UT 84108.

The MgATP binding sites of rabbit muscle adenylate kinase and a synthetic peptide (residues 1–45) which binds MgATP with comparable affinity (Hamada et al. *A.B.B. 195*, 155) were studied by NMR. Interproton NOEs in peptide-bound MgATP measured at 250 and 500 MHz were used to calculate correlation times and absolute interproton distances. The conformation-insensitive H1′ to H2′ distance obtained (3.1 Å), is within the range found in molecular models (2.9 ± 0.2 Å). Using this standard, distances determined for enzyme-bound MgATP at 250 MHz agreed with those found for peptide-bound MgATP, except that from H5′ to H8. On both peptide and enzyme, the conformation of MgATP was 3′-endo, with $\chi = 65 \pm 20°$. With the enzyme, intermolecular NOEs indicated proximity (≤4 Å) of H8, H2, and H1′ to methyl and methylene groups of Leu, Ile, Val, and/or Thr residues, and possibly a His C2H. With the peptide, a similar pattern was seen; however, no NOEs were seen to H1′, nor from His C2H. A model of the peptide, based on the X-ray structure of the enzyme (Sachsenheimer and Schulz, *J.M.B. 114*, 37), accommodates MgATP in a manner consistent with all of the NOE data, and successfully incorporates distances to Cr^{3+} obtained using the paramagnetic analogue Cr^{3+}ATP.

59. Kinetic and Magnetic Resonance Studies of the Interaction of a Spin-Labeled Substrate Analogue with Δ^5-3-Ketosteroid Isomerase (KSI). *Athan Kuliopulos*, Paul Talalay, and Albert S. Mildvan. Johns Hopkins Medical School, Baltimore, MD 21205.

KSI from *Pseudomonas testosteroni* is a dimeric enzyme (MW 27 000) which converts Δ^5-androstene-3,17-dione (I) to

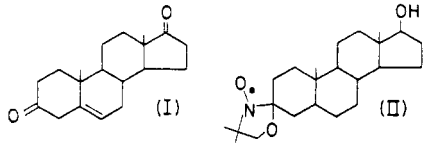

its Δ^4 derivative by a proton transfer mechanism (*The Enzymes 6*, 591). The spin-labeled substrate analogue, 3-doxyl-17β-hydroxy-5α-androstane (II), is a linear competitive inhibitor of the enzyme ($K_i = 25 \pm 5$ μM). Binding studies of II, by EPR and by paramagnetic effects on the longitudinal relaxation rate ($1/T_{1p}$) of water protons, revealed 0.7 ± 0.2 binding sites/monomer and a K_D of 43 ± 20 μM comparable to the K_i. The binding of II to KSI resulted in a peak to peak broadening of the EPR spectrum of II to 59 ± 1 G, and a 6 ± 1-fold enhancement of its effect on $1/T_{1p}$, indicating a highly immobilized nitroxide portion of II which remains accessible to water protons. Both of these effects were removed upon displacing II, either with the product (4-androstene-3,17-dione) or with 19-nortestosterone, a potent competitive inhibitor.

60. New Models for the Investigation of Chromophore–Protein Interactions (Opsin Shifts) in Rhodopsin and Bacteriorhodopsin. *G. D. Mateescu* and M. Iqbal. Department of Chemistry, Case Western Reserve University, Cleveland, OH 44106.

We report the first NMR results obtained with visual chromophore models which mimic the combined wavelength regulation function of the quaternary (Schiff base) nitrogen and a functional (carboxylic) group capable of placing a negative charge in the proximity of the retinylidene chain. The inductive effect of the positively charged nitrogen in **1** and **2**

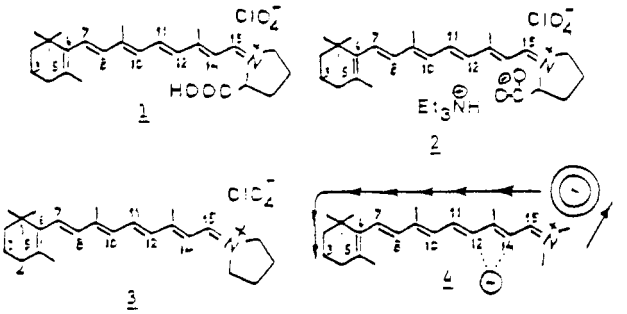

and the field effect of the negatively charged carboxylate ion in **2** can be observed, particularly when using retinylpyrrolidiniminium perchlorate **3** as reference. The results will be interpreted in terms of bond polarization, charge delocalization, counterion, and external charge (**4**) effects on the chemical shifts of key carbon atoms such as 4, 5, 6, 12, 13, 14, and 15. Solvent effects will also be discussed. An attempt to correlate trends in NMR and UV-vis spectra will be made.

61. Evidence for a Second Allosteric Binding Site for Inositol Hexaphosphate on Human Hemoglobin. *W. N. Poillon* and Bak C. Kim. Howard University Center for Sickle Cell Disease, Washington, DC 20059.

The solubility profile (c_{sat} vs. effector/Hb molar ratio) observed for deoxy-Hb S in the presence of inositol hexaphosphate (IHP) is composed of three distinct regions: (1) one of negative slope in the molar ratio range 0–1, (2) one of positive slope in the range 1–2, and (3) one of zero slope in the range 2–3. This behavior suggests the presence of a second binding site for IHP (zone 2) that is separate and distinct from the DPG binding cleft between the β chains (zone 1). In companion O_2 affinity experiments we were able to show that in the presence of the drug ethacrynic acid (ECA), which has been shown by others (Kennedy et al. (1984) *J. Med. Chem. 27*, 103) to raise the O_2 affinity of Hb A and to bind in the central cavity between the α chains (Abraham et al. (1983) *PNAS 80*, 324), the allosteric effect of IHP (lowering of the O_2 affinity) is abolished. Moreover, in the presence of ECA the decreased solubility evoked by IHP in zone 1 is partially eliminated, while the increased solubility exhibited in zone 2 is left intact. Thus it appears, that the allosteric effects of IHP and ECA are exerted independently of each other, which means they cannot both be binding at the same site. We suggest the existence of a second allosteric binding site for IHP on the Hb molecule, which is the same as the binding site for ECA.

62. Evidence That Microwaves Stimulate the Autoxidation of Hemoglobin To Produce Superoxide Anion. *R. P. Liburdy* and R. G. Positano. Institute of Environmental Medicine, New York University Medical Center, New York, NY 10016.

Autoxidation of hemoglobin (HbO_2) occurs spontaneously in vivo with 3% of HbO_2 converted to methemoglobin (MetHb) and superoxide anion (O_2^-) daily. Superoxide dismutase (SOD) is present in the erythrocyte to reduce O_2^- to H_2O_2, and catalase further reduces H_2O_2 to H_2O and O_2. We report that when 20 mM bovine HbO_2 in buffered saline (pH 7.4, 37 °C) is exposed to 2450 MHz (CW) microwave radiation for 30 min at 37 °C a reduction in absorbance occurs at 430 nm, characteristic of the HbO_2 to MetHb conversion ($\Delta\epsilon = 4.2 \times 10^4$ M^{-1} cm^{-1}). No change in absorbance is detected at isosbestic wavelengths of 475 and 525 nm, or at 430 nm for sham exposed samples at 37 °C. The microwave effect is dependent on absorbed power (3–60 mW/g) and on the presence of oxygen. In addition, the microwave effect is not observed during exposures conducted in the presence of SOD (10 μg/mL). These results provide evidence that microwaves stimulate the production of O_2^- from HbO_2.

63. Effect of Environmental Parameters on the Folding of the α Subunit of Tryptophan Synthase. *Mark R. Hurle* and C. Robert Matthews. Department of Chemistry, The Pennsylvania State University, University Park, PA 16802.

The urea-induced unfolding of the α subunit of tryptophan synthase from *E. coli* has been analyzed for the dependence of the equilibrium constant and time constants on temperature, viscosity, pH, and ionic strength. The activation energy for the single observed kinetic phase in unfolding, which has been attributed to dissociation of two stable domains, is 4.8 ± 0.1 kcal mol^{-1} and the activation entropy is −47 ± 2 cal deg^{-1} mol^{-1}. The negative value for the entropy suggests that solvent is being ordered around hydrophobic groups buried at the interface between domains in the folded protein. 20% sucrose (w/w) increases the stability of the protein by about 1 kcal mol^{-1}, but *decreases* the time constant of refolding, the opposite effect of what might be expected from simple considerations of viscosity. Ionic strength and pH studies show small effects on stability but no dramatic effects on the kinetics of folding. These results may be explained by a model for the domain association reaction in which the two folded domains are in close proximity and associate by a mechanism which is not sensitive to bulk solution properties.

64. The Influence of Single-Site Replacements on the Folding and Stability of Dihydrofolate Reductase from *E. coli*. C. R. Matthews, *K. M. Perry*, and N. A. Touchette. Department of Chemistry, The Pennsylvania State University, University Park, PA 16802.

The urea-induced unfolding of three isozymes of dihydrofolate reductase (DHFR) has been monitored by UV difference spectroscopy. Two of the enzymes differ only by the amino acid at position 28, whereby Leu is replaced by Arg. The third enzyme is a single site mutant of the Arg-28 form, where Lys replaces Glu at position 139. The equilibrium unfolding transition of all three forms is consistent with a two-state model. Differences in stability and cooperativity have been observed. The Arg-28 DHFR exhibits 2.0 kcal mol^{-1} greater stability than the Leu-28 enzyme at 15 °C while the Lys-139 form is 5.0 kcal mol^{-1} less stable than the Glu-139–Arg-28 reductase at 15 °C. The 2.0 kcal mol^{-1} enhancement may be related to an ionic interaction between Asp-27 and Arg-28 that is not present in the Leu form. Crystal structure data suggest that the destabilization demonstrated by the Lys-139 mutant may be attributed, in part, to the disruption of a salt bridge between Glu-139 and His-141. Kinetic studies of the folding of these isozymes have shown differences that are consistent with those found in the equilibrium studies and provide a more refined view of the way in which the amino acid replacements alter the energetics of the transition.

65. Charge Effects of Single Amino Acid Substitution in the Folding of Tryptophan Synthase α Subunit. *Neil Tweedy*, Mark Crisanti, and C. R. Matthews. Department of Chemistry, The Pennsylvania State University, University Park, PA 16802.

An individual amino acid side chain can play a crucial role in the folding and stability of a globular protein. The urea induced unfolding of two variants of the α subunit of *E. coli* tryptophan synthase with amino acid replacements at position 211 has been studied to determine the role of this residue in folding and to elucidate the proposed mechanism of folding (Matthews et al. (1983) *Biochemistry 22*, 1445). The Gly-211 → Glu substitution causes a small increase in stability and 10-fold reduction in the rate of the urea dependent unfolding reaction. In contrast, the Gly-211 → Arg substitution decreases the stability and gives a >10-fold increase in the corresponding rate. The opposing effects from side chains of opposite charge clearly demonstrate the importance of an electrostatic interaction at this position in the folding of the mutants. Unfolding studies on the the Gly-211 → Arg protein also reveal the presence of a urea independent slow phase in addition to the previously observed urea dependent phase. These results confirm the folding model and demonstrate the utility of the mutants in refining kinetic models of folding.

66. Light Scattering Labels of DNA: Resonance Enhancement from Bound Dyes. *David A. Knoll* and Victor Bloomfield. Department of Biochemistry, University of Minnesota, St. Paul, MN 55108.

According to resonance enhancement (RE) theory (Stanton, S. G., et al. (1981) *J. Chem. Phys. 75* (12), 5615), one can expect large increases in both the polarized and depolarized components of the scattered light when the wavelength of the incident light is near a strong absorption band in the scattering molecule. We have been investigating the feasibility of using resonance enhancement from bound chromophores as a means of specifically labeling macromolecules. We have chosen the dye proflavine (PF) since it has (1) strong, well-characterized binding to DNA, and (2) a strong absorption band (λ_{max} = 454 nm) which is near the 488-nm line of our Ar^+ laser. Using φ29 DNA (MW = 11.5 M) and one PF bound every 2.3 base pair, we have obtained over a 50-fold enhancement in the polarized sacttering. Thus far, we have not observed enhancement of the depolarized component. Over a range of DNA concentrations from 0.06 to 2 mg/mL, the amount of enhancement decreased with decreasing PF/DNA ratio, as expected. Extension of these studies to other dyes and wavelengths will be presented. We anticipate that the RE technique will be useful in studying the scattering of DNA at low concentration.

67. Δ^1-Piperidine-2-carboxylate Reductase of Rat Brain and Liver. *Y. F. Chang*. Department of Biochemistry, University of Maryland Dental School, Baltimore, MD 21201.

The enzyme responsible for reducing Δ^1-piperidine-2-carboxylic acid (P2C) to L-pipecolic acid, P2C reductase, was partly purified from rat brain and liver. The enzyme reaction requires NADH as a coenzyme in stoichiometric quantity. P2C reductase has an optimal pH of 6.2 and is quite stable at 4 or −20 °C in 0.005 mM K-PO_4 buffer, pH 6.2. Preliminary analysis of enzyme kinetics indicates that the brain but not the liver enzyme is inhibited by high P2C concentration (>0.1 mM) which can be overcome by increasing NADH concentration. At 0.045 mM NADH, the K_m and V_{max} values for the brain and liver enzyme are 0.013 and 0.026 mM, and 0.043 and 0.014 mmol min^{-1} mg^{-1}, respectively. Both the brain and the liver enzymes are, however, inhibited by high NADH concentration (>0.04 mM). At 0.5 mM P2C, the K_m and V_{max} values for the brain and the liver enzymes are 0.010 and 0.018 mM, and 0.033 and 0.034 mmol min^{-1} mg^{-1}, respectively. Since L-pipecolic acid is a major product of L-lysine metabolism in the brain and is believed to have a relation with the γ-aminobutyric acid (GABA) neurotransmission, P2C reductase may have a role in brain function.

68. 2-[(4-Bromo-2,3-dioxobutyl)thio]-1,N^6-ethenoadenosine 2′,5′-Diphosphate: A New Affinity Label for $NADP^+$-Binding Enzymes. *Jerome M. Bailey* and Roberta F. Colman. Chemistry Department, University of Delaware, Newark, DE 19716.

A new reactive fluorescent adenine nucleotide has been synthesized: 2-[(4-bromo-2,3-dioxobutyl)thio]-1,N^6-ethenoadenosine 2′,5′-diphosphate (BDB-TϵADP). Starting with $NADP^+$, 2′-phosphoadenosine 5′-diphosphoribose (PADPR) was generated enzymatically and was converted to 2′-phospho-1,N^6-ethenoadenosine 5′-diphosphoribose (ϵPADPR) by reaction with chloroacetaldehyde. Treatment with NaOH, followed by reaction with CS_2 yielded 2-thio-1,N^6-ethenoadenosine 2′,5′-diphosphate (TϵADP). The final product was generated by reaction of TϵADP with 1,4-dibromobutanedione. The structure of BDB-TΔADP was determined by UV, fluorescence, ^1H, and ^{13}C NMR spectroscopy as well as by bromide and phosphorus analysis. BDB-TϵADP inactivates $NADP^+$-specific isocitrate dehydrogenase of pig heart. The dependence of the inactivation rate on [BDB-TϵADP] exhibits saturation kinetics. Protection against inactivation is provided by $NADP^+$, NADPH, PADPR, and adenosine 2′,5′-diphosphate, but not by NAD^+ or Mn isocitrate. These results suggest that BDB-TϵADP acts as an affinity label of the coenzyme binding site of $NADP^+$-specific isocitrate dehydrogenase and that it may have general applicability as an affinity label of $NADP^+$ sites in enzymes.

69. Effect of Single Amino Acid Replacements on the Thermodynamics of the Reactive Site Peptide Bond Hydrolysis in Ovomucoid Third Domains. *Wojciech Ardelt* and Michael Laskowski, Jr. Department of Chemistry, Purdue University, West Lafayette, IN 47907.

It was well accepted that the equilibrium constants, $K_{hyd}°$, for the hydrolysis of the reactive site peptide bonds in protein proteinase inhibitors are all of the order of unity. The inhibitors on which this generalization was based belong to several nonhomologous families. Therefore, after finding that turkey ovomucoid third domain has K_{hyd} of 0.97 (Ardelt, W., & Laskowski, M., Jr. (1983) *Acta Biochim. Polon. 30*, 115–126), we expected that all other avian ovomucoid third domains will show closely similar values. We were therefore surprised to find that, of 20 third domains surveyed at pH 6, K_{hyd} (we believe this is probably $K_{hyd}°$) varies from 0.4 for Japanese quail to 25 for chicken. We are in the process of examining as many of the 53 different sequenced avian third domains as possible. Equilibrium is approached from both directions at pH 6 in reactions catalyzed by aspergillopeptidase B or *S. griseus* proteinase B. Aliquots are analyzed by anion-exchange (Mono Q) chromatography at pH 9 and monitored at 206 nm. We expect to develop a sequence to K_{hyd} algorithm from the sequence of the ovomucoid third domain.

70. The Binding of Substrates and Effectors to Yeast and Rabbit Muscle Pyruvate Kinase. Charles E. Brown, Jacqueline M. Taylor, Mary C. Portis, and *Lai-Man Chan.* Department of Chemistry, Jackson State University, Jackson, MS 39217.

The interactions of fructose 1,6-diphosphate (FDP), phosphoenolpyruvate, ADP, and ATP with pyruvate kinase from yeast and muscle have been studied utilizing the quenching of protein fluorescence at 330 nm (excited at 295 nm) by these ligands. The major difference between the muscle and the yeast enzyme is their interaction with FDP. FDP binds to the muscle enzyme with an apparent dissociation constant of 8.5 mM and a Hill coefficient of 1.0; the binding is independent of pH. On the other hand, FDP binds to the yeast enzyme with an apparent dissociation constant of 2×10^{-9} M and a Hill coefficient of 2.0 at pH 6.5; the affinity decreases sharply as the pH increases.

71. The Inhibition of Elastases and Chymotrypsin by Gossypol. *M. Philipp*, H. James, S. Maripuri, and A. Cohen. Lehman College and Graduate Center, City University of New York, Bronx, NY 10468 (M.P. and S.M.), and University of Texas Health Center at Tyler, Tyler, TX 75710 (H.J. and A.C.).

We have studied the inhibition of human neutrophil elastase, procine pancreatic elastase, and bovine chymotrypsin by gossypol. Gossypol is a compound of interest since it has been shown to act as a male contraceptive in human trials. The compound is also capable of inhibiting various other enzyme systems. Its mechanism of action as a contraceptive is under active investigation. We have found that gossypol's dissociation constants range from 0.7 μM for chymotrypsin to 1 μM for pancreatic elastase and 6 μM for neutrophil elastase. In the case of neutrophil elastase, gossypol's inhibition constants are pH dependent, with better inhibition at pH values below 7. The implications of the pH profile and the shifts in the gossypol absorbance spectrum on binding will be discussed.

72. Metallocene Inhibition of Type I Procollagen *N*-Proteinase. *Kenneth E. Dombrowski*, Darwin J. Prockop, and John E. Sheats. Department of Biochemistry, UMDNJ-Rutgers Medical School, Piscataway, NJ 08854 (K.E.D. and D.J.P.), and Department of Chemistry, Rider College, Lawrenceville, NJ 08648 (J.E.S.).

Metallocenes are a class of organometallic compounds which have the generalized structure of a transition metal in the 2+ valence state "sandwiched" between two cyclopentadiene (cp) rings. A series of derivatives of ferrocent (Fc) (I) and cobaltocene (II) were shown here to selectively inhibit type I procollagen *N*-proteinase, the enzyme responsible for cleaving the NH_2-terminal propeptide from type I procollagen. The K_i appears to be dependent upon the degree of modification of the cp rings. In an assay using [^{14}C]procollagen as a substrate the mono- and dicarboxylic acid derivatives of I and II inhibited the enzyme with K_i's in the range of 300–400 μM,

$FcCH_2CH_2COOH$ (K_i = 3000 μM) (III), FcCH=CHCOOH (K_i = 500–1000 μM) (IV), and $FcC(O)CH_2CH_2COOH$ (K_i = 10–50 μM) (V). The monocarboxylic acid derivative of I showed no inhibitory activity with either mammalian or bacterial collagenases nor thermolysin at concentrations less than 4 mM. Ferrocinium chloride was equally effective as V. Effects due to Fe^{3+} were ruled out since this ion did not inhibit *N*-proteinase at concentrations less than 500 μM.

73. The Uncoupling of Rat Liver Mitochondria by Coumarin Derivatives. Mark A. Valentini and *Leo A. Miller*. Department of Chemistry, San Francisco State University, San Francisco, CA 94132.

The mitochondrial uncoupling activity of the coumarin derivative β-methyl umbelliferone (BMU) was ascertained by means of four parameters and compared to that of 2,4-dinitrophenol (DNP) under similar conditions. In the presence of BMU and DNP, P:O ratios were decreased, ATPase activity was increased, respiratory control ratio (RCR) values were increased, and passive swelling was increased. DNP exerted its uncoupling effect at lower concentrations per mg of mitochondrial protein compared with BMU. The BMU analogues 7-hydroxycoumarin (7-HC) and 4-methyldaphnetin (4-MDAPH) exhibited uncoupler activity using ATPase and RCR assays. The BMU analogues 4-methyl-5,7-dihydroxycoumarin (4-MDC) and 4-hydroxycoumarin (4-HC) showed no uncoupler activity. However, 4-HC inhibited increased O_2 uptake produced by BMU and 4-MDAPH while 4-MDC inhibited the DNP mediated increased in O_2 uptake. The inhibition of BMU, 4-MDAPH, and DNP uncoupling by analogues of BMU having little or no uncoupling activity per se indicates the possible existence of mitochondrial membrane sites to which coumarin derivatives can bind and dissipate the high-energy gradient thus producing uncoupling.

74. Abstract withdrawn.

75. Tuftsin, a Natural Phagocyte Activator. Isolation of Its Receptor. Nancy J. Bump and *Victor A. Najjar*. Protein Chemistry, Tufts University School of Medicine, Boston, MA 02111.

Tuftsin, Thr-Lys-Pro-Arg, a natural activator of known functions of phagocytic cells, binds to specific receptors on rabbit peritoneal neutrophils and mouse macrophages with a K_d of 0.61–0.85 $\times$ 10^{-7} M for neutrophils and 50000 receptors per cell. Scatchard plots indicated the presence of one type of receptor. The receptor from rabbit neutrophils was isolated in pure form as follows: cell membranes were prepared and dissolved in 8 mM CHAPS and fractionated on an affinity column to which was bound covalently the pentapeptide tuftsin analogue, Thr-Lys-Pro-Pro-Arg. The analogue binds tuftsin receptor with an affinity 4× that of tuftsin. The column was washed 3× with ammonium acetate in CHAPS, pH 5, and 3× with ammonium carbonate in CHAPS, pH 8. The receptor was then eluted with 1 mM pentapeptide analogue in CHAPS. Adsorption of the eluate on Dowex 50 removed all traces of the pentapeptide. SDS–PAGE yielded an apparent M_r of 480–520K. Similar determination on Sephadex G200 showed an apparent M_r of 450–550K.

76. Proteolytic Dissection of the Human Erythrocyte Glucose Transport Protein. *R. Leslie Shelton, Jr.*, and *Robert G. Langdon*. Department of Biochemistry, University of Virginia School of Medicine, Charlottesville, VA 22908.

The functions of the various domains of the 100000-dalton erythrocyte glucose transporter were probed by limited proteolytic dissection. Removal of the cytoplasmic domain from the carrier, either in the native membrane or after reconstitution into pure lipid vesicles, inactivates it. The resulting inactive peptide has electrophoretic properties reminiscent of the 55000-dalton protein that was isolated by other groups and proposed to be the native glucose transporter, but which we demonstrated to be a partially active proteolytic fragment of the true carrier. Chymotryptic digestion limited to the exoplasmic region cleaves the transporter into complementary intrinsic peptides of 55000 and 38000 daltons; the larger one alone is capable of saturable transport when reconstituted into phospholipid vesicles, although sensitivity to the inhibitor phloretin requires the presence of the smaller one as well. The functional organization of the transporter suggested by these results will be discussed.

77. Mammalian Metabolism of the Trichothecene Mycotoxin Diacetoxyscirpenol (Anguidine). *Michael A. Marletta* and Joanne Recchia. Department of Nutrition and Food Science, M.I.T., Cambridge, MA 02139.

The trichothecenes are a group of naturally occurring sesquiterpenoids produced by various fungi and have been implicated in animal and human mycotoxicoses. In vitro incubations with rat liver microsomes (control, phenobarbital (PB) and β-naphthoflavone (BNF) induced) produced three major products resulting from hydrolysis of the ester bonds. The metabolites were characterized by HPLC and GC–MS. DAS was a noncompetitive inhibitor of ethoxyresorufin deethylation in BNF microsomes but had no effect on benzphetamine demethylation in PB microsomes. Using [^{3}H]DAS, no products were produced with the glutathione *S*-transferases or microsomal epoxide hydrolase. BNF microsomes in the presence of uridinediphosphoglucuronic acid and [^{3}H]DAS generate a glucuronide which has been isolated by HPLC. The glucuronide is resistant to hydrolysis by β-glucuronidase. Structure proof of this product is under way. Preliminary in vivo experiments with rats indicate that many of the in vitro generated metabolites are also produced in vivo.

78. Ether-Knobbed Fatty Acids Lengthen the *Neurospora* Circadian Period. J. C. Callaway and *Daniell L. Mattern*. Chemistry Department, University of Mississippi, University, MS 38677.

9- and 10-alkoxystearic acids with alkoxy groups of varying size were synthesized by solvomercuration of oleic acid esters. These "knobbed" fatty acids were used to supplement a *Neurospora* strain carrying the *cel* mutation, which confers a partial fatty acid deficiency. It was expected that the supplemental fatty acids would be incorporated into the *Neurospora* membranes as the acyl groups of phospholipids, thereby fluidizing the membranes as unsaturated or short-chain fatty acyl groups do. Unsaturated or short-chain fatty acids are known to dramatically lengthen the circadian period of spore formation (conidiation) in *cel* strains. A similar dramatic lengthening was obtained with the ether-knobbed supplements. However, the change in period did not correlate with the size of the knob. Further, analysis of total lipids by gas chromatography gave no evidence that the knobbed supplements were incorporated intact into *Neurosproa* membranes, even though they were depleted from the medium.

79. Preparation of Farnesyl Pyrophosphate Synthetase by Affinity Chromatography. *Desiree L. Bartlett*, Richard H.

S. King, and C. Dale Poulter. Department of Chemistry, University of Utah, Salt Lake City, UT 84112.

Farnesyl pyrophosphate synthetase (EC 2.5.1.1), the prenyl transferase of sterol biosynthesis, produces a key intermediate in the isoprenoid pathway. An affinity column for farnesyl pyrophosphate synthetase based on a nonreactive substrate analogue of geranyl pyrophosphate has been synthesized. Farnesyl pyrophosphate synthetase from ammonium sulfate precipitates of avian liver and yeast homogenates has been purified 460–600-fold with recoveries of enzyme activity from the affinity column of 60–90%. The procedure permits the enzyme to be purified to homogenity from crude preparations rapidly and in a single affinity step. The derivatized gel is stable and a single packed column has been used repeatedly for eight months without detectable degradation.

80. Glycoside and Diazoketone Photoresponsive Reagents for Neuraminidases. *S. W. Tanenbaum*, V. Kumar, M. Sharma, K. Rasmussen, and M. Flashner. SUNY College of Environmental Science & Forestry, Syracuse, NY 13210.

Little is known at the molecular level about catalyses promoted by neuraminidases (sialidases). We now describe two series of affinity reagents for identifying active site regions. The first consists of ketosides of AcNeu in which the aglycones possess intrinsic reactivity, exemplified by AcNeu-α-2′,2′,2′-trichloroethyl, AcNeu-α-*o*-nitrobenzyl, AcNew-α-2′,3′-epoxypropyl, and AcNew-α-propargyl glycosides. In the second, transition-state intermediates based upon "2,3-dehydro-AcNeu", such as 5-acetamido-2,6-anhydro-3,5-dideoxy-D-glycero-D-galactonon-2-en-1-diazoketone (DAK) and its 4-epimer were made. The syntheses of these substrate analogues will be detailed. Photoinactivations of a model enzyme obtained from an *Arthrobacter* isolate with 10^{-4} M each of the trichloroethyl and *o*-nitrobenzyl glycosides, as well as with the two DAK's and "4-keto-2,3-dehydroAcNeu", were time dependent. Nullification of these reactions by 10^{-4} M 2,3-dehydroAcNeu methyl ester provided evidence for their specificity. These ligands should prove applicable toward elucidation of enzyme mechanisms and as probes for the study of neuraminidase comparative biochemisty.

81. Proteins of the Milk Fat Globule Membrane: Isolation of Major Components by Preparative Electrophoresis and Comparison of Amino Acid Compositions. *Jay J. Basch*, Rae Greenberg, and Harold M. Farrell, Jr. Eastern Regional Research Center, ARS, U.S. Department of Agriculture, Philadelphia, PA 19118.

Fat globule membranes (MFGM) of milk are derived from the apical plasma membrane secretory cells. Six methods of preparation of MFGM suggested by various authors were tested by the use of discontinuous SDS–gel electrophoresis. Four major bands, which stain for protein and carbohydrate were present independent of the method of preparation. The apparent molecular weights of these proteins as determined by SDS gels (15% T) were 142000, 64000, 49000, and 46000, respectively. After delipidation and salt (NaCl) fractionation, five major protein bands were isolated from preparative slab gels by use of an electrophoretic concentrator. Amino acid compositions were obtained and compared with each other. The 142K band is composed of the salt soluble xanthine oxidase and an insoluble glycoprotein. The latter protein is closely related by amino acid composition to the 64K band and to the salt insoluble 49K and 46K glycoproteins. This suggests that either these fractions form a closely related family of membrane glycoproteins or that they are proteolytic fragments of each other.

82. Effect of Differentiation Inducing Agents on Plasminogen Activator (PA) Secretion. *M. D. Prager*, S. C. Dacus, and N. F. Nelson. University of Texas Health Science Center, Dallas, TX 75235.

PA, which is secreted by many malignant cells, may contribute to their invasive and metastatic potential. PA secretion into serumless medium by human renal carcinoma (hRC: Cur and Caki) and murine B16 melanoma (F10 and BL6) cell lines was determined by degradation of [^{3}H]acetylcasein in the absence and presence of added plasminogen. In each case plasminogen increased the rate of degradation, consistent with plasmin generation. The hRC cells secrete both urokinase and tissue type PA as indicated by (1) chromatography on Con A–Sepharose and (2) binding to fibrin. Both types were characterized by multiple MW components. Part of the PA secreted by B16 was in an inactive form which could be activated by trypsin. After halting tryptic action with Tyrasylol, increased PA activity was observed by measuring hydrolysis of pyroGlu-Gly-Arg *p*-nitroanalide. Dimethyl sulfoxide (1%) markedly inhibited PA secretion by all cell lines, an effect shown to be reversible for Cur cells. Retinoic acid (1 μM) inhibited secretion by B16, and butyrate (2 mM) inhibited secretion by hRC cells. Morphologic changes accompanied the altered PA secretion by Cur cells, but it remains to be ascertained whether this represents a more highly differentiated state.

83. Partial Sequence of the Heavy and Light Chains of *botulinum* Neurotoxin Type E. V. Sathyamoorthy and *B. R. DasGupta*. Food Research Institute, University of Wisconsin, Madison, WI 53706.

Mild trypsinization of botulinum neurotoxin (NT) type E, produced by *Clostridium botulinum*, results in over 100× increase in toxicity and cleavage of the single-chain molecule (M_r 150000) to a dichain form (M_r 150000) (*Biochem. Biophys. Res. Commun. 48*, 108, 1972). The light (M_r 50000) and heavy chains (M_r 100000) of the dichain NT, held together by –S–S– bond(s), were separated and purified by ion-exchange chromatography in the presence of DTT and urea. The purified chains were carboxymethylated and placed in an automatic gas phase sequencer (Applied Biosystems Model 470A). The PTH derivatives were identified using reverse-phase HPLC (IBM instruments LC/9533 and CS9000). The following partial sequences were obtained: light chain, Pro·Lys·Ile·Asn·Ser·Phe·Asn·Tyr·Asn·Asp·Pro·Val·Asn; heavy chain, Lys·Lys·Ile·Cys·Ile·Glu. The partial sequences of the L chain and the N terminal of the single-chain NT (not trypsinized; *Fed. Proc. 42*, 1811, 1983) match; hence we prove that (i) the light-chain region constitutes the amino-terminal end of the single-chain NT prior to its cleavage by trypsin and (ii) the site of this cleavage is one-third the distance from N to C terminal.

84. Physicochemical Properties of Isocitrate Dehydrogenase from Lactating Bovine Mammary Gland: Effects of Metal Substrate. *V. L. Seery*, T. F. Kumosinski, and H. M. Farrell, Jr. Eastern Regional Research Center, Philadelphia, PA 19118.

The cytosolic form of isocitrate dehydrogenase is a major source of the NADPH required for fatty acid synthesis in lactating bovine mammary gland. The purified enzyme ex-

hibits a distinct lag time in stopped-flow kinetic experiments that can be eliminated by preincubating the enzyme with its metal–substrate complex. The physicochemical basis for this phenomenon was investigated. Analytical ultracentrifugation showed that the enzyme behaves as a rapidly reequilibrating monomer–dimer system whose aggregation properties are only slightly influenced by the presence of the metal–substrate complex. Circular dichroism (CD) spectra in the far-UV indicate a moderate content of α-helix which is unchanged by the presence of isocitrate and Mn^{2+}. The CD spectrum in the chromophoric region exhibits three main features: a positive peak at 292 nm, a negative trough at 280 nm with a shoulder at about 276 nm, and a broad positive band centered at about 262 nm. Upon addition of metal–substrate, the trough is abolished and the broad band at 262 nm is partially resolved into two components. These changes observed in the chromophoric region of the CD spectrum may reflect a subtle conformation change related to activation of the enzyme by its metal–substrate complex.

85. Distal Histidine-Mediated Effects on Hemoglobin-Bound Carbon Monoxide. *William H. Fuchsman*, Anna Huttenlocher, Joseph D. Varley, and Phillip C. Liu. Chemistry Department, Oberlin College, Oberlin, OH 44074.

Acidification increases the C–O stretching frequency (ν_{CO}) of CO bound to hemoglobin (Hb) and leghemoglobin (Lb). Soybean LbCO is affected the same way by low pH and the presence of Zn(II). Human HbCO is affected the same way by low pH and the presence of Zn(II), Cd(II), Co(II), Ni(II), or Pb(II). Bloodworm (*Glycera dibranchiata*) monomeric HbCO is not affected by either low pH or the presence of Zn(II). Soybean Lb and human Hb, but not bloodworm Hb, contain a distal histidine in each heme pocket. Therefore, pH and metal ion effects appear to be mediated by changes in distal histidine-bound CO interactions. Literature data, together with ν_{CO} of bloodworm monomeric HbCO, suggest that ν_{CO}'s above 1956 cm^{-1} characterize hemoglobins which lack distal histidines. However, lamprey (*Petromyzon marinus*) HbCO exhibits two ν_{CO}'s above 1956 cm^{-1} even through it has a distal histidine. Relative ν_{CO} band intensities of lamprey HbCO are dependent upon pH and Zn(II) concentration. Therefore, sensitivity of ν_{CO} to pH and certain metal ions is a better indicator of the presence of a distal histidine than is the value of ν_{CO}.

86. Detection and Purification of Cytochromes P-450 in Animal Tissues with Monoclonal Antibodies. *K. C. Cheng*, F. K. Friedman, B. J. Song, S. S. Park, and H. V. Gelboin. National Cancer Institute, Bethesda, MD 20205.

Monoclonal antibody (MAb) based radioimmunoassay (RIA) and immunopurification procedures were used to probe the immunochemical relatedness of cytochromes P-450 in tissues from different species. RIAs based on MAbs 1-7-1 and 1-31-2, both to the major 3-methylcholanthrene (MC) induced rat liver microsomal cytochrome P-450, detected antigenically related forms of cytochrome P-450 in liver microsomes from MC-induced rats, C57BL/6 and DBA/2 mice, hamsters, and guinea pigs; and in lung and kidney microsomes of MC-induced rats. Immunoaffinity-purified cytochromes P-450 of different molecular weights were obtained from the microsomal fraction of the following tissues from MC-treated animals: liver of rats (56K and 57K), liver of C57BL/6 mice (56 K and 57K), liver of DBA/2 mice (57K), liver of hamsters (57K), liver of guinea pigs (53K), and lung of rats (57K). Studies are in progress to determine the degree of structural homology among these purified cytochromes P-450.

87. Monoclonal Antibody-Based Immunopurification of Cytochrome P-450. *R. C. Robinson*, F. K. Friedman, S. S. Park, and H. V. Gelboin. National Cancer Institute, Bethesda, MD 20205.

Several cytochromes P-450 have been isolated from rat liver microsomes by immunoaffinity purification with Sepharose-bound monoclonal antibodies (MAbs) to 3-methylcholanthrene (MC) and phenobarbital (PB) induced rat liver cytochrome P-450. The immunoadsorbents bound cytochromes P-450 from livers of MC- and PB-treated rats, but not from untreated rats. The purified species therefore represent induced cytochromes P-450. The purified isozymes were characterized by spectral and electrophoretic analyses, and with respect to catalytic activities. Immunopurifications based on different MAbs not only provide purified cytochromes P-450 for subsequent analyses but also serve to classify the individual isozymes on the basis of MAb-specific epitope content.

88. Detergent Solubilization in the Study of Acetylcholine Receptor/Lipid Associations. *J. M. Gonzalez-Ros*, M. Llanillo, A. Paraschos, J. A. Ferragut, and M. Martinez-Carrion. Department of Biochemistry, Virginia Commonwealth University, Richmond, VA 23298.

Acetylcholine receptor (AcChR) is an optimal system for the study of lipid–protein interactions. Lipids surrounding integral proteins within the bilayer may act as modulator of the functionality of membrane-bound proteins. In the AcChR, the importance of the lipid environment on the properties of the former has also been suggested through reconstitution experiments, enzymatic action of phospholipases, etc. Partial solubilization of AcChR-rich membranes with the nonionic detergent octyl β-D-glucoside (OG) has been carried out in an attempt to cosolubilize intimately related lipid with the receptor. Treatment of membranes with increasing OG concentrations was followed by sucrose gradient centrifugation in order to fractionate the solubilized components. The samples were analyzed by polyacrylamide gels in the presence of SDS and α-bungarotoxin binding (as indicative of AcChR protein) and lipid composition for each fraction was determined. Thermodynamic transitions of the membrane protein accompanying the solubilization process were monitored by differential scanning calorimetry. Lipid–protein relationships are discussed in terms of preferential lipid cosolubilization with AcChR.

89. Biosynthesis of Deoxycoformycin (Pentostatin) by *Streptomyces antibioticus*. *J. C. Hanvey*, E. Smal, D. C. Baker, and R. J. Suhadolnik. Temple University School of Medicine, Philadelphia, PA, and University of Alabama, Tuscaloosa, AL.

The carbon–nitrogen skeleton of deoxycoformycin (I) is derived from a purine nucleoside and carbon-1 of D-ribose.

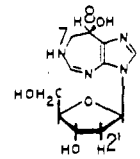

DEOXYCOFORMYCIN (I)

The six-membered pyrimidine ring of the purine is expanded to the seven-membered 1,3-diazepine ring by a novel reaction in which the anomeric carbon of D-ribose serves as a one-carbon donor for carbon-7 of deoxycoformycin. The tetra-

hydrofolate/one-carbon pool is not involved in this one-carbon addition. The mechanism of the ring expansion and its possible relationship to histidine biosynthesis has been investigated. The addition of [6-^{18}O]inosine to *S. antibioticus* cultures resulted in no incorporation of ^{18}O into the C-8 of deoxycoformycin, indicating that inosine is not the direct precursor of deoxycoformycin. Further, the reduction of carbon-2′ with the possibility of coformycin as an intermediate in deoxycoformycin biosynthesis has been explored.

90. Effect of Plumbous and Ferric Ions on (2′–5′) and (3′–5′) Oligoadenylates and Inosinates. Alice George, Pete Draganac, and *W. R. Farkas*. Department of Environmental Practice, University of Tennessee, College of Veterinary Medicine, Knoxville, TN 37901-1071.

Cells treated with interferon produce a 2′,5′-oligoadenylate (oligo-A). Experiments were conducted to determine if this oligo-A is degraded by Pb^{2+} at physiological pH and temperature as was previously shown for tRNA. The degradation of oligonucleotides was monitored by reverse-phase high-performance liquid chromatography. A number of metals were incubated with the oligo-A "cores", (2′–5′) ApApA and (3′–5′) ApApA, and several, including Pb^{2+} and Fe^{3+} were found to degrade both oligonucleotides. The fact that Fe^{3+} degraded oligo-A is surprising since Fe^{3+} does not degrade tRNA and at physiological pH does not exist in solution but is present as a colloidal suspension. The degradation by both Pb^{2+} and Fe^{3+} was found to proceed via a cyclic intermediate at 85 °C but no cyclic intermediate was detected at 37 °C. The corresponding oligoadenylates phosphorylated at the 5′ end, 2′ pApApA and 2′ pppApApA, were degraded by Pb^{2+} at a much greater rate than the core compound. Triinosinic acid, both (2′–5′) IpIpI and (3′–5′) IpIpI were degraded by Pb^{2+}. Fe^{3+} also degraded the inosinic acid trimers but at a slower rate then Pb^{2+}.

91. Structure and Synthesis of the Crown Gall Tumor Metabolite Histopine. *Hans Aaron Bates*, Alka Kaushal, and Ping-Nan Deng. Department of Chemistry, State University of New York at Stony Brook, Stony Brook, NY 11794.

Histopine (**1**) is an unusual metabolite produced by dicotyledonous host plants infected with the crown gall tumor-producing bacterium *Agrobacterium tumefaciens*. The

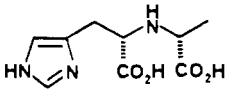

1

structure of histopine, including the absolute configuration at both chiral centers, has been elucidated by synthesis from optically active starting materials. Synthetic histopine is able to serve as the sole source of carbon and nitrogen for the bacterium *A. tumefaciens*.

92. L-Homoserine, L-Canaline, and L-Canavanine Derivatives for Biological Studies. A. J. Ozinskas and G. A. Rosenthal. T. H. Morgan School of Biological Sciences, University of Kentucky, Lexington, KY 40506.

L-Canavanine and L-canaline are highly toxic nonprotein amino acids synthesized by higher plants. These natural products have proven outstanding model compounds for a variety of biological, biochemical, and toxicological investigations. Homoserine, serine, and methionine analogues were investigated as starting materials leading to site-specific isotopic labeling of canavanine and canaline and their related metabolic derivatives. The various chemical strategies developed for the isotopic synthesis of these nonprotein amino acids, predicted upon synthesis of amino acid hydroxamates and lactones, are considered. These efforts have resulted in development of chemical methods for the production of cycloserine, canaline, and canavanine derivatives.

93. Modification of Membrane Lipid Classes and Activity of Cytochrome P-448 in Liver Rough and Smooth Microsomes by Dietary Trans Fatty Acids. *Mary G. Enig*, Joseph Sampugna, and Mark Keeney. Department of Chemistry, University of Maryland, College Park, MD 20742.

The activity of mixed-function oxygenase cytochrome P-450-448 is found in both the rough and smooth microsomes and is reported to be affected by the membrane lipid composition, e.g., phosphatidylcholine (PC), phosphatidylserine (PS), phosphatidylinositol (PI), phosphatidylethanolamine (PE), sphingomyelin (SPH), free fatty acids (FFA), cholesterol (C), and triglycerides (TG). Rough (RM) and smooth (SM-I, SM-II) microsomes isolated from C57B16J male mice fed a control diet (10% fat w/w) or an experimental diet (10% fat w/w containing 25% trans fatty acids from margarine) were examined for major changes in distribution of lipid classes. Relative to controls, liver microsomes isolated from animals on the experimental diet showed the following: decreased PC, PS, PE, SPH and increased FFA, C, TG in RM; decreased PE and increased FFA, C in SM-I; decreased PE, FFA, C and increased SPH, PI, TG in SM-II. Increased specific activity of cytochrome P-448 in the experimental group as measured by ethoxyresorufin O-deethylation appeared to be related to decreases in SPH, PC, PS, PI and increases in C, TG.

94. Guanidinoacetate Methyltransferase Activity in Tissues and Cultured Cells. *Marie M. Daly*. Department of Biochemistry, Albert Einstein College of Medicine, Bronx, NY 10461.

S-Adenosylmethionine:guanidinoacetate *N*-methyltransferase, the enzyme catalyzing the last step in creatine biosynthesis, has been thought to have a restricted, species-specific organ distribution, but we found that this enzyme is more widespread than previously reported. Activity was demonstrated in 100000*g* supernatants prepared from cultured cells (H4AzC2 hepatoma, N4TG1 neuroblastoma, and IMR-90 fibroblasts) and rat skeletal and cardiac muscle tissues. Activity was highest in the hepatoma, but tissues and cells of nonhepatic origin had 5–20% of the activity of rat liver. [1,2-^{14}C]Guanidinoacetate, added to culture medium in physiological concentrations, was converted to creatine by intact monolayers of fibroblasts and neuroblastoma cells at rates approaching V_{max}. Those cells also have the capacity to take up creatine provided in the culture medium. Comparison of the amount of creatine synthesized with the amount that could have been taken up under the same conditions showed that endogenous synthesis can make a significant contribution to intracellular pools of creatine + phosphocreatine.

95. Xenobiotic Metabolizing Enzymes in English Sole from Puget Sound. *Tracy K. Collier* and Usha Varanasi. NOAA, NMFS, NWAFC, Seattle, WA 98112.

English sole (*Parophrys vetulus*) which live in polluted marine environments have been shown to develop hepatic neoplasia. Hepatic glutathione *S*-transferase (GST) and epoxide hydrolase (EH), two xenobiotic metabolizing enzymes

which are linked with hepatocarcinogenesis in mammals, have been measured in female sole from both polluted and reference areas of Puget Sound, WA. GST activity in the 100000*g* supernatant was assayed spectrophotometrically with chlorodinitrobenzene as the substrate, and microsomal EH was measured with [^{3}H]styrene oxide as the substrate. Assays were linear with time and protein concentration. It was found that GST levels were 600% higher in fish from a polluted area (360 ± 62 nmol·mg^{-1}·min^{-1}) as compared to those from a reference area (52 ± 22 nmol·mg^{-1}·min^{-1}), but EH activity was not significantly different (2.9 ± 0.4 and 1.9 ± 0.6 nmol·min^{-1}·mg^{-1} in fish from polluted and reference areas, respectively). EH, but not GST, was shown to be higher in males than in females for fish from the reference area (p <0.01). The relationship between activities of these enzymes and the exposure of English sole to pollutants will be discussed.

96. Identification of a Critical Interaction That Determines Productive Substrate Binding to Pancreatic Ribonuclease A. *R. P. Carty*, C. F. Hummel, and M. R. Pincus. Department of Biochemistry, SUNY, Downstate Medical Center, Brooklyn, NY 11203 (R.P.C. and C.F.H.), and Department of Pathology, Columbia College of Physicians & Surgeons, New York, NY 10032 (M.R.P.).

Five bromoacetamidopyrimidine nucleosides were synthesized and used as affinity labels for RNase A. Analysis of the alkylation products and inactivation kinetics reveals the existence of a critical interaction necessary for proper orientation of 3′,5′-phosphodiester substrates of the enzyme. All nucleoside derivatives show saturation kinetics. 2′-Bromoacetamido-2′-deoxyuridine, 2′-BAMUrd (K_m = 0.11 M, k_3 = 0.0058 s^{-1}), 2′-bromoacetamido-2′-deoxyxylofuranosyluracil, 2′-BAMxylU (K_m = 0.18 M, k_3 = 0.17 s^{-1}), 3′-bromoacetamido-3′-deoxyarabinofuranosyluracil, 3′-BAMaraU (K_m = 0.04 M, k_3 = 0.00066 s^{-1}), and 3′-bromoacetamido-3′-deoxythymidine, 3′-BAMT (K_m = 0.094 M, k_3 = 0.00027 s^{-1}) show exclusive or preferential reactivity for N-3 of His-12. 3′-Bromoacetamido-3′-deoxyuridine, 3′-BAMUrd (K_m = 0.06 M, k_3 = 0.00033 s^{-1}) reacts only with His-119, preferentially at N-1. The greater reactivity of 2′-derivatives with His-12 indicates that the imidazole ring of this residue lies close to the 2′-OH group of nucleotide substrates. Absence of the "down" 2′-OH group in 3′-BAMT and 3′-BAMaraU allows the 3′-bromoacetamido group to react with N-3 of His-12. When the 2′-OH is "down" as in 3′-BAMUrd and 3′,5′-dinucleoside phosphates, it interacts strongly with His-12 and positions 3′-substituents close to His-119, a condition required for catalysis. The 30-fold greater alkylation rate of 2′-BAMxylU over 2′-BAMUrd indicates that the "down" 3′-OH group interacts with His-12; however, this interaction does not align 2′-substituents near His-119 and accounts for the failure of 2′,5′-dinucleoside phosphates to act as substrates.

Tuesday Morning—Pfizer Award Symposium in Honor of Robert Tjian—D. Koshland, Symposium Chairman

97. Mechanisms for Increased Sensitivity in Regulatory Control. *D. E. Koshland, Jr.* Department of Biochemistry, University of California, Berkeley, CA 94720.

Regulatory systems show many elements and thus it seems logical that some of the devices shown to exist in metabolic pathways will apply to developmental gene expression. In particular, high sensitivity to control should be as important in gene expression as in the acceleration and shutting down of metabolic pathways. Two new mechanisms for achieving high sensitivity have recently been described. One of these, "zero order ultrasensitivity", can give sensitivity equivalent to allosteric enzymes during reversible phosphorylation of a protein. A second mechanism, "branchpoint ultrasensitivity", can give equivalent sensitivity if the competing enzymes at the branchpoint have appropriate kinetic constants. The evidence for these mechanisms and then application to pathway control and gene expression will be discussed.

98. Regulation of Transcriptional Enhancement by Glucocorticoid Receptor Protein. *K. R. Yamamoto.* Department of Biochemistry and Biophysics, University of California, San Francisco, San Francisco, CA 94143.

Glucocorticoid receptor, complexed with cognate steroid ligands, selectively stimulates transcription initiation at the single promoter on mammary tumor virus (MTV) DNA in cultured mammalian cells. Purified receptor binds with high affinity to multiple widely separated regions within MTV DNA in vitro. DNA fragments containing a specific binding region were fused to the intact HSV thymidine kinase promoter, which is not normally hormonally regulated; subsequent DNA transfections revealed that the binding region acts in vivo as a receptor-dependent transcriptional enhancer element; i.e., it confers hormone responsiveness upon a heterologous promoter, functioning in cis in both orientations and at many positions relative to the promoter. A discrete region of altered genome structure, detected by its hypersensitivity to DNase I cleavage in isolated nuclei, forms over this same region with a time course, that parallels hormonal stimulation of transcription initiation. Thus, specific receptor–DNA interactions may alter the configuration of DNA or chromatin, thereby creating an active transcriptional enhancer.

99. Transcriptional Control Signals of the Herpes Simplex Virus Thymidine Kinase Gene. *Steven McKnight*, Stephen Eisenberg, and Barbara Graves. Basic Sciences Division, Fred Hutchinson Cancer Research Center, Seattle, WA 98104.

Transcriptional expression of the herpes simplex virus thymidine kinase (tk) gene is modulated by the interaction of cellular transcription factors with DNA sequence signals located "upstream" of the tk gene. We have studied these transcription signals by creating specific mutations and assaying their effects by one of several expression assays. Three discrete transcription signals occur within a 100 base pair domain that flanks the tk mRNA start site. One such signal, termed the "proximal signal" is located between 16 and 32 base pairs "upstream" of the start site. This region houses the "TATA homology" of the tk gene. Two additional signals are located "upstream" of the "TATA homology": these are termed the "distal transcription signals". Each of the "distal signals" contains a G/C-rich hexanucleotide sequence. Analyses of single point mutations in the hexanucleotide repeats indicate that these components of the "distal signals" are functionally homologous. However, the "distal signal" that is located farthest from the tk gene exhibits properties that distinguish it as a "stronger" transcription signal. We have developed a model for distal signal function that may account for the disparate properties of the two distal signals that predicts the use of two cellular transcription factors.

100. The Molecular Biology of Papilloma Viruses. *M. Botchan*, M. Lusky, L. Berg, K. Singh, and J. Reynolds.

Abstract not available at time of publication.

101. Positive and Negative Regulation of Transcription by Binding of Sp1 and T Antigen to the SV40 Early Promoter Region. *R. Tjian.* Department of Biochemistry, University of California, Berkeley, CA 94720.

The temporally regulated synthesis of SV40 early messenger RNA is thought to depend both on positive transcription factors from the host cell and negative control elements encoded by the virus. We have developed an in vitro transcription system comprised of isolated cellular transcription components and viral regulatory proteins that mimic the regulation expression of SV40 early RNA in vivo. Fractionation of cell extracts reveals at least two fractions in addition to RNA polymerase II that are required for accurate in vitro transcription of the SV40 early promoter. One of these factors, Sp1, is a promoter-specific component that discriminates between different RNA polymerase II promoters. Transcription of promoter mutants and DNAse footprinting reveals that Sp1 specifically recognizes and binds to the 21 bp tandem repeats located in the upstream control region of the SV40 early promoter. By contrast, the product of the viral A gene, large T antigen, acts as a specific repressor of early transcription by binding to tandem recognition sites located downstream of the SV40 early promoter region. Analysis of T antigen binding site mutants both in vivo and in vitro indicate that efficient repression of transcription occurs only when both sites I and II are occupied.

Tuesday Afternoon—Eli Lilly Award Symposium in Honor of David Goeddel—M. Sporn, Symposium Chairman

102. Transforming Growth Factors from Human, Bovine, and Murine Sources: Their Chemistry and Biology. *Michael B. Sporn,* Mario A. Anzano, Richard K. Assoian, Joseph E. De Larco, Charles A. Frolik, Anita B. Roberts, and Lalage M. Wakefield. National Cancer Institute, Bethesda, MD 20205.

Transforming growth factors (TGFs) are peptides defined by their ability to induce anchorage-independent growth in nonneoplastic indicator cells that ordinarily will not growth in soft agar. They have been found in many tissues, both neoplastic and nonneoplastic, of human, bovine, and murine origin. Two different peptides must be present to cause nonneoplastic NRK cells to grow in soft agar, a type α TGF, which binds to the receptor for epidermal growth factor (EGF), and a type β TGF, which does not bind to the EGF receptor, but binds to its own receptor. TGF-β controls the synthesis and down-regulation of the EGF receptor in NRK cells. Type α TFFs have structural homology with EGF and consist of a single chain, MW approximately 5–6K, cross-linked by three disulfide bridges. We have recently purified type β TGFs to homogeneity from human platelets, human placentas, and bovine kidneys. The MW of these three peptides is approximately 25K; they are composed of two similar (possibly identical) disulfide-bridged subunits. In collaboration with Drs. Rik Derynck and David Goeddel (Genentech), work is currently in progress to clone the gene for human TGF-β.

103. Biochemical Studies Using Synthetic DNA. *M. H. Caruthers.* Department of Chemistry, University of Colorado, Boulder, CO 80309.

During the past few years, dramatic new developments in nucleic acid chemistry have led to rapid procedures for synthesizing deoxyoligonucleotides. Current methodologies utilize inorganic polymer supports such as silica gel and protected nucleoside 3′-phosphoramidites as synthons. Recent improvements which will be presented include the use of bis-dialkylaminophosphines for synthesizing deoxynucleoside phosphoramidites in situ and new amidine protecting groups for deoxynucleoside bases. The mechanism whereby proteins recognize and bind to specific DNA sequences remain largely unknown despite considerable effort. We have directed our research toward studies on the interaction of cro protein with cro operator DNA. Using rapid methods for synthesizing DNA, we have constructed genes for many mutated cro proteins and have studied how these mutations affect operator recognition. Our results support the current hypothesis on cro recognition of cro operator. We have also designed weaker and tighter binding cro repressors and measured the affinities of these proteins for cro operator. These results will be reported and discussed relative to the possibility of a specific code controlling the recognition of DNA sequences by DNA binding proteins.

104. Applying Old and New Genetic Technology toward Understanding the Cytoskeleton of Yeast. *D. Botstein,* D. Shortle, P. Novick, J. H. Thomas, T. Huffaker, and P. Schatz. Department of Biology, M.I.T., Cambridge, MA 02139.

Mutations in the major cytoskeletal proteins of yeast have proved to be difficult to isolate by classical genetic screening of random mutations. In recent years, technology has been developed which has allowed us to proceed from knowledge of the protein to isolation, characterization, and most important, to specific alteration of any gene of interest. These methods will be illustrated with examples taken from recent work in our laboratory. Application of the idea of "gene disruption" via integration of plasmids bearing DNA fragments internal to the coding sequence of cloned genes made it possible to show that the single actin and tubulin genes of yeast are essential for viability. Use of in vitro mutagenesis techniques in conjunction with variants of the gene disruption principle made possible the isolation of conditional-lethal point mutations in these genes without knowledge of phenotype beyond the lethality associated with loss of function. The conditional-lethal mutations then allowed the assessment of phenotype. Finally, application of knowledge about recombination mechanisms in yeast have made possible the development of simple and general mapping methods both at the chromosomal and fine-structure level so that mutations can be followed by function as well as by DNA sequence. More classical genetic methods, particularly pseudo-reversion methods, have made it feasible to find new genes whose products interact with the cytoskeleton. These are found as loci which yield suppressors of cytoskeleton mutations which, under some condition, are themselves conditional-lethal mutations. In general, these have phenotypes strikingly similar to the original mutations affecting cytoskeletal proteins. The products of these genes should be accessory proteins (e.g., microtubule associated proteins [MAPs] in the case of suppressors of tubulin mutants).

105. Activation and Function of Human *ras* Protooncogenes. *Arthur D. Levinson.* Genentech Inc., South San Francisco, CA 94080.

There are three known members of the human *ras* gene family (Ha-ras, Ki-ras, and N-ras), all of which encode related proteins of 21 000 daltons. Each of these protooncogenes has been demonstrated to be involved in a variety of tumor types, although to date little is known about the mechanism by which the gene products functions in either normal or tumor cells. Typically, *ras* genes are activated in tumors by somatic mutations involving amino acids 12 (glycine) or 61 (glutamine).

To extend these descriptions of activated genes, we have systematically mutated codon 12 of c-Ha-ras and examined the effects of such mutations using the NIH3T3 transfection assay. Our results indicate that most amino acids other than glycine and proline at position 12 activate the protein. As a means of determining the function of the polypeptides encoded by normal and activated *ras* genes, we have expressed both version of c-Ha-ras genes in *E. coli* and yeast. Using p21 purified from heterologous hosts, we have determined that one property of the p21 polypeptide, the binding of guanine nucleotides, is not significantly affected by alterations at amino acid 12 as determined by in vitro measurements. Although it is known that p21 encoded by v-Ha-ras can autophosphorylate, known human analogues (both normal and activated) lack this ability. We have demonstrated that this inability results from the lack of the appropriate phosphoacceptor residue (Thr-59) in the human protein. Further biochemical characterizations and enzymatic studies involving normal and activated *ras* polypeptides will be discussed.

106. Genes for Human Interferons and Transforming Growth Factors. *David V. Goeddel.* Department of Molecular Biology, Genentech, Inc., South San Francisco, CA 94080.

The human interferons (IFNs) can be classified into three groups based on antigenic properties: IFN-α, -β, and -γ. Single genes code for IFN-β and IFN-γ. There are two distinct classes of IFN-α genes. The well-characterized class I gene family codes for more than 12 distinct but homologous proteins ($\sim$85% homology). A second (class II) family has been found which encodes gene products having about 50% amino acid homology with the class I IFNs-α. The proteins encoded by these IFN genes have been synthesized in active form in a variety of heterologous cell systems. There are two classes of transforming growth factors (TFGs): TGF-α and TGF-β. When used together, these TGFs are very potent at inducing the reversible phenotype transformation of normal mammalian cells. We are currently examining the structure and expression of the genes for human TFG-α and -β.

Tuesday Afternoon—Symposium on Mechanism-Based Enzyme Inhibitors—Organized by the Division of Biological Chemistry, Cosponsored with MEDI—J. J. Villafranca, Symposium Chairman

107. Cyclopropylamines as Mechanism-Based Inactivators of Monoamine Oxidase. *Richard B. Silverman*, R. Bryan Yamasaki, Paul A. Zieske, and Michael L. Vazquez. Department of Chemistry, Northwestern University, Evanston, IL 60201.

A unified picture has developed for the mechanism of inactivation of monoamine oxidase (MAO) by cyclopropylamines. *N*-Cyclopropylbenzylamine (N-CBA), *N*-(1-methyl)cyclopropylbenzylamine, *N*-cyclopropyl-α-methylbenzylamine, *trans*-2-phenylcyclopropylamine, and 1-phenylcyclopropylamine are shown to be mechanism-based inactivators of MAO. Radioactively labeled analogues of each of these compounds are utilized to determine the stoichiometries of binding; chemical reactions, carried out on the radioactively labeled enzyme, are used to elucidate the structures of the enzyme–inactivator adducts. Based on these collective results, the mechanism of inactivation of MAO by *all* of the cyclopropylamines studied [including N-CBA whose mechanism of inactivation was proposed previously as occurring by a different pathway (Silverman, R. B., & Hoffman, S. J. (1980) *J. Am. Chem. Soc. 102*, 884–886)] can be generalized as a one-electron transfer from the amine to the flavin cofactor followed by homolytic cyclopropyl ring cleavage and capture of the incipient radical by another active site radical. Evidence to support this mechanism and to more clearly define the nature of the active site radical and the general structure of the active site will be presented.

108. Mechanism-Based Inhibitors of Dopamine β-Hydroxylase. *J. J. Villafranca*, G. Colombo, B. Rajashekher, P. Fitzpatrick, and D. Flory. Department of Chemistry, The Pennsylvania State University, University Park, PA 16802.

Several mechanism-based inhibitors of dopamine β-hydroxylase have been synthesized and their properties as substrates and inhibitors have been investigated. The molecules fall into three classes: (1) ring-substituted 2-X-(Y-phenyl)-1-propenes where X = H, Cl, Br, and Y are m and p substituents, (2) ring-substituted benzyl cyanides, and (3) substituted phenylpropynes. Based on extensive kinetic analyses involving isotope effects on V_{max} and V/K, a catalytic mechanism involving formation of an intermediate benzylic radial and radical cation is proposed. The intermediates can partition between formation of product and enzyme inactivation.

109. Suicide Inhibition of Steroid Biosynthesis. *Brian W. Metcalf.* Smith Kline & French Laboratories, Philadelphia, PA 19101.

Approaches to the specific control of androgen biosynthesis via testosterone 5α-reductase and of estrogen biosynthesis via aromatase will be presented. These approaches demonstrate the design of suicide inhibitors for the inactivation of NADPH and cytochrome P-450 dependent enzymes, respectively.

110. Strategies for the Specific Inhibition of Cytochrome P-450^{scc} Catalysis of the Conversion of Cholesterol to Pregnenolone. *W. H. Orme-Johnson*, Atsushi Nagahisa, Ricky J. Krueger, Stephen R. Wilson, and Marcel Gut. Department of Chemistry, Massachusetts Institute of Technology, Cambridge, MA 02139 (W.H.O.-J., A.N., and R.J.K.), Chemistry Department, New York University, New York, NY 10003 (S.R.W.), and Worcester Foundation for Biological Research, Shrewsbury, MA 01545 (M.G.).

The cytochrome P-450^{scc} in steroid hormone synthesizing tissues catalyzes three rounds of oxygenation of cholesterol, ultimately producing cholesterol and isocaproaldehyde. We found that cholesterol analogues retaining the tetracyclic nucleus but with alterations at C-22 such as replacement of C by S, replacement of the isopentyl group with trimethylsilylmethyl, desaturation of the C-22,23 bond, or substitution of an amino group for a hydrogenation all were either effective competitive inhibitors or were acted on by the oxygenase to become inhibitory. The central theme to be explored is that addition of P-450-generated oxenoid species or abstraction of hydrogen from these steroids by such species yields potent reactants in the active site. We will discuss the evidence for clean regio- and stereospecific reactions of these types and show that these compounds act similarly in the isolated enzyme and in intact adrenal cortical cells.

Wednesday Morning—Symposium on Drug–Metal Complexes. Chemistry and Mechanism—J. W. Kozarich, Symposium Chairman

111. Mechanistic Analysis of DNA Fragmentation by Bleomycin. *J. W. Kozarich*, J. C. Wu, and J. A. Stubbe. De-

partment of Pharmacology, Yale University School of Medicine, New Haven, CT 06510, and Department of Biochemistry, University of Wisconsin, Madison, WI 53706.

Specifically tritiated DNA models have been constructed and used as probes for determining the mechanism of deoxyribose fragmentation leading to the generation of free nucleic acid base and base propenal by bleomycin–metal complexes. Analyses have been carried out for various activated metallobleomycins under several different reaction conditions. The results are consistent with a rate-determining cleavage of the 4′-C–H bond of the deoxyribose moiety by the activated metallobleomycin which is uniquely responsible for the production of both free base and base propenal.

112. DNA Strand Scission by Bleomycin Group Antibiotics. *S. M. Hecht*, N. Murugesan, R. Kilkuskie, G. Ehrenfeld, L. Rodriguez, and C. Xu. Departments of Chemistry and Biology, University of Virginia, Charlottesville, VA 22901.

Bleomycin is the generic name used to describe members of a family of clinically useful antitumor antibiotics. The bleomycins are glycopeptide-derived molecules, whose therapeutic value is believed to derive from their ability to effect strand scission of chromosomal DNA. We have studied the nature of DNA cleavage by several activated metallobleomycins following three different methods of activation. Presently, we describe the nature of the products formed and some novel characteristics of DNA strand scission by bleomycin.

113. Cobalt Bleomycins and Deoxyribonucleic Acid: Sequence-Dependent Interactions, Action Spectrum for Nicking, and Indifference to Oxygen. C.-H. Chang and *C. F. Meares*. Department of Chemistry, University of California, Davis, CA 95616.

Light-induced strand scission of DNA by cobalt bleomycins is more likely to occur at certain base sequences than others. By use of ^{32}P-end-labeled DNA restriction fragments as the substrates for cleavage, products have been analyzed on high-resolution polyacrylamide gels and compared to those produced by iron bleomycin. The results indicate that the sites of damage to DNA are similar in both cases: pyrimidine residues located at the 3′ side of a guanine are preferentially attacked. Consistent with the observed nicking specificity, interactions between cobalt bleomycin and guanine residues in the trinucleotide sequence GGT are revealed in a dimethyl sulfate methylation experiment. The action spectrum for the light-induced DNA cleavage reaction correlates with the absorption spectrum of cobalt bleomycin in the wavelength range between 330 and 450 nm. In contrast to iron bleomycin, the extent of DNA degradation by light-activated cobalt bleomycins appears to be indifferent to the concentration of dissolved oxygen in the reaction medium, and little or not base propenal is produced. Bases (e.g., thymine) are released by both agents.

114. Bleomycin Activation Is Analogous to That of Cytochrome P-450. *R. M. Burger*, S. B. Horwitz, and J. Peisach. Albert Einstein College of Medicine, Bronx, NY 10461.

Bleomycin (BLM), a 1550-dalton glycopeptide antibiotic, catalyzes the oxidative degradation of DNA. It forms metal complexes of which Fe–BLM is the most active against DNA. Like P-450, high-spin Fe(II)–GLM is activated by addition of O_2 to form an oxygenated complex which then undergoes a one-electron reduction to form 'activated BLM', a species kinetically competent in DNA degradation. Like its P-450 counterpart, it can also be formed directly from Fe(III)–BLM and peroxide. Unlike its P-450 counterpart, activated BLM is moderately stable. Activated BLM is a complex of BLM and low-spin Fe(III) which is ligated to oxygen derived from either O_2 or peroxide. The net oxidation state is 5+. Its decay to Fe(III)–BLM is accompanied by attack on DNA to yield two types of products. DNA is cleaved, releasing base propenals comprising nucleic base plus deoxyribose carbons 1–3, only if O_2 is available subsequent to drug activation. A second product is nucleic base whose formation is unaffected by the presence or absence of O_2. Like P-450, BLM forms a Mn(II) complex which in the presence of peroxide, but not of O_2 plus reductants, cleaves DNA, releasing the same products as with Fe, but in different proportions and in lower yield.

Wednesday Afternoon—Symposium on Mechanism of Conformational Change in Proteins—G. Rose, Symposium Chairman

115. Point Mutations and Protein Folding. Anne Beasty, Mark Crisanti, Mark Hurle, Joanna Manz, Kathleen Perry, Thomas Stackhouse, Nancy Touchette, and *Robert Matthews*. Department of Chemistry, Penn State University, University Park, PA 16802.

Although it is generally accepted that the amino acid sequence of a protein determines its three-dimensional structure, the mechanism by which a protein folds to its native conformation is not yet known in detail for any protein. Our approach toward solving this problem is to investigate the effects of single amino acid replacements on the folding and stability of globular proteins. We presume that residues which play a key role in folding and stability will have observable effects on kinetic and thermodynamic parameters for the folding process. Results on a two-domain protein, the α subunit of tryptophan synthase, support this hypothesis and demonstrate the utility of the mutations in identifying the structural basis of several of the kinetic phases observed in folding. In particular, one slow phase in folding can be convincing assigned to domain association. Similar studies on dihydrofolate reductase, a single domain protein, show the single amino acid substitutions can serve to either increase or decrease the stability of the protein. Insights into the molecular basis for these changes can be obtained for the X-ray structure. We believe that mutagenesis will play an ever increasing role in elucidating the mechanism of protein folding.

116. Insights into Protein Dynamics and Hydration Using Neutron Diffraction. *A. A. Kossiakoff* and J. Shpungin. Genentech, South San Francisco, CA 94080 (A.A.K.), and Department of Biology, Brookhaven National Laboratory, Upton, NY 11973 (J.S.).

Neutron diffraction has the capability of directly locating hydrogen atoms in molecules as large as proteins, and further, it has the ability to distinguish them from deuteriums. This attribute has been used to study the dynamic and hydration properties of several proteins. Two classes of conformational fluctuation can be probed by this technique: (1) "protein breathing"—by analyzing the rotational properties of side-chain methyl groups and (2) "regional melting"—by H/D exchange experiments. Together these two classes of fluctuation span nearly the full range of all motions which might play a role in biological activity. A new method has been developed to look at the structural details of water binding in proteins using neutron solvent-difference maps. Such maps

are obtained by comparing the changes in intensity between two data sets, one taken with H_2O as the solvent and a second set where D_2O is the solvent medium. With neutrons, H_2O and D_2O have very different scattering properties which are accentuated in these difference maps to reveal an accurate representation of the solvent structure. Results will be discussed showing that substantially more information on the positions of bound water can be obtained from these solvent maps than from conventional X-ray methods.

117. Transmission of Conformational Change in Proteins. *Arthur M. Lesk* and Cyrus Chothia. MRC Laboratory of Molecular Biology, Cambridge, UK (A.M.L. and C.C.), and University College London, London, England (C.C.).

Recent X-ray structure determinations of multiple conformers of proteins, at high resolution and well refined, have made it possible to analyze mechanisms of conformational change. In insulin, α-helices tend to move as rigid bodies. Relative displacements of packed helices of up to about 1.5 Å are accommodated by small adjustments in torsion angles retaining the pattern of residue packing. We call this the *helix interface shear* mechanism of conformational change. The closure of the interdomain cleft of citrate synthase upon binding its substrate and cofactor is also the cumulative effect of similar shifts in pairs of packed helices. The large interface between the domains precludes a simple hinge mechanism. It is the limit to the size of allowable shifts of packed helices—the limit of plastic deformation of helix interfaces—which limits the extent to which a conformational perturbation can be accommodated locally. In turn, it is the limit to the local dissipation of helix movements that can propagate over long distances—and in some cases can even amplify—conformational change. In insulin an impulse at the surface of the molecule sets off a train of conformational changes that breaks the dimer symmetry at Phe B25, 20 Å away.

118. Self-Recognition in Proteins. *Richard H. Lee* and George D. Rose. Department of Biological Chemistry, The Milton S. Hershey Medical Center, The Pennsylvania State University, Hershey, PA 17033.

When a protein folds, its secondary structural units fit snugly together, squeezing out waters of hydration. Thus, the self-assembly process may be regarded as a sequence of molecular recognition events between the complementary surfaces of such units. We have devised a docking algorithm that identifies favorable modes of association between rigid units abstracted from the native structure. The method first develops a list of prominent topographic surface features for a given structural unit, i.e., its hills and valleys. Complementarity between units is taken to be the degree of volume overlap between features of opposite type. A search strategy that systematically mates features in pairwise fashion is made possible due to the limited combinatorics of the problem. Initial results using two α-helices will be presented. Extension of the method to other instances of rigid-body docking such as subunit–subunit and receptor–ligand interactions will also be discussed.

119. Assembly of Triple Helices in Models of Collagen and of α-Helical and Other Regular Structures in Globular Proteins: A Conformational Energy Study. *G. Némethy*, K.-C. Chou, M. Gerritsen, and H. A. Scheraga. Baker Laboratory of Chemistry, Cornell University, Ithaca, NY 14853.

Conformational energy computations have been used to determine the energetically favorable ways of packing of regularly folded polypeptide structures. In modelling the microfibril assembly of collagen, the preferred relative orientation and longitudinal alignment of two triple helices composed of various regularly repeating poly(tripeptide) chains was studied. Very short triple helices can pack in a variety of orientations but, for longer chains, a parallel packing arrangement is energetically preferred. A high content of Pro residues is necessary for this strong preference. In the packing of α-helices of poly(amino acids), several packing arrangements can occur, but an antiparallel arrangement is energetically most favorable. The computed low-energy arrangements also occur frequently in globular proteins. A computation of the packing of three α-helices in myoglobin indicated that the presence of nearby helices can influence the packing of a given pair of α-helices. The analysis of α-helix–α-helix and α-helix–β-sheet packings indicates that it is possible to account for frequently observed packing arrangements of regular structures in proteins in terms of local interaction energies.

Wednesday Afternoon—Symposium on Carbohydrate Processing Enzymes—Organized by the Division of Biological Chemistry, Cosponsored with CARB—V. Schramm, Symposium Chairman

120. Chitin Synthetase, a Membrane-Bound Enzyme That Catalyzes Vectorial Synthesis of a Polysaccharide. *E. Cabib*, M. S. Kang, N. Elango, E. Mattia, and J. Au-Young. National Institutes of Health, Bethesda, MD 20205.

Chitin, the polysaccharide that forms the primary septum of yeast, is found in the cell outside the plasma membrane; however, its precursor, uridine diphosphate *N*-acetylglucosamine, is synthesized in the cytoplasm. Chitin synthetase is attached to the plasma membrane. We have shown that isolated plasma membranes are able not only to synthesize the polysaccharide, but to extrude it to the outside face of the membrane, as occurs in vivo. To further expand these studies, the synthetase has been solubilized from membranes with digitonin and purified 8000–10000-fold. The key step in the purification was trapping of the enzyme in its own reaction product, i.e., in insoluble chitin that forms during incubation with UDP-*N*-acetylglucosamine. When the purified enzyme was subjected to nondenaturing gel electrophoresis and the gel was incubated with UDP-*N*-acetylglucosamine and Mg^+, chitin precipitated in the gel, forming an opaque band that indicated the position of chitin synthetase. Thus, it appears that synthesis of the polysaccharide can occur in the absence of a primer, unless this is tightly bound to the synthetase itself.

121. Transmembrane Movement of Sugar Residues during Asparagine-Linked Oligosaccharide Synthesis. *M. D. Snider*. Department of Embryology, Carnegie Institution of Washington, Baltimore, MD 21210.

Sugar residues are exported from the cytoplasm during glycoprotein synthesis, since the oligosaccharides of secreted and cell surface molecules are made from cytoplasmic sugar nucleotides. This export occurs by two different mechanisms during asparagine-linked oligosaccharide synthesis, which begins in the endoplasmic reticulum (ER) and is completed in the Golgi complex. During the synthesis of the lipid-linked precursor oligosaccharide $Glc_3Man_9NAc_2$ and its transfer to protein, no water-soluble molecules cross the ER membrane. Synthesis of oligosaccharide–lipid is begun on the cytoplasmic face of the ER and completed on the luminal face. Sugar residues appear to cross the ER membrane by the transmem-

brane movement of lipid-linked precursors. In contrast, during the extensive processing of oligosaccharides in the Golgi, transmembrane movement of water soluble precursors does occur. Sugar nucleotides enter the Golgi lumen via specific transport carriers, where they are utilized by glycosyltransferases. Possible explanations for the differences in the topography of oligosaccharide synthesis in ER and Golgi will be discussed.

122. A Processive Bacterial Glucoenzyme—The Endogenous Autolytic Peptidoglycan Hydrolase of *Streptococcus faecium*. *G. D. Shockman*, J. Barrett, D. Dolinger, and V. L. Schramm. Department of Microbiology and Immunology and Department of Biochemistry, Temple University School of Medicine, Philadelphia, PA 19140.

An endogenous autolytic peptidoglycan hydrolase of *S. faecium* ATCC 9790 (muramidase 1) has been shown to be a glucoenzyme, present in cells in both a latent (M_r ~130 kd) and proteinase-activated (M_r ~87 kd) form. Hydrolysis of soluble, linear un-cross-linked peptidoglycan chains, consisting of 44 to 47 β-1,4-linked disaccharide (TlcNAc-MurNAc)-peptide (DSP) units was studied. Muramidase 1 has a high affinity for these chains, with hydrolysis resulting in the release of a single product, DSP monomers. Muramidase 1 hydrolysis of purified s-peptidoglycan chains extrinsically labeled with ^{14}C at the nonreducing terminus (by the addition of [^{14}C]-galactose) and with ^{3}H at the reducing terminus, resulted in an immediate and rapid release of ^{14}C and a delayed release of ^{3}H. These and other experiments were consistent with the binding of muramidase 1 to the nonreducing terminus, followed by processive hydrolysis of MurNAc-β-1,4-GlcNAc bonds and the sequential release of DSP_i units. Sequential hydrolysis of susceptible bonds within chains was followed by slow release of enzyme from the distal, reducing terminus.

123. Anatomy of an Unusual Phosphoribosyltransferase: Glutamine PRPP Amidotransferase from *Bacillus subtilis*. *Robert L. Switzer* and Steven J. Vollmer. Department of Biochemistry, University of Illinois, Urbana, IL 61081.

Glutamine 5-phosphoribosyl-α-1-pyrophosphate (PRPP) amidotransferase catalyzes the first reaction of purine nucleotide biosynthesis:

glutamine + PRPP →
phosphoribosylamine + glutamate + PP_i

In addition to catalyzing displacement reactions at C-1 of PRPP that are typical of phosphoribosyltransferases, this enzyme catalyzes hydrolysis of glutamine to glutamate plus NH_3. The amidotransferase from *B. subtilis* contains an essential [4Fe-4S] cluster, which is apparently involved in regulation of the enzyme rather than catalysis. Characterization of the [4Fe-4S] cluster will be presented. The glutamine-hydrolyzing site was shown by reaction of the enzyme with [^{14}C]-6-diazo-5-oxo-L-norleucine to include the sulfhydryl group of the amino terminal cysteinyl residue. The amino acid sequence of the enzyme was determined by DNA sequencing of its gene by C. Makaroff and H. Zalkin, Purdue University. Comparison of the sequence to those of other proteins allowed tentative identification of regions of the primary structure involved in glutamine hydrolysis, phosphoribosyltransferase activity, binding of an allosteric inhibitor, and attachment of the Fe-S cluster.

124. Ribulose-1,5-bisphosphate Carboxylase: Mechanisms Involved in CO_2 and Cation Activation. *H. M. Miziorko*. Medical College of Wisconsin, Milwaukee, WI 53226.

Ribulosebisphosphate (RuBP) carboxylase must be activated by incubation with CO_2 and cation in order for the enzyme to become catalytically functional. The mechanisms involved in enzyme activation have been elucidated in experiments involving a model complex formed upon mixing $E–CO_2–M^{2+}$ with the transition-state analogue carboxyarabinitol bisphosphate (CABP). Simultaneous binding of activator CO_2 and CABP indicates that distinct CO_2 molecules serve as activator and substrate. Treatment of a $^{14}CO_2$-containing model complex with diazomethane, followed by exhaustive proteolytic digestion, permitted isolation of [^{14}C]methoxycarbonyllysine. This indicates that enzyme activation by CO_2 involves carbamylation of the ε-amino group of a lysine. The role of the cation activator has been investigated using ESR techniques. Mn^{2+}-containing model complexes produce ESR spectra which suggest marked distortion of the cation's coordination sphere. When ^{17}O is used to label the oxygens of the carboxyl group or the C-2 alcohol of CABP incorporated into the model complex, the observed ESR spectra are broadened due to superhyperfine coupling between Mn^{2+} and ^{17}O. Inner-sphere coordination must occur to account for the ESR data, which indicate involvement of the activator cation at the enzyme's catalytic site.

125. Kinetic Isotope Effects in N-Glycosidic Bond Hydrolysis by AMP Nucleosidase. David W. Parkin and *Vern L. Schramm*. Department of Biochemistry, Temple University School of Medicine, Philadelphia, PA 19140.

AMP nucleosidases are prokaryotic enzymes which hydrolyze the N-glycosidic bond of AMP to adenine and ribose 5-PO_4. Allosteric activation by MgATP causes a 10^2–10^3-fold increase in V_{max} for the enzyme from *Azotobacter vinelandii*. The primary ^{14}C and secondary ^{3}H kinetic isotope effects of glycosidic bond hydrolysis of AMP and dAMP have been measured with AMP nucleosidase in the presence and absence of MgATP. Significant isotope effects both occur in the presence and absence of the activator, but the secondary isotope effect is larger without MgATP. Isotope effects of acid-catalyzed N-glycosidic bond hydrolysis are larger than with the enzyme-catalyzed reactions. The results demonstrate that bond breaking by AMP nucleosidase is sufficiently rate limiting to express an isotope effect. If intrinsic isotope effects are being expressed, the enzymatic transition state differs considerably from that of acid hydrolysis, and the allosteric effect alters the nature of the enzyme–substrate transition state. If several steps contribute to the observed isotope effect, the activator alters steps which influence the secondary but not the primary isotope effects.

Thursday Morning—Symposium on New Advances in the Study of Biological Phosphoryl Transfer—D. Dunaway-Mariano, Symposium Chairman

126. New Applications of Exchange-Inert Metal–Polyphosphate Complexes to the Study of Enzyme Mechanisms. *Debra Dunaway-Mariano*. Department of Chemistry, University of Maryland, College Park, MD 20742.

Exchange-inert metal complexes of polyphosphates, phosphonates, phosphoroamidates, and phosphorothioates have been prepared. The application of these complexes as probes of (1) the structure of Mg complexes of ATP, adenylimidodiphosphate, and adenylmethylenediphosphonate, (2) substrate protonation and metal coordination, and (3) enzyme metal binding sites will be described.

127. Advances in the Chemistry of Nucleoside Phosphoro-

thioates. Applications to Enzymic Stereochemistry. *Perry A. Frey*. Institute for Enzyme Research, University of Wisconsin, Madison, WI 53705.

Reaction of nucleoside phosphorothioates with BrCN in aqueous solutions in the neutral to alkaline pH range produces the corresponding desulfurized nucleotides in high yields. The reaction is accompanied by incorporation of ^{18}O into the nucleotide from ^{18}O-enriched water. Reaction of (R_p)-β-cyanoethyl-ADPαS with BrCN in ^{18}O-enriched H_2O produces (S_p)-β-cyanoethyl-[α-^{18}O]ATP, which can be readily deprotected to (S_p)-[α-^{18}O]ADP. The reaction is used to prepare ^{18}O and ^{17}O containing nucleotides with chirally substituted phosphoryl groups for use in a variety of stereochemical studies of enzymes. In the absence of a protecting group such as cyanoethyl, the reaction takes a complex course, in which the thiocyanato group formed by reaction of ADPαS or ATPβS is internally displaced by the terminal phosphoryl group. This produces *cyclo*-diphosphates as intermediates. These four member ring phosphoanhydrides undergo rapid hydrolysis by mechanisms that involve a high degree of oxygen randomization.

128. Mechanism of the Argininosuccinate Synthetase Reaction. *Frank M. Raushel*. Department of Chemistry, Texas A&M University, College Station, TX 77843.

Argininosuccinate synthetase catalyzes the transformation of ATP, citrulline, and aspartate into AMP, pyrophosphate, and argininosuccinate. Ratner and co-workers have previously shown that the ureido oxygen of citrulline is quantitatively transferred to the AMP formed during the reaction. This result is consistent with either the intermediate formation of citrulline adenylate or the adenylation of an adduct formed between aspartate and citrulline. The distinction between these and other possible mechanisms was explored utilizing rapid-quench and positional isotope-exchange experiments. In the absence of aspartate the enzyme was found not to catalyze a positional isotope exchange between the β-nonbridge oxygens and the $\alpha\beta$-bridge oxygen of ATP. However, AMP is formed after an acid quench when enzyme, ATP, and citrulline are incubated together in the absence of aspartate. The amount of AMP formed is proportional to the amount of enzyme but is independent of the time of incubation after $\sim$1 min. No AMP is formed in the absence of citrulline. These and other results indicate that ATP and citrulline react to form citrulline adenylate and pyrophosphate. The pyrophosphate that is produced is apparently torsionally immobile.

129. Determination of Ligand Hyperfine Couplings to Mn^{2+} in Creatine Kinase by Electron Spin-Echo Envelope Modulation. *Russell LoBrutto*, Georgh H. Reed, Geoffrey Smithers, and J. S. Leigh. Department of Biochemistry and Biophysics/G4, University of Pennsylvania, Philadelphia, PA 19104.

Recent technological developments have helped to make pulsed EPR spectroscopy a practical and affordable tool for the study of structural detail in metalloenzymes. Electron spin echoes in such systems are observed in response to an appropriate microwave pulse sequence, and the echo amplitude decays as interpulse spacing is increased. Modulation of the spin echo decay envelope due to weakly coupled nearby nuclei is often observed. We have detected modulations of the Mn^{2+} spin echo in creatine kinase due to ^{14}N and ^{15}N of thiocyanate. The frequency spectrum obtained from the Fourier transform of the modulations reveals a 3.8-MHz coupling for ^{15}N. Other couplings which may correspond to ^{31}P of ADP have been found; model studies of MnP_2O_7 complexes in single crystals of MgP_2O_7 are in progress to aid in assigning these resonances. Preliminary studies employing nitrate as a ligand reveal a weak ^{15}N coupling from it as well.

Thursday Afternoon—Symposium on Xenobiotic Metabolizing Enzymes—Organized by the Division of Biological Chemistry, Cosponsored with MEDI—R. Armstrong, Symposium Chairman

130. Steady-State Kinetic Studies of Glutathione *S*-Transferase Using the Dead-End Inhibitors γ-L-Glu-L-SerGly and γ-L-Glu-L-AlaGly. *Wen-Jian Chen* and Richard N. Armstrong. Department of Chemistry, University of Maryland, College Park, MD 20742.

Two peptide inhibitors of glutathione *S*-transferase have been synthesized. The tripeptide analogues of glutathione (GSH), γ-L-Glu-L-SerGly (GOH) and γ-L-Glu-L-AlaGly (GH) are linear competitive inhibitors vs. GSH and linear noncompetitive inhibitors vs. the electrophilic substrate 1-chloro-2,4-dinitrobenzene with isozyme A_2 of rat liver glutathione *S*-transferase. The results are consistent with a steady-state random mechanism suggested by product inhibition studies. Comparisons of the inhibition constants vs. GSH for GOH (K_i = 12 μM) and GH (K_i = 180 μM) to the thermodynamic dissociation constant of GSH ($K_D \approx 7$ μM) suggest that recognition of the tripeptide by the enzyme is insensitive to substitution of oxygen for sulfur. Furthermore, replacement of the sulfhydryl (or hydroxy) group of GSH (or GOH) with hydrogen results in a loss of about -2 kcal/mol in the free energy of binding of the tripeptide to the enzyme.

131. Regulation and Genomic Organization of Rat Liver Glutathione *S*-Transferase Genes. *C. B. Pickett*, C. A. Telakowski-Hopkins, G. J.-F. Ding, G. S. Rothkopf, V. D.-H. Ding, and A. Y. H. Lu. Merck Sharp & Dohme Research Laboratories, Rahway, NJ 07065.

The glutathione *S*-transferases are a family of isozymes with broad overlapping substrate specificites which catalyze the conjugation of glutathione to electrophilic ligands. Using polysome immunoabsorption techniques, we have purified mRNAs specific for the Ya, Yc, and Yb transferase subunits and have used these purified mRNAs as templates to construct full-length cDNA clones. We have identified by hybrid-select translation two cDNA clones, pGTA/C43 and pGTA/C44, which are complementary to Yb mRNAs. Although these two cDNA clones share significant sequence homology, their restriction maps indicate they are complementary to two distinct Yb mRNAs. Another clone, pGTB42, has also been identified and characterized. This clone hybrid-selects the Ya/Yc mRNAs, hybridizes to pGTB38, a Ya/Yc cDNA clone we have characterized previously; however, based on its restriction map, pGTB42 is complementary to a distinct Ya/Yc mRNA. We have utilized the cDNA clones in nuclear run-off experiments to demonstrate that the transcriptional rates of the glutathione *S*-transferase genes are augmented by phenobarbital and 3-methylcholanthrene administration. Finally, structural genes encoding the rat liver glutathione *S*-transferases have been isolated from a rat genomic library and are being characterized.

132. The Partial Purification and Characterization of the Cytochrome P-450 Monooxygenase Enzyme System of *Cunninghamella bainieri* (*echinulata*). *James P. Ferris*, Robert A. Aleksejczyk, and Michael A. Martin. Department of Chemistry, Rensselaer Polytechnic Institute, Troy, NY 12181.

The cytochrome P-450 and cytochrome P-450 reductase of *Cunninghamella bainieri* (*echinulata*, ATCC 9244) were solubilized with Emulgen 913 and partially purified. The cytochrome P-450 was purified to 5.6 nmol/mg of protein by DEAE-cellulose, ω-amino-*n*-octyl-Sepharose 4B and hydroxylapatite chromatography. SDS–PAGE indicated this partially purified fraction contained three main bands of apparent molecular weight 48 700, 44 900, and 40 300. The cytochrome P-450 reductase was separated from the cytochrome P-450 by chromatography on DEAE-cellulose. The reductase does not bind to a 2′,5′-ADP Sepharose 4B affinity column and its cytochrome *c* reductase activity is enhanced by the addition of 1 μM FAD and FMN. The AHH activity of *C. bainieri* was reconstituted by combining the partially purified cytochrome P-450, a presumed lipid fraction from the DEAE-cellulose column, and either the fungal or rat hepatic reductase.

133. Inhibition of Cytochrome P-450 by Flavonoids. *Michael A. Marletta*, Rosemary L. Sousa, and Lionelle Nugon-Baudon. Department of Nutrition and Food Science, M.I.T., Cambridge, MA 02139.

Some naturally occurring flavonoids are potent inhibitors of cytochrome P-450. Our work has focused on the kinetic nature and mechanism of this inhibition. Quercetin (3,3′,4′,5,7-pentahydroxyflavone) at nM concentrations inhibited ethoxyresorufin deethylation catalyzed by β-naphthoflavone (BNF) induced microsomes and at μM concentrations inhibited benzphetamine demethylation in phenobarbital (PB) induced microsomes. In both cases the pattern of inhibition was dependent on quercetin concentration. Specific steps in the P-450 reaction pathway were examined for sensitivity to quercetin inhibition: the reduction of cytochrome P-450 by NADPH/P-450 reductase was not inhibited, but quercetin did inhibit the cumene hydroperoxide supported deethylation of ethoxyresorufin. Quercetin also inhibits the formation of chlorophenols from chlorobenzene and demonstrates a differential effect on the isomeric product ratio. We are currently testing the in vivo biological activity of quercetin with chlorophenol formation as an end point and are assessing the ability of quercetin to inhibit macromolecular binding of selected chemical carcinogens in vivo.

134. Primary Isotope Effects on Cytochrome P-450 Catalyzed Reactions. *G. T. Miwa*, J. S. Walsh, N. Harada, and A. Y. H. Lu. Department of Animal Drug Metabolism, Merck Sharp & Dohme Research Laboratories, Rahway, NJ 07065.

Oxidative O- and N-dealkylation reactions catalyzed by cytochrome P-450 proceed with the cleavage of a C–H bond. Since this bond cleavage step must occur after dioxygen activation, the study of kinetic isotope effects makes possible the elucidation of mechanistic features around this step. Large ($k_H/k_D > 10$) deuterium isotope effects have been determined for an O-dealkylation reaction catalyzed by two purified isozymes of cytochrome P-450. The marked rate reduction caused by deuterium labeling results in a change in regiospecificity without consequence to the overall turnover rate of the enzyme. We interpret these data to indicate that an irreversible step precedes hydrogen abstraction–oxygen recombination during the formation of an intermediate hemiacetal. In contrast, low isotope effects ($k_H/k_D < 3$) have been observed during N-dealkylation reactions catalyzed by these enzymes. This and other data implicate a one-electron nitrogen oxidation–α-carbon deprotonation mechanism during the formation of an intermediate carbinolamine.

Thursday Afternoon—Poster Session—Rowena Matthews, Chairman

135. Cleavage of Short Oligonucleotides by Bleomycin. *Thomas J. Keller*, Norman J. Oppenheimer, and Corey Levinson. Pharmaceutical Chemistry Department, University of California, San Francisco, CA 94143 (T.J.K. and N.J.O.), and Cetus Corp., Emeryville, CA 94608 (C.L.).

Bleomycin is an anticancer drug for which the presumed cell killing mechanism is the cleavage of DNA. Double-strand cleavages are expected to be particularly lethal because they are less likely to be repaired. Previous research demonstrated that the drug does not react at random sequences. In fact, recognition of specific base sequences has been suggested; however, the molecular basis for the drugs selectivity has not been worked out. We report results indicating there are two distinct kinds of cleavage sites. First, the well-recognized reaction at 5′-G(C/T)-3′ sequences in which damage occurs at the pyrimidine 5′ to guanine is confirmed. Second, bleomycin is shown to react at 5′-GA-3′ sequences. Here, the drug can apparently react at either the adenine or the complimentary thymine nucleotide. Further results indicate base-labile damage associated with specific cleavage sites. The molecular basis for the specificity of bleomycin's interaction with DNA will be discussed.

136. Oligonucleotide-Mediated Mutagenesis of Dihydrofolate Reductase. *Cinda S. Herndon*, Arthur D. Riggs, and C. Robert Matthews. Department of Chemistry, Pennsylvania State University, University Park, PA 16802 (C.S.H. and C.R.M.), and City of Hope Research Institute, Duarte, CA 91010 (A.D.R.).

Dihydrofolate reductase (DHFR; EC 1.5.1.3) binds NADPH 100-fold more tightly than NADH, presumably due to the interaction of the 2′-phosphate of NADPH with arginine-44. Substitution of leucine for arginine at this position would allow assessment of the role of this ion pair in ligand binding by the reductase. An Arg → Leu mutation is effected by site-directed mutagenesis of the *fol* structural gene using a synthetic 17-base oligonucleotide bearing three base mismatches with the wild-type sequence. A 5.3-kb plasmid containing the *fol* gene is nicked at a unique *Eco*RI site within the gene and gapped with exonuclease III. Subsequent to annealing with the oligonucleotide, the gap is filled and ligated using DNA polymerase I (Klenow fragment) and T4 DNA ligase. Transformation of *E. coli* HB101 with the heteroduplex DNA, isolation of plasmid, and a second transformation yields transformants containing either the wild-type or mutant plasmid. Colonies are screened by hybridization with the ^{32}P-labeled oligonucleotide, which selectively hybridizes with the mutant sequence. The mutation is verified by restriction mapping and sequencing of the *fol* gene. Preliminary characterization of the mutant DHFR will involve comparisons with wild type of ligand binding, catalytic activity, and stability.

137. Solid-Phase Synthesis of Oligonucleoside Methylphosphonates. *M. Parameswara Reddy*, Akira Murakami, Cheryl H. Agris, Scott A. Glave, Paul S. Miller, and Paul O. P. Ts'o. Division of Biophysics, School of Hygiene and Public Health, The Johns Hopkins University, Baltimore, MD 21205.

Nonionic oligodeoxyribonucleoside methylphosphonates, d-Np(N*p*)$_n$N, contain methylphosphonate groups (*p*) in place of the natural phosphodiester linkages (p) of nucleic acids. Protected 5′-dimethoxytritylnucleoside 3′-methylphosphonic

imidazolides, d-[$(MeO)_2$Tr]N*p*Im, are readily prepared by reaction of protected nucleoside with methylphosphonic bis(imidazolide) in acetonitrile and are stable for several weeks when stored in solution at −20 °C. Reaction of d-[$(MeO)_2$Tr]N*p*Im with thymidine on a polystyrene support for 6 h gives dimers in 90% yield. In the presence of tetrazole, the yield is 95% after 1 h. Longer oligomers (n = 6–10) were prepared by stepwise addition of [$(MeO)_2$Tr]N*p*Im to nucleosides or oligomers on a polystyrene support with an average yield of 83–91% per step. Deprotected oligomers were purified in one step by ion-exchange chromatography. While d-Np-$(Np)_n$N serve as substrates for both polynucleotide kinase and reverse transcriptase, d-N$p$$(Np)_n$N are not phosphorylated by polynucleotide kinase.

138. The Origin of the Major Small Cytoplasmic RNAs (scRNAs). V. L. Cash and *T. O. Sitz*. Department of Biochemistry and Nutrition, Virginia Tech, Blacksburg, VA 24061.

In the cytosol of rat liver there is a population of nonpolysomal 40S mRNPs which can be translationally inactive. This fraction contains several low molecular weight RNAs (scRNAs) which may be involved in translational control. One of these, α1RNA, is capped and resembles the 3′-end of 18S rRNA while another major form, β1RNA, is not capped (Villringer et al. (1983) *Mol. Biol. Rep. 9*, 65–74). We have found a 4.5S RNA in membrane bound polysomes which is the 3′-terminal fragment of 18S rRNA and is identical to the α1RNA except for the 5′-end sequences and the cap group. In comparing sequences with the rDNA sequences for 18S rRNA (Chan et al. (1984) *J. Biol. Chem. 259*, 224–230) we found that the β1RNA is identical to a 5′-fragment from 18S rRNA. The two major scRNAs (α1 and β1) would appear to derive from the ends of 18S rRNA. The possible origin of the 4.5S RNA (related to the α1RNA and the 3′-end of 18S rRNA) and its function will be presented.

139. *cis*-Diamminedichloroplatinum(II) Cross-Links High Mobility Group 1 and 2 Proteins to DNA in Micrococcal Nuclease Accessible Regions of Chromatin. *William M. Scovell*, Nancy Muirhead, Lee R. Kroos, and Jeff Hayes. Department of Chemistry, Bowling Green State University, Bowling Green, OH 43403.

The antineoplastic agent, *cis*-$(NH_3)_2PtCl_2$ (*cis*-DDP), covalently modifies both DNA and proteins and is found to cross-link these components in cellular chromatin, although the identity of the proteins involved has not been determined. To gain further insight into chromatin structure, we reacted *cis*-DDP with nuclei and observed a progressive cross-linking of (1) low mobility group (LMG) proteins and also (2) the high mobility group (HMG) proteins 1, 2, and E to DNA in micrococcal nuclease accessible regions of chromatin. These findings imply that the HMG 1, 2, and E proteins directly interact with or are sensitive to limited micrococcal nuclear digestion. These data are of interest on at least two counts. First, they reveal a novel mechanism by which *cis*-DDP may inhibit DNA replication and other biological functions. Second, the data provide new insights into chromatin structure and specifically the location of the HMG 1 and 2 proteins in chromatin. A model for this protein–DNA interaction is currently being evaluated will be presented.

140. The Effect of *cis*-$(NH_3)_2PtCl_2$ Binding on the Native Structure of the Simian Virus 40 Minichromosome. F. R. Collart and *W. M. Scovell*. Department of Biochemistry, MCO, Toledo, OH 43699 (F.R.C.), and Department of Chemistry, Bowling Green State University, Bowling Green, OH 43403 (W.M.S.).

cis-$(NH_3)_2PtCl_2$ is an effective antineoplastic agent which interacts covalently with DNA and chromosomal material. The Simian virus 40 minichromosome (SV40 MC) exhibits many characteristics which permits it to serve as a useful model for the structural and functional aspects of nuclear chromatin. The higher order and structural characteristics of the drug-modified SV40 MC are compared to the unmodified MC by both physicochemical and nuclease probes. Sedimentation studies and nucleoprotein gel electrophoresis indicate that no gross conformational changes occur in the MC as a result of the *cis*-$(NH_3)_2PtCl_2$ binding. Protein–DNA cross-links are evident at even low r_i levels. A set of single-cut restriction endonucleases, each of which cleaves at widely different sites on the MC, and DNases, which exhibit cleavage at hypersensitive sites in the nucleosome-free and the regulatory region, have been used to monitor the degree of alteration in the local structure produced at specific sites on the MC as a result of *cis*-$(NH_3)_2PtCl_2$ binding. Possible implications of these findings to cellular chromatin will be discussed.

141. Thermodynamic and Mechanistic Studies of the Interactions of RNA Polymerase with the λP_R Promoter. J.-H. Roe and *M. T. Record, Jr.* Department of Chemistry and Biochemistry, University of Wisconsin, Madison, WI 53706.

Interactions of the cationic binding sites of proteins with the DNA polyanion behave at a thermodynamic level like ion-exchange reactions (Record, Lohman, and deHaseth, *J. Mol. Biol.* (1976) *106*, 145–158). Consequently both the equilibria and kinetics of these interactions are sensitive functions of the ionic environment. We have used this effect to probe the thermodynamics and mechanism of the interaction of *E. coli* RNA polymerase with the λP_R promoter, using the nitrocellulose filter assay. We find that approximatly 20 monovalent ions are released in the formation of the transcriptionally competent open complex at this promoter and that the entropic contribution from release of these ions is the dominant thermodynamic driving force for complex formation under approximately physiological ionic conditions ($K_{eq} \simeq 2.6 \times 10^{10}$ M^{-1} at 25 °C, pH 7.5, 0.20 M NaCl). At least two intermediates must exist on the pathway between the initial collision complex and the open complex, as determined from the magnitude of the salt dependence of the second-order association rate constant and the negative activation energy of the first-order dissociation rate constant. The slow interconversion of these intermediates may correspond to nucleation of DNA opening.

142. Isolation and Expression of Fungal Cellulase Genes. *G. E. Willick*, F. Moranelli, and V. L. Seligy. Division of Biological Sciences, National Research Council, Ottawa, Canada K1A 0R6.

Culture filtrates from *Schizophyllum commune* grown on cellulose contain at least three cellulolytic activities: β-glucosidase (cellobiase), endoglucanase, and cellobiohydrolase. Antibodies have been prepared to purified proteins expressing each of these activities. Each enzyme is initially secreted as one glycosylated protein. Tunicamycin (5 μg/mL) blocked asparagine-linked glycosylation, resulting in intracellular accumulation of lower molecular weight species of each enzyme. Some of these were secreted, but with lowered efficiency. The antibodies were used to detect the presence of mRNA tran-

scripts coding for these enzymes. Transcripts were present in at least 100-fold greater amounts when the organism was grown on cellulose as opposed to glucose, and were present in the largest amount when the rate of secretion of cellulases was maximum. cDNA was prepared to the mRNA extracted from *S. commune* grown on cellulose, and this cDNA was inserted into the expression vector λgt11. Clones expressing determinants for the endoglucanase and β-glucosidase have been isolated.

143. Acrylonitrile Reacts with 2′-Deoxynucleosides and in Vitro with Calf Thymus DNA To Form Cyanoethyl Adducts with Gua and Thy and Carboxyethyl Adducts with Ade and Cyt. An Autocatalyzed Hydrolysis Is Postulated for Conversion of the Nitrile Moiety to a Carboxylic Acid. *A. Segal* and J. J. Solomon. Department of Environmental Medicine, New York University Medical Center, New York, NY 10016.

Acrylonitrile (AN), a rodent carcinogen, was reacted with dAdo, dCyd, dGuo, dIno, N^6-Me-dAdo, and dThd at pH 5.0 and/or 7.0 for 10 and/or 40 days. Products isolated were cyanoethyl (CNE) adducts at N-7 of Gua, N-1 of Hyp and N-3 of Thy and carboxyethyl (CE) adducts at N-1 of Ade, N^6 of Ade (by Dimroth rearrangement of N-1 of Ade), N-3 of Cyt and N-1 of N^6-Me-Ade. Reaction products were not detected after 4 h. When initial cyanoethylation (via Michael addition) occurred at a ring nitrogen adjacent to an exocyclic nitrogen the nitrile group was rapidly converted (autocatalysis) to a carboxylic acid. AN was reacted in vitro with calf thymus DNA (pH 7.0, 37 °C, 40 days) and the relative amounts of adducts isolated after various hydrolysis (nonenzymatic) procedures was 1-(2-CE)-Ade (25.8%), N^6-(2-CE)-Ade (7.6%), 3-(2-CE)-Cyt (1.3%), 7-(2-CNE)-Gua (25.8%), 7,9-bis-(2-CNE)-Gua (4.3%), imidazole ring-opened 7,9-bis(2-CNE)-Gua (18.9%), and 3-(2-CNE)-Thy (16.3%). Thus a carcinogen once adducted to a base in DNA was shown to be subsequently modified.

144. Comparison of Chain Length Distribution of in Vitro Generated and in Vivo Existing Poly(ADP-ribose). *Alaeddin Hakam*, Jerome McLick, and Ernest Kun. Department of Pharmacology and Cardiovascular Research Institute, University of California, San Francisco, CA 94143.

Poly(ADP-ribose) is a nucleic acid like homopolymer of eukaryotic cell nuclei (Kun et al. (1983) *Adv. Enzyme Regul. 21*, 177). Although its precise biological function at a molecular level is still unknown, there is evidence that the control of neoplastic transformation appears to depend on poly(ADP-ribosylation) (Kun et al. (1983) *Proc. Natl. Acad. Sci. U.S.A. 80*, 7219). Chain lengths of poly(ADP-ribose) fall into two groups: short oligomers (up to $n = 30$) and long chains ($n > 100$). Until now, chain lengths were determined by degradation of the polymer to AMP and PR-AMP yielding only average values. Furthermore, the biological significance of the chain length (oligomers vs. long chain) cannot be studied unless direct detection of intact oligomers and polymers is possible. An HPLC method has now been developed which separates the oligomeric from the long-chain population and further resolves the oligomeric group into distinct peaks according to the individual chain lengths. Comparison of poly(ADP-ribose) generated in vitro and occurring in vivo in rat tissues indicates that in the physiological steady state, poly(ADP-ribose) appears to exist as predominantly long polymeric chains, whereas in isolated nuclei distribution of oligomers spreads over a wider spectrum, with only 16–18% as long chains.

145. Base and Conformational Specificity of Covalent Amine Addition to DNA. *Douglas Maibenco*, Shirley Chang, Catherine Chen, and Sue Hanlon. Department of Biological Chemistry, University of Illinois College of Medicine, Chicago, IL 60612.

Amines can be covalently coupled to DNA and polydGdC, using nondenaturing concentrations of CH_2O (2%) at 25 °C in 20 mM NaCl, 10 mM Na/PO_4, pH 7 (SSP). This addition stabilizes a B conformation of higher winding angle. In an effort to explore the base and conformational specificity of the addition, we have examined reactions with natural DNAs of different base composition, polydAdT, polydIdC, polydGdm^{5}C, and their CH_2O controls. The extent of *n*-butylamine addition, stable to dialysis, to the natural DNAs is proportional to their GC content, with polydAdT exhibiting only 0.007 mol of amine/mol of nuc. PolydIdC in the reaction mixture converts from a "Z" type CD spectrum to a "B" type. The dialyzed product, however, reverts to the "Z" spectrum and contains no amine. PolydGdm^{5}C in the Z form (SSP + 3 mM Mg^{2+}) exhibits similar low reactivity (0.03) compared to polydGdC in the same solvent (0.21) and polydGdm^{5}C in the B form in SSP (0.22). On the basis of these results, we have concluded that the predominant product which survives dialysis is an amine addition to the exocylic amino group of C in a polynucleotide whose stable conformer in the dialysis solvent is a classical B form.

146. Premelting and the Hydrogen Exchange Open State in Synthetic RNA Duplexes. *R. S. Preisler*, S. W. Englander, and N. R. Kallenbach. Department of Chemistry, Towson State University, Towson MD 21204, and Departments of Biochemistry & Biophysics and Biology, University of Pennsylvania, Philadelphia, PA 19104.

"Premelting" transitions are conformational changes in double-stranded nucleic acids that occur at temperatures far below the onset of the helix–coil transition. Hydrogen–deuterium exchange (HX) measurements detect base pair opening at premelting temperatures in two synthetic RNA duplexes, poly(rA)·poly(rU) and poly(rI)·poly(rC). We are attempting to relate this phenomenon to transitions manifested in ultraviolet circular dichroic (CD) spectra and in the vibrational bands of bases in the infrared (IR). Isoelliptic or isosbestic points are consistent with a well-defined two-state premelting process. Using a least-squares analysis and a two-state model, we obtain enthalpies from the CD and IR spectra substantially greater than those calculated for HX opening. Thus the HX open state represents only one premelting reaction among several responsible for the major equilibrium changes in helix geometry. The premelting effects monitored by CD and IR appear to be dominated by processes that do not affect HX rates.

147. The Hydrophobicities of Four Isometric Viruses. *S. Boatman*. Department of Chemistry, Hollins College, VA 24020.

In order to assess the extent to which certain viruses bind to hydrophobic surfaces or ligands, four viruses were submitted to hydrophobic chromatography on a series of alkyl agaroses. Equal amounts of Brome (BMV), Cucumber (CMV), and Southern Bean (SBMV) or Turnip Yellow (TYMV) mosaic viruses were applied to measured amounts of C4, C6, and C8 alkyl agaroses under varied conditions of pH and ionic strength; the columns were washed until no further material eluted. BMV and SBMV (pH 5.6, 0.1 M NaCl) had very little

affinity for alkyl agaroses up to C8. TYMV apparently had greater affinity than CMV for C4 and C6 alkyl agaroses. CMV's affinity for C8 alkyl agaroses was the greatest of the four viruses. The "swollen" forms of BMV (pH 7.0) and SBMV (pH 8.0 and EDTA) had affinities for C8 alkyl agaroses similar to that of CMV. SBMV (pH 8.0 and 1 M Ca^{2+}) had an affinity like that of "compact" SBMV. Swelling of BMV and SBMV may expose hydrophobic sites which had been areas of subunit contact and may bind C8 chains like CMV. The binding behavior of TYMV and models to explain the behavior of the other viruses will be discussed.

148. Cocoa (*Theobroma cocoa*) Seed cDNA Library. *Melinda R. Wilson* and Paul J. Fritz. Department of Pharmacology, The M. S. Hershey Medical Center, The Pennsylvania State University, Hershey, PA 17033.

Messenger RNA isolated from cocoa seeds was used to establish a cDNA library in *E. coli* HB101 cells. The population of recombinant plasmids was constructed using the vector primer from pCDV1 and the SV40 linker from pL1 [*Mol. Cell Biol. 3*, 280 (1983)]. Preliminary data from agarose and polyacrylamide gel electrophoresis of restriction endonuclease treated cDNA clones demonstrated insert sizes ranging from 1.5 to 4.5 kilobase pairs. Data also indicated that larger inserts were obtained using mRNA isolated from pods picked 160 days after pollination (DAP) compared to mRNA from pods obtained 100 DAP. Current studies involve enzymes related to triacylglycerol biosynthesis. Initial use of the cocoa cDNA library will be to identify colonies containing gene(s) encoding glycerol-3-phosphate acyltransferase.

149. Abstract withdrawn.

150. Cocoa Seed Glycerol-3-phosphate Acyltransferase: Purification and Characterization. *P. J. Fritz*, J. M. Kauffman, C. A. Robertson, and M. R. Wilson. Department of Pharmacology, The M. S. Hershey Medical Center, The Pennsylvania State University, Hershey, PA 17033.

Glycerol-3-phosphate acyltransferase (G-3-PAT) was purified over 1000-fold from the postmicrosomal supernatant of cocoa (*Theobroma cacao*) seed extracts using differential ammonium sulfate solubility followed by DEAE-cellulose and Sephacryl S-300 gel filtration chromatography. Further purification was achieved by isoelectric focusing (IEF) which revealed a series of five proteins with G-3-PAT activity having isoelectric points close to 5.2. Stearoyl and palmitoyl acyl carrier proteins are tightly bound to the enzyme even after IEF and serve as acyl donors in the G-3-PAT catalyzed reaction. The product of the G-3-PAT catalyzed reaction is exclusively 1-acylglycerol 3-phosphate. The molecular weight of cocoa seed G-3-PAT is around 180000 daltons as determined by gel filtration chromatography and nondenaturing polyacrylamide gel electrophoresis (PAGE). The IEF purified G-3-PAT was used to raise antibodies in rabbits. Immunological screening following denaturing PAGE and Western blotting revealed at least 4 and possible 5 subunits ranging from 15 to 44000 daltons.

151. Synthesis, Purification, and Characterization of Thymosin α_{11}, a New Thymic Peptide. *E. P. Heimer*, M. Ahmad, T. J. Lambros, and A. M. Felix. Bio-Organic Chemistry Department, Roche Research Center, Hoffmann-La Roche Inc., Nutley, NJ 07110.

A new peptide, isolated from preparations of calf thymus fraction 5, has been characterized and synthesized. The peptide, designated thymosin α_{11}, is homologous to thymosin α_1 and contains seven additional amino acid residues at the COOH terminus. The synthesis was accomplished by the solid-phase method employing the 4-(aminoacyloxymethyl)-phenylacetamidomethyl-copoly-1%-divinylbenzene resin [PAM]. The synthetic material was purified by preparative high-performance liquid chromatography and was found to be equivalent to the natural compound in its chemical and biological properties. Thymosin α_{11} protects susceptible inbred murine strains against opportunistic infections with *Candida albicans* (at doses <300 ng/mouse) and is ~30 times as potent as thymosin fraction 5 and equal in potency to thymosin α_1.

152. Disposition and Metabolic Fate of ^{14}C-Labeled 4-[3-[3-[2-(1-Hydroxycyclohexyl)ethyl]-4-oxo-2-thiazolidinyl]-propyl]benzoic Acid (I-^{14}C), a New Renal Vasodilator. *Ling L. Lee*, Anthony G. Zacchei, and David W. Cochran. Merck Sharp & Dohme Research Laboratories, West Point, PA 19486.

The disposition and metabolism of the enantiomers of I-^{14}C were studied in beagle dogs and rhesus monkeys following intravenous dosing. Although considerable differences in pharmacological response have been observed for the enantiomers, no disposition/metabolism differences were noted. The enantiomers of I-^{14}C, which were cleared rapidly from the plasma, represented less than 50% of the AUC radioactivity profile. Biliary excretion was the major mechanism for I elimination. In either species, about 50% of the fecal radioactivity (50–90% of dose) was intact I. Enterohepatic recycling was evident in the dog. Seventeen and 35% of the radioactive dose was recovered in the urine of dog and monkey, respectively. Less than 4% of the dose was identified as intact I (either enantiomer). The following metabolites of (+)-I were isolated from the urine and characterized using solvent extraction, HPLC, derivatization, MS, and NMR techniques: the sulfoxide and sulfone analogues of (+)-I, the 4-hydroxy analogue, and traces of the glucuronide conjugate. A similar metabolic profile was noted for (−)-I. HPLC and EC-GLC methods were utilized to estimate the levels of I.

153. Analysis of Free and Esterified Sterols of *Crithidia fasciculata* at Various Times of Culture. *Collins Jones* and Chester E. Holmlund. Department of Chemistry, University of Maryland, College Park, MD 20742.

Crithidia fasciculata was cultured in a serum-free medium. Culture aliquots were removed at various times over a 70-h period. Lipids were extracted (Sobus & Holmlund, 1976) and the free and esterified sterols were resolved by chromatography on Biosil A. Analysis of free and esterified sterols (after saponification) was conducted by gas–liquid chromatography. Turbidometric measurements suggested that the culture reached stationary phase by 70 h. Free sterol represented from 70 to 90% of the total sterol over the 70-h period. There was no indication of increased sterol esterification with increased age of the culture. Ergosterol represented 90–100% of the free sterol at all times. Sterol esters from younger cultures (up to 38 h) contained ergosterol and equal or greater amounts of zymosterol and one or two unidentified sterols. In older cultures, ergosterol represented up to 85% of the sterols in sterol esters.

154. Nucleated Cells of the Human Circulatory System Secrete Plasminogen Activator and Respond to *C. atrox* Venom. *Nancy E. Kirschbaum*, Andrei Z. Budzynski, and

Gwendolyn J. Stewart. Department of Biochemistry, Temple University School of Medicine, Philadelphia, PA 19140.

The process of fibrinolysis, whose function is the dissolution of a blood clot, is initiated by activators converting plasminogen to plasmin. The amount of plasminogen activators (PA) secreted from the cells regulate fibrinolysis. Secretion of PA from cells occurring either in blood, i.e., erythrocytes (RBC), platelets (PLT), polymorphonuclear leukocytes (PMN), or in the blood vessel wall, i.e., smooth muscle cells (SMC), endothelial cells (EC), was measured by plasmin-dependent fibrinolysis. Only nucleated cells secreted PA. RBC and PLT secreted no PA. EC, SMC, and PMN secreted 0.13, 0.12, and 0.001 urokinase units of PA activity per 10^6 cells, respectively. Analogous phenomenon was observed when testing the cellular response to stimulation by *Crotalus atrox* venom. PMN exhibited a 400-fold increase in the amount of PA activity secreted. EC and SMC had a 40-fold maximal stimulation. The activating agent in the venom had M_r 25–55 kD. The calculation of EC, SMC, and PMN number in veins of different diameter demonstrated that EC are the main source of PA in capillaries and in veins with a diameter below 20 μm. As the vessel diameter increases, SMC and PMn overtake EC number and will be the major contributors to PA output in large veins, especially those above 1-mm diameter.

155. New Protein Sequencing Techniques. High Sensitivity Solid-Phase Protein Sequence Analysis Using a Commercial Gas-Phase Sequencer. *P.-H. Lai* and R. Everett. Amgen, Thousand Oaks, CA 91320.

Since its introduction in 1981, the method of automated gas phase protein sequence analysis has been effectively used for determining the primary structure of polypeptides of limited availability. Similar to the liquid phase sequencing, the gas-phase procedure requires the sample be prepared essentially free from reagents and salts. This is a serious problem when purifying minutely available proteins to the state of sequencing purity. To circumvent this problem and to increase the sensitivity, we combined the solid-phase and gas-phase methods. The protein samples were coupled on to solid supports, which can be performed in the presence of denaturants and/or a high concentration of salts, and sequenced with a commercial gas-phase sequencer. This combined method of protein sequencing offers highly sensitive analysis at pmol level and can tolerate salts and denaturants in sample preparations. Several rDNA protein products including *E. coli* interferons have been analyzed by this method.

156. The Product-Selective Blot: A New Tool for Measuring Enzyme Activities in Large Numbers of Samples and Native Electrophoresis Gels. *Gregory A. Thompson*, H. Maelor Davies, and Nancy McDonald. Calgene, Inc., Davis, CA 95616.

As part of studies of nitrogen assimilation in maize, we have developed a method for screening large numbers of samples for glutamate synthase (GOGAT) activity. Enzyme reaction mixtures in microtiter wells are deproteinized with TCA and aliquots are blotted by suction into a 5 mm thick layer of 0.75% agarose containing an immobilized ligand (Dowex 1 or 50) which selectively binds one of the products (glutamate). After washing to remove unbound substrate, bound product is measured by radiometric or fluorometric (*o*-phthalaldehyde) methods. Activities measured correspond to values from conventional assay protocols. Alternatively, the method may be used to detect enzyme activities in native electrophoresis gels by running reactions in the gel and then blotting into the agarose layer. This variation of the method has been demonstrated for detection of glutaminase. Details of each version will be presented along with a discussion of other potential uses.

157. HPLC Determination of Cilastatin in Biological Fluids. *J. L. Demetriades*, P. R. Souder, L. A. Entwistle, W. C. Vincek, D. G. Musson, and W. F. Bayne. Drug Metabolism, Merck Sharp & Dohme Research Laboratories, West Point, PA 19486.

Cilastatin, a dehydropeptidase I inhibitor, is coadministered with the β-lactam antibiotic imipenem. The described procedure for the quantitation of cilastatin in plasma and urine was developed. The assay involved sample purification on a bonded-phase extraction cartridge, reverse-phase HPLC, postcolumn derivatization, and fluorescence detection. Standard curves were linear from 0.75 to 75.0 μg/mL in plasma and from 2.5 to 200.0 μg/mL in urine. The intraday mean coefficients of variation at concentrations within the standard curve range were 4.2 ± 2.4% and 3.0 ± 1.6% in plasma and urine, respectively. The interday coefficients of variation for analyses of cilastatin in plasma (1.0 and 50.0 μg/mL) were <10% after 31 days of analysis while those for urine (5.0 and 75.0 μg/mL) were <11% after 44 days of analysis. This procedure met the sensitivity and specificity requirements for the analysis of samples from clinical pharmacokinetic studies.

158. A Reverse-Phase High-Performance Liquid Chromatographic Method for the Quantification of Famotidine in Human Plasma and Urine. W. C. Vincek, *M. L. Constanzer*, G. A. Hessey II, and W. F. Bayne. Department of Drug Metabolism, Merck Sharp & Dohme Research Laboratories, West Point, PA 19486.

The new H2-receptor blocker, famotidine, is a potent inhibitor of gastric acid secretion in man. A specific and sensitive analytical method was developed for the quantification of famotidine in both human plasma and urine samples. Initial attempts to derivatize famotidine (pre- and postcolumn) with fluorescent or ultraviolet light absorbing tags were fruitless. Electrochemical oxidation of famotidine, either amperometrically or coulometrically, also was not suitable for routine analysis. It was possible to detect reliably 5 ng of drug in plasma (1 mL) or 500 ng in urine (1 mL) using UV absorption alone (λ_{max} = 267 nm, ϵ = 1.58 E04, plasma – 0.002 AUFS). A straight-forward, high-recovery, sample preparation procedure was developed using silica cartridges. The diluted urine or neat plasma sample was added to the cartridge, the cartridge was washed with water and the famotidine eluted by the proper choice of solvent. Resolution of famotidine from endogenous interferences was accomplished on a RP-8 column using a water–acetonitrile–phosphoric acid (82.4:10:7.6) mobile phase.

159. A High-Performance Liquid Chromatographic Method for the Quantification of Amiloride in Human Serum and Urine. W. C. Vincek, *G. A. Hessey II*, M. L. Constanzer, and M. R. Dobrinska. Department of Drug Metabolism, Merck Sharp & Dohme Research Laboratories, West Point, PA 19486.

Amiloride is an effective antikaliuretic–diuretic agent which is neither protein bound nor metabolized in man (Baer et al., *J. Pharmacol. Exp. Ther. 157*, 475, 1967). Due to the low concentrations of amiloride in serum after therapeutic doses, analytical methods have been confined to scintillation counting ([^{14}C]amiloride; Weiss et al., *Clin. Pharm. Ther. 10*, 401,

1969). The described procedure permitted the low level measurement of amiloride in human serum (1 ng/mL) or urine (25 ng/mL) samples. In brief, amiloride was adsorbed onto silica and eluted with acetonitrile. The acetonitrile alone (urine) or after mixing with a solution of sodium perchlorate (serum) was injected into the HPLC system. The mean recovery of amiloride from urine samples was 65% and from serum samples was 70%. Intraday variability was less than 4% for serum (curve range 1.0–25.0 ng/mL) and less than 8% for urine samples (curve range was from 0.025 to 5 μg/mL). Instrumental conditions: Waters 6000 pump (flow = 1.0 mL/min); Waters micro-Bondapak C18 column (30 cm × 3.9 mm, 10 micron); Perkin-Elmer 650-10S (ex = 368 nm/em = 417 nm). Representative results from a human clinical study will be presented.

160. Deamination Reactions at the ϵ-Amino Group of Lysine. *Edyth L. Malin*, Rae Greenberg, Edwin Piotrowski, Thomas A. Foglia, and Gerhard Maerker. Eastern Regional Research Center, ARS, USDA, Philadelphia, PA 19118.

Three peaks were observed in the amino acid analysis elution profile of HCL hydrolysates of poly-L-lysine deaminated by nitrous acid. The major peak appeared just before the elution time of glycine; GC–MS analysis of this material after isolation by preparative TLC showed that it contained both δ- and ϵ-isomers of hydroxynorleucine. Chlorinated substitution products of these isomers, formed during HCl hydrolysis, appeared as a single peak just before the elution time of tyrosine. This peak did not appear in analysis of mercaptoethanesulfonic acid hydrolysates. The third peak, observed at the position of glutamic acid, was not identified. The γ-isomer of hydroxynorleucine was not seen in amino acid analysis. However, it was formed during the deamination reaction and observed as a component isolated by preparative TLC. The amino acid analysis chromatogram was useful in detecting the occurrence of deamination in proteins after reaction with nitrous acid since two of the three components resulting from deamination were observed as unique peaks.

161. Properties of the Antibacterial Agent Hypothiocyanous Acid (HOSCN). *K. M. Pruitt*, J. O. Tenovuo, B. Mansson-Rahemtulla, and P. G. Harrington. University of Alabama in Birmingham, Birmingham, AL 35294, and University of Turku, Turko, Finland 20520.

Peroxidases catalyze the oxidation of the thiocyanate ion (SCN^-) by hydrogen peroxide to generate HOSCN. The hypothiocyanite anion ($OSCN^-$, produced by ionization of HOSCN, pK = 5.3) is a normal component of human saliva at pH 7. The antibacterial activity of HOSCN/$OSCN^-$ is greater at low pH. We have studied the properties of HOSCN in acid solution. The HOSCN was generated by mixing SCN^-, H_2O_2, and bovine lactoperoxidase (LP) in 0.1 M phosphate at pH 3.0. The UV spectrum of HOSCN at this pH showed a nearly symmetrical peak at 240 ± 2 nm, extinction coefficient ϵ = 95 M^{-1}. In order to record this spectrum, the contributions of unreacted SCN^- (ϵ_{240} = 290 M^{-1}) and H_2O_2 (ϵ_{240} = 45 M^{-1}) had to be eliminated or compensated for. The HOSCN is stable at pH 3 but rapidly decomposes when the pH is adjusted to 8. The uncatalyzed reaction between SCN^- and H_2O_2 is slow, but equilibrium is reached rapidly in the presence of excess LP. The equilibrium constant for the reaction $H_2O_2 + SCN^- = HOSCN + OH^-$ was estimated to be $5 \pm 2 \times 10^{-9}$. The rate of decomposition of HOSCN was not significantly affected by the presence of excess SCN^-, LP, or H_2O_2.

162. Oxidation and Interconversions of Pyruvate, Lactate, and Alanine in the Metabolism of Neonatal Rat Heart Cells in Culture. *Nancy A. Schroedl*, C. Richard Bacon, and Charles R. Hartzell. Alfred I. duPont Institute, Wilmington, DE 19899.

Facile cellular interconversions between pyruvate, lactate, and alanine, as well as complex cellular compartmentalization resulting in substrate pooling, give rise to an emerging picture of intricate metabolic control and regulation in the developing heart. In the steady-state metabolism of glucose by neonatal rat heart cells in culture, the following products are produced under normal conditions (% of original medium glucose), lactate (80%), CO_2 (12%), glycogen (5%), and alanine (3%) [Schroedl, Ross, McCarl, and Hartzell (1982) *J. Cell. Physiol. 113*, 231–239]. Medium lactate and alanine levels often increased severalfold over original concentrations and subsequently are reused, even in the presence of glucose, by the heart cells for synthtic processes and oxidative energy metabolism. Surprisingly, when CO_2 evolution rates were measured, these cells showed a marked preference for oxidizing lactate over either pyruvate or glucose. In aerobic glucose-free conditions, the heart cells used lactate, pyruvate, or alanine to maintain the beating response to the detriment of synthetic processes. The utilization of lactate is complicated by continuous dilution of the labeled lactate in the medium. Algorithms have been developed for data treatment to account for interconversions and pool dilution.

163. Propranolol Depression of NAD-Linked Glycerol-3-phosphate Dehydrogenase Activity in Cultured Heart Cells. *Deborah L. Freerksen* and Charles R. Hartzell. Research Department, Alfred I. duPont Institute, Wilmington, DE 19899.

The direct effects of chronic exposure (11 days) to the β-adrenergic blocking drug, propranolol (10 $\mu g \cdot mL^{-1}$), on myocardial muscle metabolism were studied using rat heart cells in culture. Heart cell beating rate, glucose uptake rate from the medium, and protein content were not altered by propranolol. NAD-linked glycerol-3-phosphate dehydrogenase (NAD-G3PDH, EC 1.1.1.8) activity was depressed in cells maintained with propranolol. This enzyme has previously been shown to be a sensitive indicator of the metabolic state of the heart cell [Freerksen, D. L., & Hartzell, C. R. (1983) *Biochemistry 22*, 16A; Freerksen, D. L., Schroedl, N. A., & Hartzell, C. R. (1984) *Arch. Biochem. Biophys. 228*, 474–479]. NAD-G3PDH is important in synthesis of the glycerolipid precursor, glycerol 3-phosphate, in heart. Inhibition by propranolol of NAD-G3PDH activity may serve the same purpose as inhibition of phosphatidate phosphohydrolase (which has been shown to occur in several tissues), i.e., to decrease the biosynthesis of diglycerides, triglycerides, and polar lipids. Glucose-6-phosphate dehydrogenase (EC 1.1.1.49) activity was elevated by chronic exposure of heart cells to propranolol.

164. Microradiorespirometry Applied to Cells Attached to Petri Dishes. *C. Richard Bacon*, Nancy A. Schroedl, and Charles R. Hartzell. Alfred I. duPont Institute, Wilmington, DE 19899.

Methods developed to measure $^{14}CO_2$ evolution from specifically ^{14}C-labeled substrates by various tissues and tissue preparations have over the years yielded a wealth of biochemical information. We reported an early version of a

radiorespirometer to measure $^{14}CO_2$ evolution from cells attached to Petri dishes [Ross, McCarl, and Hartzell (1981) *Anal. Biochem. 112*, 378–386]. A controlled gas flow was humidified, passed through the culture medium, and trapped with an organic base in scintillation vials. Reported improvements will include (a) gas flow regulation, (b) gas humidification, (c) Petri dish capping, (d) gas introduction to the culture medium by means of a "soft" bubble, (e) medium mixing by a rocking mechanism, and (f) efficient $^{14}CO_2$ trapping. The apparatus may be sterilized and operated under aseptic conditions. $^{14}CO_2$ evolution from various ^{14}C-labeled substrates by neonatal rat heart cells in culture will demonstrate the accuracy and precision that can be obtained by the redesigned apparatus.

165. A Role for Citrate in the Synthesis of Acetylcholine in Nerve Terminals. *G. V. W. Johnson* and Charles R. Hartzell. Alfred I. duPont Institute, Wilmington, DE 19899, and University of Delaware, Newark, DE 19711.

The mechanism whereby mitochondrial acetyl-CoA becomes available for cytoplasmic acetylcholine (ACh) synthesis in neurons of the CNS is not well understood. Our data indicate that citrate, by utilizing ATP citrate lyase (EC 4.1.3.8), plays an important role in supplying the cholinergic synaptoplasm with acetyl-CoA for ACh synthesis. After a 3-h incubation, the percentages of ^{14}C-ACh synthesized from total substrate taken up by the synaptosome were 2.40 ± 0.16, 2.24 ± 0.26, and 0.47 ± 0.07 for [2,3-^{14}C]succinate, [6-^{14}C]glucose, and [3-^{14}C]pyruvate, respectively. ACh synthesis continued to increase after 3 h for [2,3-^{14}C]succinate and [6-^{14}C]glucose, while steady-state conditions were reached within 60 min for [3-^{14}C]pyruvate. Then millimolar 1,2,3-benzenetricarboxylic acid, a competitive inhibitor [K_i = 0.16 mM] of citrate transport from mitochondria, reduced ACh synthesis from [2,3-^{14}C]succinate by 70%. This information and additional data support the concepts that (1) citrate serves to introduce acetyl-CoA to the synaptoplasm, (2) partitioning occurs between exogenous pyruvate and endogenous pyruvate derived from glucose and succinate, and (3) per mole metabolized, glucose and succinate are preferential substrates for ACh synthesis.

166. Cancer Detection: Assay Procedure for B-Protein Adapted to a Variety of Clinical Situations. *E. T. Bucovaz* and W. D. Whybrew. Departments of Biochemistry, Obstetrics, and Gynecology, University of Tennessee Center for the Health Sciences, Memphis, TN 38163.

B-Protein is a general serological marker used to detect cancer. The standard assay procedure is based on the interaction between B-protein and a radiolabeled binding protein, a substructure of the coenzyme A–synthesizing protein complex (CoA–SPC) of Bakers' yeast. The B-protein–binding protein complex is separated from interfering proteins utilizing the principal of solubility differences. Modifications have resulted in simplifications which include (1) measuring the rate of filtration, (2) measuring UV absorption, and (3) replacing CoA–SPC with either purified radiolabeled binding protein or acyl carrier protein. These modified procedures have essentially the same degree of sensitivity and are readily adaptable to the clinical laboratory environment. Subsequent studies directed at further simplification of the assay are based on the principal of agglutination inhibition. These modifications should provide substantially more versatility for use of the B-protein assay. Although many of the principals are the same as involved in the standard assay, the use of radioactivity is not required, and the assay time can be reduced to approximately one minute. Consequently, the assay, could be utilized in clinicians' offices as well as in clinical laboratories.

167. Cancer Management: Studies Conducted Utilizing the Standard and Modified B-Protein Assay Procedures. *J. C. Morrison*, W. D. Whybrew, and E. T. Bucovaz. Departments of Biochemistry, Obstetrics, and Gynecology, University of Tennessee Center for the Health Sciences, Memphis TN 38163, and the Department of Obstetrics and Gynecology, University of Mississippi Medical Center, Jackson, MS 39216.

B-Protein, a general serological marker for cancer, is used for the detection and monitoring of malignancies. The effectiveness of the standard B-protein assay procedure as a cancer management aid has been evaluated for more than two years. The results of this study show that whenever a positive B-protein result is observed prior to surgery, the assay has a high degree of efficiency in detecting the recurrence of cancer in that individual. The standard B-protein assay procedure, because of its design, is for use primarily in the clinical laboratory environment. Consequently, in many cases valuable time may be lost during the process of transporting the sample to the clinical laboratory and communicating the results to the clinician. Therefore, a modified assay procedure for B-protein based on the principal of agglutination inhibition, which can be utilized in the clinicians' office, was compared with the standard B-protein assay in the cancer management studies. This modified procedure, although qualitative in nature, proved to be effective and efficient as a cancer management aid.

168. Chlordecone Binding Proteins Isolated from Pig Liver Cytosol. *P. J. Soine*, R. V. Blanke, and C. C. Schwartz. Department of Chemistry, Randolph-Macon College, Ashland, VA 23005, and Department of Pathology, Department of Medicine, Virginia Commonwealth University, Richmond, VA 23298.

Binding of chlordecone (CD) to pig liver cytosolic proteins was studied after the simultaneous administration of ^{14}C-CD and ^{3}H-cholesterol via the portal vein. The isolation of CD binding proteins (CDBP) from liver cytosol consisted of ultracentrifugation, $(NH_4)_2SO_4$ fractionation, and chromatography on Bio-Gel A 0.5m, on carboxymethylcellulose (CMC), and on Sephadex G-100. Three proteins retained ^{14}C-CD after elution from the CMC column. CDBP I and CDBP II but not CDBP III also retained [^{3}H]cholesterol. The molecular weights, estimated by Sephadex G-100, were 33 500 and 67 000 for CDBP IA and CDBP IB, 49 000 for CDBP II, and 44 000 for CDBP III. Incubation of CDBPs, eluted from Sephadex G-100, with [^{3}H]cholesterol resulted in 2000-, 800-, 100-, and 300-fold increases of ^{3}H associated with CDBP II, CDBP IA, CDBP IB, and CDBP III, respectively. Comparison of the isolation characteristics, molecular weights, and cholesterol binding properties of the CDBPs with cytosolic cholesterol binding proteins previously isolated suggests that CD and cholesterol share a common transport pathway in the liver cytosol.

169. Bovine Molk Bombesin (BMB): Partial Purification, Characterization, and Bioactivity. *L. H. Lazarus*, G. Gaudino, W. E. Wilson, and V. Erspamer. LBNT, NIEHS, NIH, Research Triangle Park, NC 27709.

A new mammalian bombesin in milk was recently described using a radioimmunoassay against the amphibian peptide [*PNAS 81*, 578 (1984)]. Purification from the acidified whey

included (a) neutralization, (b) ammonium sulfate precipitation, (c) molecular sieving on Bio-Gel P-10, (d) preparative C-8 reverse-phase LC using stepwise acetonitrile elution, (e) semipreparative LC on ODS packing, and (f) HPLC on analytical C-8 and ODS columns. Using triethylamine, pH 5.0, and linear gradients of acetonitrile and propanol, a single immunoreactive bombesin-containing peptide was found and purified to apparent homogenity. BMB elution on ODS depended on pH and sodium sulfate in the mobile phase. Gel filtration gave a M_r of 3200. A purified sample was air oxidized suggesting the presence of a thiol group; it was susceptible to trypsin and α-chymotrypsin digestion. BMB exhibited a bombesin-specific contraction of isolated rat uterus and guinea-pig large intestine and had a particularly evident effect on rhythmic movement; stimulation was promptly removed by washing. BMB was more potent than porcine bombesin-27 (GRP) and may be as active as amphibian bombesin-14.

170. A Comparison of Triose 1,2-Enediol 3-Phosphate Stability in Solution and at Triosephosphate Isomerase. *J. P. Richard.* Fox Chase Cancer Center, Philadelphia, PA 19111.

Rate and equilibrium constants for the formation of triose 1,2-enediol 3-phosphate by quinuclidinone deprotonation of DHAP within the buffer–substrate encounter complex have been estimated from the experimentally determined rate constant for quinuclidinone catalyzed deprotonation of DHAP, and estimated equilibrium constants for DHAP ionization at carbon-3 and for encounter complex formation. Comparison of the nonenzymatic values with previously published values for triose phosphate isomerase catalysis of DHAP reaction shows that there is a 10^5-fold acceleration and DHAP deprotonation at the enzyme compared to the quinuclidinone encounter complex, and a corresponding 10^{10}-fold stabilization of the intermediate at the enzyme which is due to a 10^{10}-fold higher affinity of the enzyme for its reaction intermediate than for substrate DHAP. The utilization of the large intermediate binding energy in stabilization of the transition state for intermediate formation will be discussed.

171. The Reaction of Triosephosphate Isomerase with L-Glyceraldehyde 3-Phosphate and Triose 1,2-Enediol 3-Phosphate. *John P. Richard.* Fox Chase Cancer Center, Philadelphia, PA 19111.

Triosephosphate isomerase catalyzes the isomerization and/or racemization reactions of L-glyceraldehyde 3-phosphate (LGAP). The reaction is inhibited by the active site directed reagent glycidol phosphate. The second-order rate constants for this enzymatic reaction show little or no dependence on increasing steady-state concentrations of triose 1,2-enediol 3-phosphate caused by increasing quinuclidinone catalysis of LGAP deprotonation. Therefore enzymatic protonation of the enediol or enediolate, which would lead to net LGAP reaction, are at best minor reactions. Instead LGAP reacts directly by binding at the enzyme active site. Improbable and probable explanations for the failure of triose phosphate isomerase to protonate its putative reaction intermediate will be discussed.

172. Inhibition of Sickle Hemoglobin Gelatin by Amino Acids and Related Compounds. *Hwei-zu Lu*, Bruce L. Currie, and Michael E. Johnson. Department of Medicinal Chemistry and Pharmacognosy, University of Illinois at Chicago, Chicago, IL 60612.

Sickle cell anemia is a hereditary disease in which the glutamic acid at the β6 position of normal adult hemoglobin (Hb) is replaced by valine to produce sickle Hb. During deoxygenation, HbS aggregates together to form gels which deform and rigidify the erythrocytes. Over the last several years, a variety of studies have shown the binding interaction between hemoglobin and aromatic amino acids, peptides, and related compounds [Noguchi, C. T., and Schechter, A. N. (1978) *Biochemistry 17*, 5455–5459; Gorecki, M., Votano, J. R., and Rich, A. (1980) *Biochemistry 19*, 1564–1568], which act as stereospecific inhibitors at one of the contact region to prevent gelation. We have used tryptophan as a model compound to study the binding characteristics by ultrafiltration. The binding studies indicate that Trp binds weakly to Hb with dissociation constant about 10^{-2}–10^{-3} M. We have synthesized a spin-label analogue of phenylalanine as a gelation inhibitor probe. HbS gelation measurements indicate that it is a potent inhibitor of deoxy HbS aggregation. We have also used spin-label EPR and high-resolution proton NMR to study the binding of the Phe analogue to Hb and find a specific binding of the spin-label analogue of Phe to Hb.

173. Microorganism Characterization by Enzyme-Metabolite Induced Fluorescence Velocity Measurements. *A. P. Snyder*, T. T. Wang, and D. B. Greenberg. Chemical Research & Development Center, Aberdeen Proving Ground, MD 21010 (A.P.S. and T.T.W.), and Department of Chemical and Nuclear Engineering, University of Cincinnati, Cincinnati, OH 45221 (D.B.G.).

A methodology for the rapid characterization of microorganisms is in progress using induced fluorescence as a probe. In general, the type and substrate-induced quantity of enzymes vary to an extent in bacteria and thus can be used to ascertain their presence. Enzyme action on a nonfluorescent substrate is utilized in the production of a fluorescent compound, and with a qualitative light-scattering concentration determination, a product fluorescence rate analysis can be used to discern the presence of different types of bacteria. The various enzyme/substrate assay pairs probed are lipase/diacetylfluorescein [Snyder, A. P., & Greenberg, D. B. (1984) submitted to *Bioeng. Biotechnol.*], indoxylacetate; oxidase/luminol [Oleniacz, W. S., Pisano, M. A., & Rosenfeld, M. H. (1966) *Technicon Int. Symp.* Vol. I] and dehydrogenases/NADH, resazurin. Limits of detection of seven different organisms representing the genera *Bacillus* to *Escherichia* are 3.0×10^4 to 4.0×10^8 and 10^3 to 3.0×10^4 for the diacetylfluorescein and luminol reactions, respectively. The specificity and versatility of the method can be realized by using dyes containing similar and different functional groups.

174. Assessment of Human Glomerular Permeability with Polydisperse Dextran. *Marion P. Cullen* and Raymond M. Baker. Department of Paediatrics, Guy's Hospital Medical School, University of London, London SE1 9RT.

A semiautomatic system incorporating an ultrasensitive interference refractometer coupled to a dual-column gel-permeation HPLC apparatus has been devised for measurement of the molecular size distribution of dextrans in small samples of serum and urine from a paediatric population and volunteers, will be described. Following infusion of dextran, serial samples over 3 h are analyzed to assess the relationship between concentration and molecular sizes. The system was calibrated with 17 defined dextran fractions within the range of 1200–250 000 D. Urine samples were prepared for analysis by passage through small ion-exchange columns; serum was

pretreated by precipitation with trichloroacetic acid and centrifuged before the ion-exchange treatment. Internal standard (dextran, 2×10^6 D) was added to each sample before pretreatment. Data were analyzed with a specially written computer program, output from which gave plasma clearance for each of selected ranges of molecular size.

175. Chemotherapeutic-Induced Changes in the Accumulation of Radiolabeled Thymidine (TdR), 2-Deoxy-D-glucose (2-DG), and α-Aminoisobutyric Acid (AIB) in Rat Prostatic Adenocarcinoma. *P. S. Conti*, B. Schmall, E. L. Kleinert, H. W. Herr, and W. F. Whitmore, Jr. Memorial Sloan-Kettering Cancer Center, New York, NY 10021.

Carbon-11, a cyclotron produced, short-lived ($t_{1/2}$ = 20.4 min), positron-emitting radionuclide, has been incorporated into TdR, 2-DG, and AIB in order to study biochemical processes in neoplastic tissues in vivo by imaging with positron emission tomography (PET) (Schmall, Conti, et al., *Biochemistry 22*, 36A, 1983). We have investigated the accumulation of C-14 TdR, 2-DG, and AIB at 45 min postinjection in the fast-growing, anaplastic Dunning R3327G and slow-growing, well-differentiated R3327H prostatic adenocarcinomas in Copenhagen rats before and after chemotherapy (5 rats per group):

COMPOUND	UNTREATED G	TREATED*G	UNTREATED H	TREATED†H
TdR	2.55	0.85	1.31	1.17
2-DG	1.07	0.73	1.15	1.61
AIB	1.61	0.69	2.02	1.44

*MethylGAG: 3.5mg/rat/day(ip). Difluoromethylornithine: 2% in drinking water. †Diethylstilbestrol: 0.5mg/rat/2 weeks (ip).

(Values = DPM found/g of tumor ÷ DPM injected (ic)/g of rat mass.) The results suggest that changes in the accumulation of these molecules in tumor tissue during therapeutic intervention can be monitored with the C-11 analogues and PET.

176. Comparative Studies in Rat Prostate Adenocarcinoma with Radiolabeled Substrates for A-Type and L-Type Amino Acid Transport Systems. *P. S. Conti*, B. Schmall, E. L. Kleinert, H. W. Herr, and W. F. Whitmore, Jr. Memorial Sloan-Kettering Cancer Center, New York, NY 10021.

Carbon-11 ($t_{1/2}$ = 20.4 min) labeled synthetic, nonmetabolized amino acids such as α-aminoisobutyric acid (AIB), *N*-methyl-AIB, aminocyclopentanecarboxylic acid (ACPC), and 2-aminobicyclo[2.2.1]heptane-2-carboxylic acid (BCH) may be useful for studying amino acid transport in vivo using positron emission tomography. In order to compare the biodistribution of these amino acids, the C-14 and C-11 labeled analogues were studied in control rats and in rats bearing the Dunning R3327G prostatic adenocarcinoma. The mean relative concentration (RC) of activity in blood and tissue samples was calculated, where RC = dpm found per g of tissue/dpm injected (ic) per g of animal mass (5 rats per group):

AMINO ACID	SYSTEM	TUMOR	BLOOD	PROSTATE	MUSCLE	PANCREAS	KIDNEY	LIVER
C-14 AIB	A	1.61	0.83	0.44	0.44	10.6	13.8	3.25
C-14 N-MeAIB	A	1.34	0.86	0.39	0.41	10.7	15.6	3.25
C-14 ACPC	L	1.47	1.09	0.92	1.11	5.29	1.84	1.23
C-11 BCH	L	1.24	0.89	0.85	0.92	5.41	1.48	0.99

These values of RC at 45 min postinjection demonstrate accumulation of all four amino acids in tumor, with notable differences in the normal tissues studied.

177. Nitrite Anion Oxidation of Thiols. *Robert C. Benedict.* Eastern Regional Research Center, ARS, U.S. Department of Agriculture, Philadelphia, PA 19118.

Nitrous acid (pK_a = 3.38) reacts as the undissociated acid with thiols to form nitrosothiols (RSNO) which can react further to product disulfide (RSSR) and various nitrogen oxides. Rate of nitrosothiol formation from HONO and various thiols is affected greatly by the nature of the thiol, the pH, and the presence of chloride or other anions. At pHs above 5.0, however, nitrosothiols appear not to be forms, but disulfides are produced from a reaction of nitrite anion with the thiol. This oxidation involves formation from nitrite of an active oxygen intermediate such as superoxide anion which reacts with thiol to form disulfide. This reaction also is affected by the nature of the thiol and added anions and appears to be more important than nitrosothiol formation in nitrite inactivation of thiol enzymes and in certain reactions during meat curing occurring at pHs greater than 5.

178. Monoclonal Antibody to Human Cytochrome *c*. *Li-Mei Kuo*, Helen C. Davies, and Lucile Smith. Department of Microbiology, University of Pennsylvania, Philadelphia, PA 19104, and Department of Biochemistry, Dartmouth Medical School, Hanover, NH 03755.

We have prepared a monoclonal antibody to human cytochrome *c* which will bind only to human cytochrome *c* among the 25 cytochromes from different species tested, including that from *Macaca mulatta*. Thus the antibody binds in the area around isoleucine-58, where evidence of a conformational change is seen on oxidation–reduction. The effect of the antibody on the reaction of human cytochrome *c* with the oxidase and reductase segments of the electron transport chain of beef heart mitochondria was measured using spectrophotometric assays where binding of cytochrome *c* is rate limiting. The antibody was found to decrease the rate constant of both reactions, but the inhibitory effect was greater on that of the oxidase (50% inhibited with 0.5 antibody site to cytochrome *c*) than with the reductase (not inhibited at this ratio). In addition, increasing the pH of the assay from 6 to 8 resulted in less inhibition on the oxidase and more on the reductase. The data suggest that the change around isoleucine-58 influences the reaction of the cytochrome differently with its two redox partners, even though the binding sites appear to be localized in another area of the molecule.

179. Europium(III) as a Laser-Induced Luminescent Probe of Concanavalin A. *G. L. Richmond*, J. Maule-Schmidt, and P. Chu. Department of Chemistry, Bryn Mawr College, Bryn Mawr, PA 19010.

Substitution of luminescent lanthanide ions for spectroscopically invisible metal ions in native proteins can provide valuable information about the biomolecular structure of the metal ion binding sites. This is particularly true for europium(III) in which the relative intensities and band structure are sensitive to the detailed nature of the ligand environment about the metal ion. We report the use of europium(III) as a fluorescent probe of the metal binding sites of concanavalin A, an important plant lectin which specifically binds to polysaccharides. Upon pulsed laser excitation of the $^7F_0 \rightarrow {}^5D_0$ transition of europium ions in the protein samples, enhanced fluorescence is observed indicating Eu(III) ion binding. The excitation emission spectrum contains resolvable Lorentzian peaks characteristic of individual binding sites on the concanavalin A. The number of distinct sites range between two and three depending upon the pH of the samples. Fluorescence lifetime measurements are used to characterize the europium

ion environment with respect to the protein and water ligands. Results of the competitive addition of metals such as calcium, manganese and other lanthanides will be discussed.

180. Comparative Solvent Proton Relaxation Dispersion Studies on Solutions of Ca^{2+}-Mn^{2+}-Con A, -Lentil and -Pea Lectins. *C. F. Brewer*, Lokesh Bhattarcharyya, R. D. Brown, III, and S. H. Koenig. Department of Molecular Pharmacology, Albert Einstein College of Medicine, Bronx, NY 10461, and IBM T. J. Watson Research Center, Yorktown Heights, NY 10598.

Nuclear magnetic relaxation dispersion (NMRD) measurements have been previously employed to investigate the metal ion and saccharide binding properties of the lectin concanavalin A (Con A) (cf. Koenig, S. H., Brown, R. D., III, and Brewer, C. F. (1983) *Biochemistry 22*, 6221–6226). NMRD measurements record solvent proton longitudinal relaxation rates in solutions of metalloprotein (typically Mn^{2+}) as a function of magnetic field, corresponding to proton Larmor frequencies of from 0.01 to 50 MHz. A comparative NMRD study of the Ca^{2+}–Mn^{2+} profiles of the latter two proteins were essentially identical, but differed from the former. The results are used to demonstrate two mechanisms for solvent proton relaxation by Con A, only one of which appears present in the lentil and pea lectins.

181. Preparation and Properties of Metal Ion Derivatives of Lentil and Pea Lectins. *Lokesh Bhattacharyya*, C. F. Brewer, R. D. Brown, III, and S. H. Koenig. Department of Molecular Pharmacology, Albert Einstein College of Medicine, Bronx, NY 10461, and IBM T. J. Watson Research Center, Yorktown Heights, NY 10598.

The lentil and pea lectins are isolated as Ca^{2+}–Mn^{2+}-containing proteins. In the course of carrying our NMR studies on these lectins, we required a variety of different metal ion derivatives of the proteins. Unlike concanavalin A, a related lectin which can be acid demetallized to form the stable apoprotein and then remetallized, lentil and pea lectins do not form stable apoproteins, but rather, irreversibly form higher oligomers. We have devised a procedure which results in metal ion substitution without directly producing the apoproteins for the latter two lectins. We have replaced Mn^{2+} in the two proteins with the following metal ions: Zn^{2+}, Co^{2+}, Ni^{2+}, and Cd^{2+}. We have also prepared the Cd^{2+}–Cd^{2+} complexes of both proteins. All derivatives have been shown to have saccharide binding activity equal to the native lectins.

182. Phenylglyoxal-Modified Fe_2-Human Serum Transferrin Stability to Iron Removal and Periodate Oxidations. M. H. Penner, D. T. Osuga, C. F. Meares, and *R. E. Feeney*. Departments of Food Science and Technology (M.H.P., D.T.O., and R.E.F.) and Chemistry (C.F.M.), University of California, Davis, CA 95616.

Previous reports from our laboratory have shown the rapid inactivation of apo human serum transferrin (HST) by periodate [Geoghegan et al. (1980) *J. Biol. Chem. 225*, 11429; Penner et al. (1983) *Arch. Biochem. Biophys. 225*, 740]. Iron-saturated serum transferrin (Fe_2HST) was inactivated by periodate at different rates, depending on the buffer composition, particularly in phosphate (Penner et al., 1983). We now find that the iron in Fe_2HST is removed from the protein by phosphate ions. Phenylglyoxal-modified Fe_2HST (PG-Fe_2HST) was much more resistant to iron removal than Fe_2HST. After 2 h of dialysis against a phosphate/EDTA buffer, 80% of the iron was removed from Fe_2HST compared to only 28% from PG-Fe_2HST, which had ~15 of its 25 arginine residues modified. Also, when PG-Fe_2HST was periodate treated in a phosphate buffer for 60 min, there was no loss in iron-binding activity, but Fe_2HST lost 37% of its iron-binding activity on the same periodate treatment. It appears that the phenylglyoxal modification of Fe_2HST produces a transferrin derivative which is more resistant to iron removal by competitive ligands, such as phosphate.

183. A Model for the Transport of Iron across Hepatocellular Membranes. C. G. D. Morley, D. Delmastro, N. Prabhu, and *A. Bezkorovainy*. Department of Biochemistry, Rush-Presbyterian-St. Luke's Medical Center, Chicago, IL 60612.

Considerable interest has recently developed on the mechanism of iron transport from serotransferrin (TF) across the plasma membrane. There are two opposing views: one proposes that iron is freed from TF at the cell surface, the other suggests that the Fe–TF complex undergoes receptor-mediated endocytosis with iron removal occurring in receptosomes. Our studies show a receptor-mediated iron uptake process with no significant internalization of TF. The TF receptor obeys Michaelis–Menten kinetics and is sensitive to trypsin but not neuraminidase. Plasma membrane fragments also show the presence of an Fe^{3+} binding function and an iron-release function. None of these activities are present in mature red cell ghosts. Using selective destruction–inhibition methods, it has been determined that iron takes a three-step pathway when it is transported across the hepatocyte membrane: binding of the Fe–TF complex, loss of Fe^{3+} to the Fe^{3+} binder, and release by reduction to Fe^{2+}.

184. Relationships among Dietary Linoleic Acid Intake, Plasma Fatty Acids, and Prostaglandin E Turnover in Four Volunteers. *A. Ferretti*, J. T. Judd, and M. W. Marshall. Lipid Nutrition Laboratory, BHNRC, USDA, Beltsville, MD 20705.

The objective of the study was to determine whether changes in linoleic acid (18:2ω6) intake can modulate the systemic production of E prostaglandins (PG) concurrently with, or independently of, changes in the plasma PG precursor levels. Four male volunteers were fed each of two diets (L and H) for 6-week periods. The menu cycle was 7 days, and 35% of the energy was provided by fat. Diet L contained 10 g and diet H 30 g of 18:2ω6 per day. The PGE turnover was assessed by measuring the levels of the urinary metabolite of prostaglandins E_1 and E_2 (PGE-M) (Ferretti et al., *Anal. Biochem. 128*, 351, 1983). Initial body weight was maintained by adjusting the caloric level. As expected, we found clear and direct correlations between 18:2ω6 intakes and 18:2ω6 concentrations in the neutral lipid ($P < 0.01$) and phospholipid ($P < 0.05$) fractions of plasma. However, neither arachidonic acid (20:4ω6) concentrations in those same plasma fractions nor the urinary PGE-M output responded significantly to changes in 18:2ω6 intake. With the small number of subjects involved in this study, we could not detect an influence of moderate changes in dietary levels of 18:2ω6 on the systemtic production of PGE as measured by the levels of PGE-M in urine.

185. Dietary Fat Modification of Lipoprotein Fluidity and Composition in Miniature Swine. *Elliott Berlin*, Phyllis G. Kliman, Howard S. Kruth, James E. Cupp, and A. E. K. Ommaya. USDA, Beltsville, MD 20705, and NIH, Bethesda, MD 20205.

Feeding atherogenic diets to miniature swine resulted in rapid changes in lipoprotein fluidity as monitored by DPH fluorescence polarization. Decreases were substantial in VLDL fluidity, but only minimal changes in LDL fluidity and no changes in HDL fluidity were observed. Animals were fed the several diets for periods of up to 6 months, but fluidity changes were complete with 4 weeks. Steady-state fluorescence anisotropy, r_s, in VLDL was 0.070 in control diet animals and up to 0.151 within 4 weeks in animals fed an atherogenic diet. Similarly, r_s returned to normal within 1-month feeding of a low fat stock diet in a regression experiment with pigs previously fed the atherogenic diet for 3 months. Plasma cholesterol levels increased by 1.5–5-fold in pigs fed diets with added cholesterol and/or lard but the addition of 20% lard alone to the diet did not alter plasma triacylglycerol levels. VLDL cholesterol (C) and cholesteryl ester (CE) levels were diet dependent and controlled VLDL fluidity according to the equations $r_s = 0.089 + 0.723$ (C) and $r_s = 0.068 + 2.24$ (CE). Synthesis of the more rigid VLDL was followed by atherogenesis in the minipigs as evidenced by foam cell development and plaque deposition.

186. Effect of Dietary Trans Fatty Acids on Some Murine T and B Cell Functions. *Samuel A. Mantey*, Mark Keeney, and Joseph Sampugna. Department of Chemistry, University of Maryland, College Park, MD 20742.

Dietary fatty acids (FA), especially essential FA (EFA) and EFA metabolites, have been implicated in regulation of some immune functions. Modulation of immune function by EFA is ascribed to their role in cell membrane lipids and as precursors to eicosanoids. As trans FA can affect membrane properties and EFA metabolism, we studied mitogenesis, mixed lymphocyte response, and antibody response in lymphocytes of C57B1/6J mice fed experimental or control diets. Diets were identical, except that margarine fat (25% trans FA) was used in the experimental diet and fat in the control diet contained oleic acid in place of trans FA. Secondary antibody response to trinitrophenyl-keyhole limpet hemocyanin was significantly lower whereas mitogenic stimulation of thymocytes by concanavalin A and blastogenic stimulation of splenic lymphocytes by cells from allogenic mice were higher in cells of mice fed the experimental diet compared to those from mice fed the control diet. The significance of these observations will be discussed.

187. Effect of Dietary Trans Fatty Acids on Murine Hepatic Peroxisomes. *Yliana B. Gimenez-Gadea*, Mark Keeney, and Joseph Sampugna. Department of Chemistry, University of Maryland, College Park, MD 20742.

Liver tissue isolated from C57B1/6J mice fed experimental or control diets was examined for peroxisomal number and morphology by electron microscopy, for catalase activity, and for cyanide-insensitive B-oxidation of palmitoyl-CoA. The experimental and control diets were similar; however, the fat in the experimental diet was derived from a corn oil margarine containing ca. 25% trans fatty acids, whereas the fat in the control diet was from a blend of fats designed to yield a fatty acid composition identical to that of the margarine fat except that oleic acid replaced trans fatty acids. Compared to tissue isolated from control mice, that isolated from experimental animals contained more peroxisomes as well as vesicles associated with the endoplasmic reticulum and yielded greater specific activity for β-oxidation of palmitoyl-CoA. There was little, if any difference in catalase activity in liver tissue isolated from experimental and control mice. The significance of these observations will be discussed.

188. Intestinal Biohydrogenation and Trans Fatty Acids in Swine. *Teresa A. Cloey*, Joseph Sampugna, and Mark Keeney. Department of Chemistry, University of Maryland, College Park, MD 20742.

Biohydrogenation and possible production of trans fatty acids in swine intestine were investigated. Cecal contents were obtained from living swine that had a fistulated cecum. Cecal contents were analyzed for volatile fatty acids and total lipid fatty acids. The volatile fatty acid pattern was similar to that reported for bovine rumen contents. Trans fatty acids comprised 18.6% (weight percent as methyl esters) of the cecal lipid. Trans fatty acids were not detected in the lipid extract from the diet. When the fatty acid pattern of total lipids of intestinal sections was examined, trans fatty acids were present in progressively increasing percentages (jejunum, 0%; ileum, 0.9–1.9%; cecum, 9.9%; colon, 9.9–11.7%; and rectum, 10.9%). In addition, odd-chain and branch-chain fatty acids were found and followed a similar pattern. Small amounts of trans fatty acids (1.3% as fatty acid methyl esters) were also found in total liver lipids. Analysis of the *trans*-monoene fraction isolated from cecal lipid indicated that the major positional isomer was *trans*-vaccenic acid (68.9 mol %). These results are consistent with the hypothesis that intestinal biohydrogenation is the source of trans fatty acids in tissues of animals fed diets lacking these components.

189. Lysis of Unilamellar Liposomes by Natural and Synthetic Agents. *W. J. Litchfield*, M. E. Whiting, and J. W. Freytag. E. I. du Pont de Nemours & Company, Inc., Clinical & Instrument Systems Division, Glasgow Research Laboratory, Wilmington, DE 19898.

Liposomes are frequently used as model systems to investigate interactions between proteins and biological membranes. In this report, we describe the use of 500–2500 Å diameter unilamellar lipid vesicles, composed of egg yolk lecithin and cholesterol, to study the actions of both natural and synthetic cytolytic agents. Vesicles containing entrapped alkaline phosphatase were prepared by detergent dialysis, and lysis was monitored by measuring released enzyme activity. Melittin (a 26 amino acid peptide from bee venom) was active at concentrations above 10^{-8} M and immediately lysed vesicles. A biotinylated derivative of melittin showed similar activity, while a conjugate between melittin and ouabain was more effective. Cytotoxins I and II from *Naja naja oxiana*, as well as synthetic detergents, were lytic at levels above 10^{-7} M; however, very little lysis occurred in the presence of phospholipase A_2 or streptolysin O. In contrast, streptolysin O showed considerable lytic activity when sheep erythrocytes were substituted for liposomes. These results illustrate the importance of choosing appropriate model systems and may help explain the mechanisms of cytolysin action.

190. Laminin M, a New Subunit, Is Found in Normal but Not in Neoplastic Tissues. *M. Ohno*, A. Martinez-Hernandez, N. Ohno, and N. A. Kefalides. Connective Tissue Research Institute, University City Science Center and Hahnemann Medical College, Philadelphia, PA 19104.

Recently, we reported the discovery of a new subunit of laminin from human placental membranes which we designated laminin M. Placental membranes contain in addition laminin A and B. Since laminin M is not detected in the mouse EHS tumor matrix, we decided to compare placental

membranes from different species (human, cow, mouse, and rat) and also examine neoplastic tissues and cell lines from the above species. Preliminary data indicate that (1) all three laminin components A, M, and B are present in the normal placental membranes of all four species examined, (2) the relative amounts of the laminin components may vary among tissues but the ratio is similar among species, (3) cross-reactivity of anti-laminin antibodies varies among species, and (4) laminin M is not detectable in tumors or in neoplastic cell lines of mouse, rat, or human origin. If this is due solely to neoplastic transformation, then the absence of laminin M in a tissue may be used as a marker for neoplasia.

191. Evolution of Some Ideas about Tumor Prevention. *E. Seifter*. Albert Einstein College of Medicine of Yeshiva University, Bronx, NY 10461.

Since 1961 we have made numerous ACS presentations concerning the relationship of vitamin A (VA) and tumor growth. Because many of the underlying ideas with which we started our work received experimental substantiation, we should like to review the theory as we recorded it in 1961. VA deficiency initiates excessive cell division of some epithelial cells, inhibits normal differentiation, and stimulates metaplastic but not cancerous or precancerous changes. Although cell division increases with VA deficiency, some mechanisms of *control* remain operative so that the undifferentiated epithelium does not grow without limit, and indeed there is some differentiation of epithelium and mesenchyme. We then asked what would happen if the control mechanisms per se were damaged by certain toxic chemicals, and postulated that the balance between cell division and maturation would be upset. Would this then result in abnormal kinds of cell division, abnormal maturation, or dedifferentiation, then causing cancer in the VA-deficient animals? Conversely, then, would dietary VA prevent those chemicals from damaging control mechanisms for cell division or differentiation? This presentation addresses the results obtained over the years in pursuit of answers to those questions; it is dedicated to the late Dr. Jack Sobel who was most helpful in the discussion and planning of our early experiments.

192. Anabolic Effects of L-Arginine and L-Ornithine. *E. Seifter*, G. Rettura, S. M. Levenson, and A. Barbul. Albert Einstin College of Medicine, Bronx, NY 10461.

Supplemental arginine (Arg) evokes metabolic reactions in rodents eating Arg sufficient diets: acceleration of incisional wound healing; stimulation of thymic-dependent immune reactions such as allograft skin or tumor virus rejection; and diminution of postoperative weight loss. We hypothesized that these anabolic effects are related to polyamine biosynthesis or hormone secretion rather than direct nutritive action of Arg. If so, supplemental L-ornithine (Orn) which stimulates the secretion of insulin, growth hormone, and glucagon, but is able to generate only little Arg in vivo, would behave as supplemental Arg in the described systems. SD rats fed lab chow or lab chow supplemented with 1.0% Arg·HCl or 1.0% Orn·HCl received 7-cm dorsal skin incisions and 10 days later were killed and their wounds studied. Data show that Orn (like Arg) decreases weight loss after wounding ($p < 0.01$), prevents the decrease in thymic weight ($p < 0.005$) and increases wound strength ($p < 0.02$). In other studies C57 skin was grafted to C3H mice fed diets described above. Controls rejected skin 14 days later, whereas rejection occurred in ten days for both supplemented groups. Similar results were obtained in studies of Moloney sarcoma virus. We conclude, after the dietary Arg requirement is met, either Arg or Orn promotes similar hormone related anabolic reactions.

193. Affinity Labeling of Fatty Acid Synthase by Chloropropionyl-CoA. *H. M. Miziorko*, C. E. Behnke, P. M. Ahmad, and F. Ahmad. Medical College of Wisconsin, Milwaukee, WI 53226, and The Pap Cancer Research Institute, Miami, FL 33101.

Rat mammary fatty acid synthase (FAS) is inhibited by 3-chloropropionyl-CoA in a time-dependent, irreversible fashion. FAS inactivation occurs rapidly ($t_{1/2} \leq 10$ min; 37 °C) even at low concentrations (<30 μM) of inhibitor. Protection from inactivation is afforded by preincubating FAS with the substrate acetyl-CoA. Trichloroacetic acid precipitation of [1-^{14}C]chloropropionyl-CoA inactivated enzyme indicates covalent modification with a stoichiometry of 1.2 per site. This contrasts with the high limit stoichiometry (6 per site) observed upon FAS inactivation by the highly reactive analogue, bromodioxobutyl-CoA (Clements et al. (1982) *Biochem. J. 207*, 291–296). The covalent species formed upon chloropropionyl-CoA inactivation of FAS is not labile to performic acid oxidation, ruling out any adduct which involves only thioester linkages. Carboxyethylation of an active site nucleophile would account for FAS inactivation.